博士論文

Development of Polyaniline (PANI)-Based Conductive Thermosetting Matrix for FRPs and Their Structural Applications

(導電性ポリアニリンを用いた FRP 用熱硬化型樹脂の開発と構造部材への適用)

東京大学
THE UNIVERSITY OF TOKYO

Kumar Vipin

クマール ウィピン

Department of Aeronautics & Astronautics,

Graduate school of Engineering,

The University of Tokyo

This dissertation is submitted for the degree of

Doctor of Philosophy

June 1st, 2016

I would like to dedicate this thesis to my loving parents …

Declaration

I hereby declare that except where specific reference is made to the work of others, the contents of this dissertation are original and have not been submitted in whole or in part for consideration for any other degree or qualification in this, or any other University. This dissertation is the result of my own work and includes nothing which is the outcome of work done in collaboration, except where specifically indicated in the text.

Kumar Vipin

June 1st, 2016

Acknowledgements

First of all, I would like to thank and express my sincere gratitude to my academic supervisor Associate Professor Tomohiro Yokozeki for his kind support and guidance during the course of my Ph.D. in past three years. I am really grateful to him for introducing me to the exciting field of conducting polymers. I am highly obliged and indebted to Prof. T. Takahashi and Dr. T. Goto from Yamagata University for valuable timely discussions and continued co-operation. I extend my sincere thanks to Prof. T. Aoki for his valuable suggestions during the progress meetings.

I would like to thank Dr. S. R. Dhakate Dr. B. P. Singh and Dr. S. K. Dhawan, CSIR-NPL, New Delhi for a great discussion and guidance during my visit to their institute. I also wish to thank Mr. Takahashi Yuuki and Mr. Suganuma Yuuki for their kind help in conducting experiments during my stay in Yamagata University. I would like to thank my lab mates for their timely support both inside and outside campus. As a non-native Japanese speaker, my life would have not been comfortable without their help and support. Special thanks to Mr. Siwat Manomaisantiphap, Mr. Tigmanshu Pal and Ms. Aayushi Bajpayee for their help in conducting many experiments.

Above all, I wish to acknowledge from the bottom of my heart the untiring sacrifices made by my parents for their children. My elder sister and brother have always been a source of inspiration for me to achieve the highest degree in the field of education.

In the end, I gratefully acknowledge the MEXT scholarship. Without the scholarship, I might have not achieved this mile-stone in my life.

Abstract

In the recent years, aerospace industry has seen a gradual shift from metallic structures to the Carbon Fiber Reinforced Plastics (CFRPs) in structural applications. CFRPs has shown remarkable properties in many structural areas but, there are still some issues which need to be addressed in the near future. One of them is the loss of the electrical properties of carbon fibers in thickness and longitudinal directions in epoxy based CFRPs. This loss of electrical conductivity of the composites can be attributed to the insulating behaviour of the resin matrix. To improve the electrical properties of the composites many researchers have tried to add conductive filler into the insulating matrix. Adding CNT, carbon black, graphene etc. into the insulating matrices is the most common methodology employed. However, using this methodology, very high electrical properties have not yet been realized, especially in case of thermosetting composites. Recently, researchers have tried many other alternative ways and have also shown great interest in conductive polymer based composites. Conductive polymers have shown better process ability than traditional conductive fillers. A highly conductive composite material with good mechanical properties is the need of the hour of present industrial and academic fields. Therefore, a thermoset conductive composite with high mechanical and electrical properties has been tried to be developed in this work and its application have been investigated especially structural applications of conductive CFRPs.

Since the discovery of intrinsically conductive polymers (ICPs), they have attracted tremendous attention of researchers. Conductive polymer based composites have been researched extensively due to their outstanding properties and vast applications. Polypyrrole (PPY), ploy (3, 4-ethylenedioxythiophene) (PEDOT) and polyaniline (PANI) are the most studied conductive polymers. PANI has a special status among all the conducting polymers. PANI has been the center of research due to its ease in availability, ability to tune electrical conductivity and remarkable optical properties. It is well known that, emeraldine base form of PANI can be rendered conductive by doping with a protonic acid. In the present work dodecylebenzenesulfonic acid (DBSA) has been used as a dopant for PANI due to its surfactant properties which improves the solubility of the PANI-DBSA complex in the matrix i.e. DVB.

A unique one-step synthesis process of PANI-DBSA/DVB composite has been demonstrated in this work while choosing divinylbenzene (DVB) as the matrix. It is demonstrated that a

PANI-DBSA/DVB composite has very high electrical and good mechanical properties after curing. However, due to the low liquid state duration (early start of curing at room temperature) of this matrix, a parametric study has been done to optimize the present system. Roll-milling process and control doping process of PANI have been introduced for the mass production of this thermosetting conductive resin system. High electrical & mechanical properties with good environmental stability were aimed in the final composite. To improve electrical conductivity and mechanical properties of the system, an additional conductive filler VGCF was also used. With addition of additional conductive filler VGCF-H, higher electrical conductivity and better mechanical properties have been achieved. The idea of using additional conductive fillers was derived by the hypothesis that PANI-DBSA agglomerates are the conductive islands in the insulating DVB matrix. Therefore, additional conductive fillers can be used as the conductive connecting bridge between those islands, simultaneously improving the mechanical properties. Different combinations of dopant ratios and conductive fillers were tried with the main PANI-DBSA/DVB matrix and their effect on composite properties have been investigated.

Prepared composites have been characterized using various techniques like; Fourier transform infra-red spectroscopy (FTIR), ultra violet-visible-near infrared red spectroscopy (UV-vis-NIR), thermogravimetric analysis (TGA), thermal optical microscopy, electromagnetic interference (EMI) shielding measurements and four-probe electrical conductivity. The effect of dispersion on electrical and mechanical properties has also been elaborated using scanning electron microscope (SEM) micrographs.

Applications of this composite system have been investigated. This conductive resin system was used to impregnate FRPs to prepare highly conductive FRPs. Carbon fiber reinforced composite prepared by using PANI-based thermosetting resin (CF/PANI) has shown approximately 36 times higher electrical conductivity as compared to epoxy based CFRPs (CF/Epoxy) in the direction of thickness and approximately 6 times higher in the direction of fiber.

It is observed that high electric and dielectric properties contribute to the high EMI shielding effectiveness. Therefore, this composite find its application in EMI shielding technology as well. The composite with VGCF-H as additional conductive filler has shown maximum 73 dB shielding effectiveness at 13.2 GHz with the composition of 5 wt. % VGCF, 45 wt. % PANI-DBSA and 50 wt. % DVB in the composite. Electrical conductivity up to 1.97 S/cm with the addition of 5 wt. % VGCF-H and flexural modulus up to 1.71 GPa with 3 wt. % of VGCF-H

have also been achieved. These results confirmed that a polymer thermoset conductive composite with improved electrical, mechanical and very high EMI shielding effectiveness has been successfully prepared.

These outstanding results make the PANI-DBSA/DVB composite a potential candidate for light strike protection (LSP), structural capacitor and EMI shielding material. This work gives a start towards unravelling the new horizon of applications of **Structural Conductive Composites**.

Highlights

➢ A highly environmentally stable PANI-DBSA/DVB conductive thermosetting matrix is prepared and characterized for the use in mass production of PANI-based composites.

➢ Parametric study has been done to optimize for the best electrical and mechanical properties.

➢ Dedoping phenomenon of the PANI in the system is explained using various techniques.

➢ Improved electrical, mechanical and EMI shielding properties of hybrid nanocomposite has been reported.

Graphical Abstract

a) Initiation and growth reaction
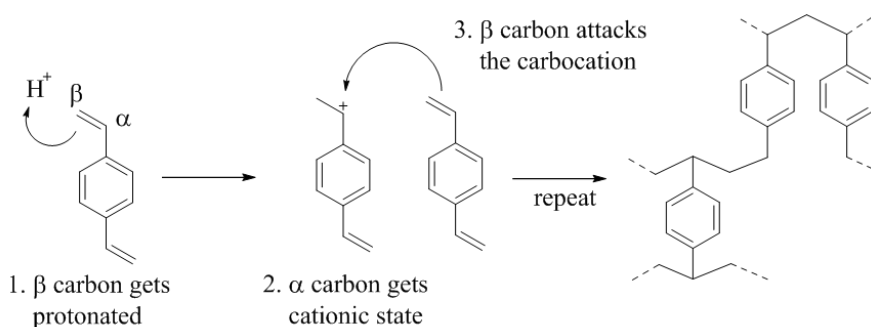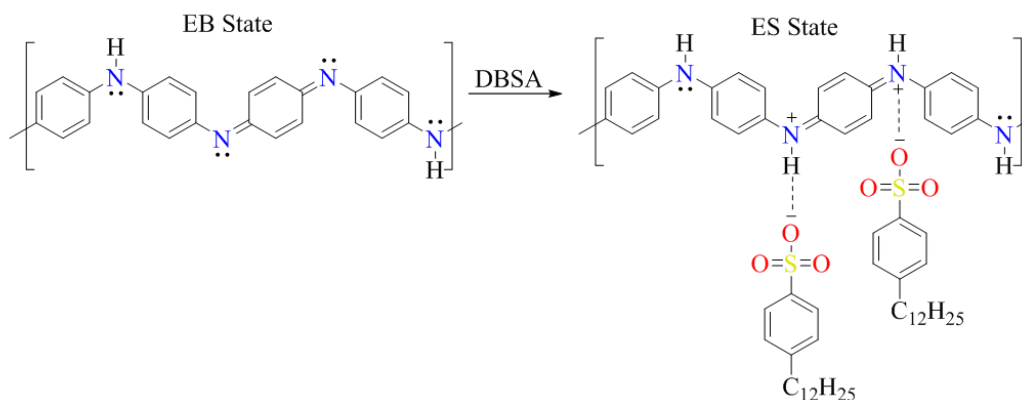
b) Terminal reaction

c) PANI Doping

Cationic polymerization of DVB polymer (a) Initiation and growth reaction (b) Terminal reaction (c) PANI doping.

Contents

PART I - Development of PANI-based conductive thermosetting matrix

PART I I - Structural applications of FRPs prepared by using conductive thermosetting matrix

List of Figures

List of Tables

Nomenclature

PANI - polyaniline

DBSA - dodecylbenzenesulfonic acid

DVB – divinylbenzene

CSA – camphor sulfonic acid

PTSA – p-toulenesulfonic acid

PM or CM – physically/centrifugally mixed

RM – roll-milled samples

CF – carbon fiber

CNF – carbon nanofiber

VGCF – vapor grown carbon fiber

LSP – lightning strike protection

TGA – thermogravimetric analysis

SEM – scanning electron microscopy

FTIR – Fourier transform infra-red spectroscopy

UV-vis-NIR – ultra violet-visible-near infrared spectroscopy

EMI – electromagnetic interference

SE – shielding effectiveness

NMP – N-Methyl-2-pyrrolidone

PART I – Development of the PANI-based conductive thermosetting matrix

Chapter 1   Introduction

In the last few decades aerospace industry has seen a gradual shift from metallic structures to composite structures. It is well known that saving on each kilogram weight in aero structures, accounts for huge fuel savings. Weight of the aircrafts become more significant during longer duration flights. As the major portion of aerospace industry is driven by economy, it was obvious to look for the material which is lighter and strong at the same time. Carbon reinforced plastic materials (CFRP composites) fulfil the aforementioned qualities. The use of composite material in the aerospace industry is increasing year by year. While composites have already been established in industry and academia, researchers are trying to find their multi-functional properties to further expand the application of this material[1]. Symbolic picture of composite uses in one of recent aircraft is shown in **Figure 1.1.**
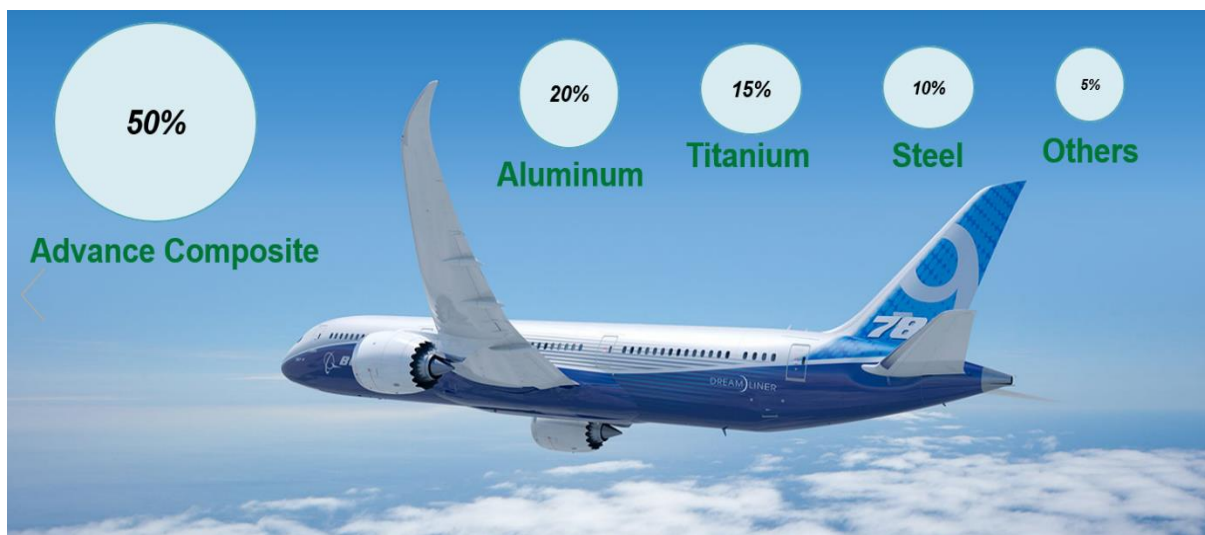
Figure 1.1 Use of composite material in Boeing 787 aircraft.
[Source: http://www.boeing.com/commercial/aeromagazine]

With the constant requirement of material with better strength and lower weight, research and development in the field of composite material has indeed come a long way. However, composites are mainly known for their structural applications but they still have a few major disadvantages. For examples loss of electrical properties of carbon fibers in the matrix. This loss of electrical conductivity of fibers can be attributed to the insulating behaviour of the conventional resins. Electrical conductivity of the CFRP composite are far lower than their counterpart metal structures. In the field of aerospace, electrical conductivity of the structures find their applications in electromagnetic interference (EMI) shielding[2] and also in protecting the structures from thunder lightning strikes[3]. Generally it is believed that a material with good electrical conductivity possesses good thermal conductivity as well. Therefore, electrical conductive structural composites are the most eligible candidate for multifunctional composites[4].

The most traditional way to prepare a conductive composite is to add conductive fillers in to the insulating matrices. Many researchers have tried to prepare conductive composite by adding a variety of conductive fillers like carbon black, carbon nanotubes (CNT), carbon nanofibers (CNF), graphene etc. Electrical conductivity from insulator-like behaviour to metal-like behaviour has been reported in the literature[5,6]. However, issues like poor process ability, complicated manufacturing process, expensive fillers are associated with the current traditional methodologies to prepare conductive composites.

These drawbacks in the traditional fillers compelled researchers to look for better and cheaper options. They found their desired material in form of intrinsically conductive polymers (ICPs)[6–8]. Conductive polymers are long repeated units which can conduct electricity upon doping. The existence of conductive polymers is known from mid-90th century, however ICPs gained their popularity when Alan J. Heeger, Alan MacDiarmid and Hideki Shirakawa reported very high electrical conductivity values of doped-polyacetylene[9]. They shared a Nobel Prize in Chemistry in 2002 for their contribution in this field. Since then ICPs are being researched extensively due to their remarkable property of tuneable electrical conductivity.

Huge number of conductive composite's applications are also being studied. For example, it was reported in literature that electrical conductivity of a conductive composite changes with

the application of load. This property gives a promising area of research to fabricate more sophisticated as well as strong piezo sensors[10,11]. Generally composites with good electric properties, possess good dielectric properties as well. Dielectric properties of conductive composite have also been investigated extensively[12–14]. Improved dielectric behaviour of PANI-based composites has been reported often[15].

Whenever, high electrical conductivity was reported, limited importance was given to the structural applications. To seek for a balance in electrical and mechanical properties for the structural applications in aerospace industries and due to the aforementioned difficulties in conductive polymer composite preparation, I gain motivation to start research in this exciting field.

In the present work, an attempt has been made to prepare & develop electrical conductive thermosetting polymer resin system which can be used to impregnate carbon and glass fibers to prepare conductive structural composites and look for their structural application in aerospace industry. To achieve these goals conducting polymer polyaniline (PANI), protonated with a dodecylbenzenesulfonic acid (DBSA) has been investigated. Divinylbenzene (DVB) is used as a cross-linked thermosetting polymer. Characteristics of each one and reasons for their choice have been explained in the following sections.

1.1 Conductive Polymers (ICPs)

A variety of different conductive polymers like poly(3,4-ethylenedioxythiophene) (PEDOT)[16], polypyrrolle[17] and polyaniline[18–20] are available in market and have been investigated by researchers. Conductive polymers have conjugated π-system (alternating single and double bond in the backbone chain) as shown in **Figure 1.2.**
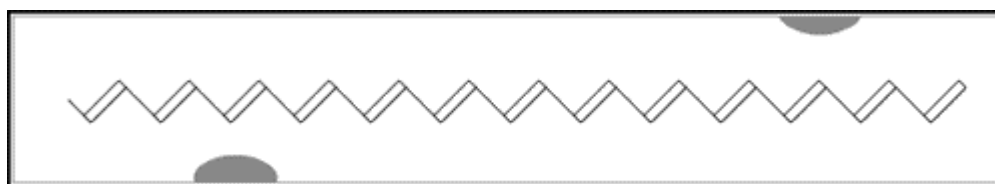
Figure 1.2 Conjugated π-system in conductive polymers.

When these conductive polymers interact with dopants, they undergo oxidation or reduction depending on the type of dopant used. Doping is the phenomenon of charge transfer from the dopant to the polymer chain either by removing electron from (oxidation), or inserting them (reduction) into the polymer chain. The introduction of these mobile charges into the conduction band of the π-system renders the polymer system conductive[21]. Charge carriers can be electrons or holes. These transferred charge carriers increase the number of mobile charges in the conduction band of the polymer chain and hence make it conductive[22]. Common electrical conductivity values of conductive polymers and some metals and semiconductor are shown in **Figure 1.3.**

Among all the conductive polymers, PANI gained popularity as one of the most studied intrinsic conducting polymer and has been studied most extensively among all ICPs due to its remarkable properties such as low cost, high thermal stability, environmental stability and controllable conductivity.
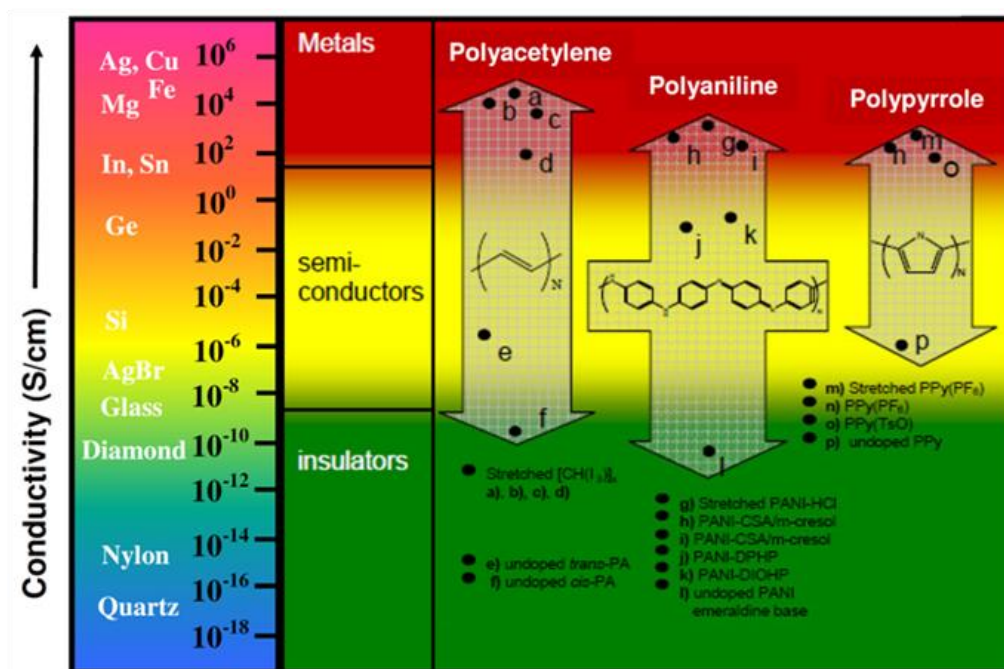
Figure 1.3 Conductivity of some of the most common conductive polymers compared to metals and semi-conductors[23].

1.1.1 PANI Structure

PANI is a cost effective polymer, polymerized from inexpensive aniline monomers. PANI can be found in one of the three different states: fully oxidized [(per)nigraniline], fully reduced [leucoemeraldine] and neutral state [emeraldine] as described in **Table 1.1** (n and m are denoted in **Figure 1.4**). These three states of PANI can be understood clearly from the basic structure of PANI. The basic structure of PANI has two parts namely amine links (reduced unit) and imine links (oxidized unit) as shown in **Figure 1.4.**

Reduced Unit (Amine)   **Oxidized Unit (Imine)**
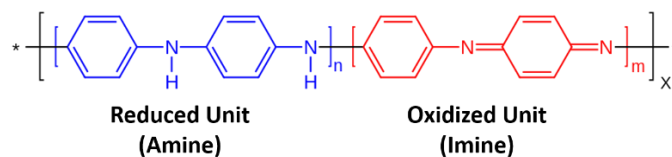
Figure 1.4 Structure of polyaniline (PANI)[24].

Table 1.1 Three different form of PANI and their characteristics[24].

Leucoemeraldine	Emeraldine	(Per)nigraniline
white/clear & colorless $(C_6H_4NH)_x$	green for the emeraldine salt, blue for the emeraldine base $([C_6H_4NH]_2[C_6H_4N]_2)_x$	blue/violet $(C_6H_4N)_x$
(n = 1, m = 0)	(n = m = 0.5)	(n = 0, m = 1)
fully reduced state	partially oxidized	fully oxidized state

1.2   Dopants

Dodecybenzenesulfonic acid (DBSA)[25], Hydrochloric acid (HCL)[26], camphorsulfonic acid (CSA)[27] and p-toulenesulfonic acid (PTSA)[28] are some the most widely used dopants for conductive polymers. Mohd. Khalid et al.[29] studied the doping of PANI with three different dopants and demonstrated preparation of self-assembled PANI in the presence of three different sulfonic acids namely camphorsulfonic acid, tetrakis(4-sulfonatophenyl)porphyrin and p-toulenesulfonic acid by polymerization technique using ammonium peroxydisulfate as

the oxidant. They showed that the electrical properties of PANI largely depends on the dopant used. They reported highest conductivity of greater than 100 S/cm in case of TSA-PANI. Trznadel et al.[30] studied the PANI-CSA doping in the presence of m-cresol. They reported a strong competition between solvent and dopant for doping with PANI. Long et al.[5] studied PANI-CSA and PANI-DBSA polyblends and explained electronic transportation in them. They compared the electrical and thermal properties of PANI-CSA/PANI-DBSA polyblends. Li and his partners[26] synthesized hydrochloric acid-doped polyaniline and reported the effect of acid concentration on the electrical conductivity and thermoelectric behavior of the HCL-doped PANI. However, among all the studied dopants, DBSA captured the major portion in research due to its remarkable ability to make PANI dispersible in common organic solvents.

1.2.1 DBSA Structure

The basic structure of DBSA has polar and non-polar head as shown in **Figure 1.5.** Dodecylbenezesulfonic acid is a bulky molecule with a polar head and a non-polar chain which functions as a surfactant as well as a dopant. The dodecyl group $CH_3(CH_2)_{10}CH_2$ is unbranched and attached to the 4th position of the benzene ring.
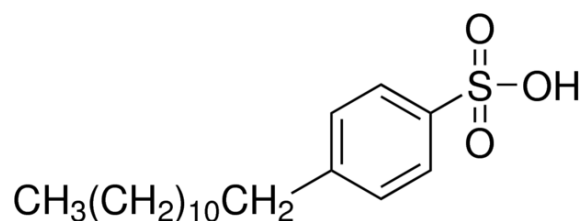
Figure 1.5 Basic structure of dodecybenzenesulfonic acid (DBSA).

Sodium dodecylbenzenesulfonate is a major component in the laundry detergent. Babazadeh[31] reported that the excess DBSA forms micellar formation and stabilizes the PANI-DBSA dispersion by creating strong hydrogen bonds within the PANI-DBSA system. Solubility of DBSA-doped PANI revolutionized the research in the field of conductive polymers. It was found that DBSA-doped PANI is soluble in many common organic solvents like toluene, m-cresol and xylene.

Moreira et al.[14] prepared epoxy/amine system containing polyaniline doped with DBSA. They reported two distinct exothermic peaks in differential scanning calorimeter. They suggested that the second peak is due to the curing of epoxy by PANI-DBSA present in the system. Similarly Patrick et. al.[32] patented their work in which they reported the resin system curing with acid catalysts like PTSA and DBSA. These results confirm that DBSA can also be used as curing agent for some polymers.

1.3   Matrices for PANI-DBSA complex

The PANI-DBSA complex are usually mixed with different insulating polymers like polyamides (PA), polystyrene (PS) and epoxy resin to prepare conductive polymer composites[33–36]. There are numerous studies trying PANI-DBSA system with different epoxies. Researchers tried different kind of epoxies to make a conductive thermosetting resin system[36–39]. Thermoplastic polymer matrices also have been studied extensively. Jeon et al.[40] used polycarbonate (PC) as a matrix to prepare PANI-DBSA/PC composites by using emulsion polymerization in which DBSA acts both as a surfactant and dopant. They reported the electrical conductivity of 10^{-2} S/cm of PANI-DBSA/PC composite with 13 wt. % of PANI. Other than solution blending technique, Zilberman et al.[41] used melt processing technique to prepare conductive blends of thermally DBSA-Doped PANI with thermoplastic polymers. They prepared PANI-DBSA/PS, PANI-DBSA/PE and PANI-DBSA/Co-PA blends by melt processing. It was found that with the same ratio of PANI-DBSA to matrix polymer, the electrical conductivity varied with different polymer matrix. Haba et al.[25] reported new PANI-DBSA/polymer blending via aqueous dispersion. They obtained PANI-DBSA/polymer blends by mixing an aqueous PANI-DBSA dispersion with an aqueous emulsion of the matrix polymer, followed by water evaporation. They reported the electrical conductivity of the composite at a very low PANI-DBSA content (0.5 wt. %). They achieved highest conductivity up to 10^{-2} to 10^{-3} S/cm at 4.5 wt. % of PANI-DBSA. In all aforementioned studies, researchers have reported the conductivity values ranging from 10^{-8} to 10^{-1} S/cm [42]. Some of the selected electrical conductivity results from literature are presented in **Table 1.2**.

Table 1.2 PANI-dopant combinations with different resin systems[42].

Fillers	Matrix	Curing agent	Conductivity (S/cm)
PANI-TSA	Epoxy system from bisphenol A	Cis-1,2,3,4-tetrahydrophthalic anhydride	10^{-8}-10^{-3}
PANI-CSA	Phenol novolac	BF_3-based Lewis acid	10^{-8}-10^{-3}
PANI-DBSA	Bisphenol A epoxy	Phthalic anhydride	0.118
PANI-DBSA	Epoxy resin with modifier	anhydride	10^{-16}-10^{-2}
PANI-DBSA	Bisphenol A epoxy	BF_3-complex	10^{-14}-10^{-7}

1.3.1 DVB as a matrix

In the conventional resin system, PANI could not achieve its highest potential due to the dedoping phenomenon. It was demonstrated by Tsotra et al.[43] that PANI system shows different conductivity with different hardener types. The dedoping of PANI ES can be attributed to such behavior. Therefore, it was proposed by our colleagues in Yamagata University to use DVB as a matrix due to its good compatibility with PANI ES system.

Divinylbenzene (DVB) is an aromatic monomer generally used as a cross-linking agent to improve polymer properties. Faster curing time, improved gloss of molded composite, improved chemical and physical properties were the deciding factors to choose DVB as a matrix. But the property to dissolve PANI-DBSA complex into DVB without any detrimental effect on PANI-DBSA doping state was the most crucial factor. DVB can be polymerized by cationic as well as radical polymerizations. Detailed polymerization mechanism is explained in the next section. Basic chemical structure of DVB monomer is presented in **Figure 1.6.**

DVB is often used to manufacture adhesives, plastics and ion exchange resins. At room temperature DVB is found in liquid phase with addition of some inhibitors to avoid self-polymerization.
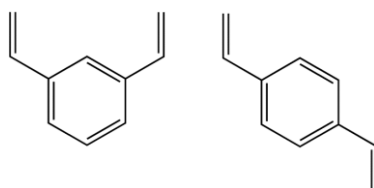
Figure 1.6 Basic structure of divinylbenzene (DVB monomer).

According to the Dow chemical company, only small amount of DVB is needed to improve both physical and chemical properties. DVB reacted with styrene can be used as a reactive monomer in polyester resins. Styrene and DVB form a cross-linking polymer S-DVB which is mainly used in production of ion exchange resins[44]. This is the most common known application of DVB monomers. However, in this work DVB is being used as whole matrix and not just as a curing agent.

1.4   Introduction of PANI-DBSA/DVB composite

1.4.1 PANI-DBSA doping phenomenon

The main problem associated with PANI was poor process ability of PANI both in melt and solution form. As mentioned in earlier section, EB form of PANI is insoluble in common solvents except a few, like the 1-methyl-2pyrrolidinone (MNP) solvent. This problem was due to the stiffness of PANI backbone. Heeger et al. reported that PANI doped with heavy functional protonic acids have better solubility and processability[45]. These acid with long tail can be used as dopants as well as surfactants in common organic solvents. After this discovery research on PANI-based polymer composites gained momentum.

The conductive emeraldine salt (ES) form of PANI can be obtained by doping emeraldine base (EB) form of PANI with a strong protonic acid. Protonic acids usually have a basic structure of $H^+(M^-R)$, where H^+M^- is a protonic group and R is an organic group. Example of such protonic acids are dodecylbenzenesulfonic acid (DBSA), hydrochloric acid (HCL) and camphorsulfonic acid (CSA)[45]. When the protons reacts with the imine links in the PANI chain, emeraldine base form of PANI changes to the emeraldine salt form, making the system

conductive. Simultaneously, R functional group enhances the solubility with common organic polymers[46]. PANI-DBSA doping has been shown in the **Figure 1.7**.
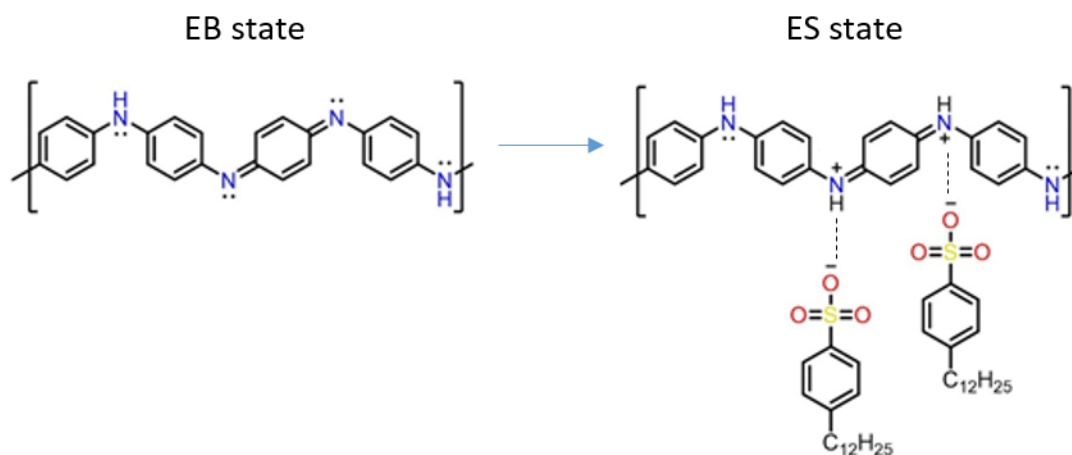
Figure 1.7 Change of PANI EB form in to PANI ES after doping with DBSA[47].

Different doping phenomenon, have been studied and compared in past. Haba et al.[48] reported new PANI-DBSA/polymer blending technique via aqueous dispersion. Goto et al.[49] studied the thermal doping without the application of shear.

1.4.2 Mechanism of DVB polymerization

Generally, DVB can be polymerized with cationic initiator as well as radical initiator. DVB can also self-polymerize by radical polymerization without initiator at high temperature. Therefore, inhibitor is usually added with DVB to avoid self-polymerization while storing. When DBSA reacts with DVB monomers a cationic polymerization takes place between them and a stable and highly cross-linked poly-DVB is formed. If the reaction is too fast and exothermic, it is very difficult to control the DVB polymerization. However, DVB can't undergo radical polymerization in doped PANI-based resin because doped PANI acts as a radical scavenger[50,51]. The initial step of cross linking polymerization is the protonation of the β carbon of DVB in presence of initiator (Strong protonic acid DBSA), subsequently α carbon of DVB forms carbocation in the cationic polymerization. The carbocation attacks the β carbon of another DVB monomer, and hence the reaction continues. The repetition of such protonation and propagation mechanism leads to the complete poly-DVB. The cationic reaction terminates

via the counter ion of DBSA[47]. The initiation, growth and terminal reaction of DVB polymerization can be seen in **Figure 1.8**.

a) Initiation and growth reaction
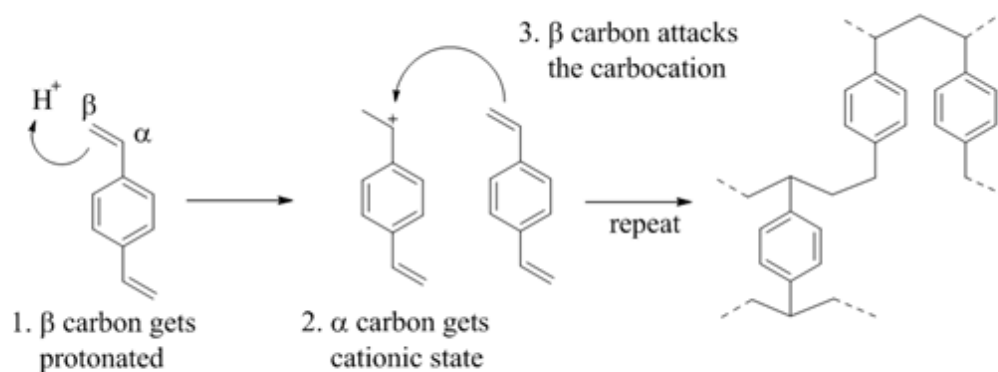
b) Terminal reaction
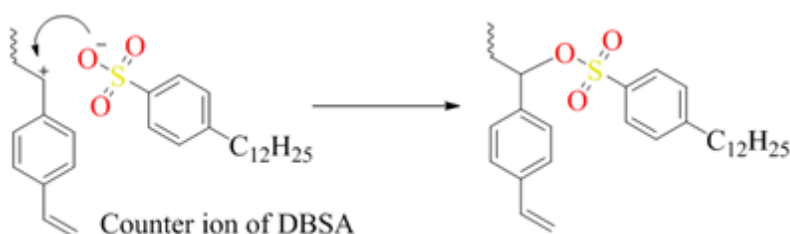
Figure 1.8 Cationic polymerization of DVB polymer (a) Initiation and growth reaction (b) Terminal reaction[47].

1.5 Unique one-step synthesis

In the past, different techniques have been used to fabricate conductive composites. Few of them have already been explained above, but it is further more interesting to know about the most common manufacturing techniques. Most known methods to prepare PANI-base conductive composites are emulsion polymerization[40], mechanical mixing[52], oxidative polymerization of absorbed PANI onto an insulating matrix[53] and casting from solution of Intrinsic conductive polymers i.e. ICPs and insulator polymer matrixes using solvents[34]. In the above mentioned manufacturing methods, generally two distinct steps are common i.e. doping (strong acid like DBSA, CSA as dopants) and curing (using curing agents). However, in the

present work a simplified one-step method to prepare PANI-based conductive composites, where doping of PANI and curing of the composite take place simultaneously, has been reported. This single step technique makes the manufacturing process really simple and hence save time and efforts. Graphical representation of this single step synthesis process of PANI-DBSA/DVB composite has been shown in the figure 1.9.
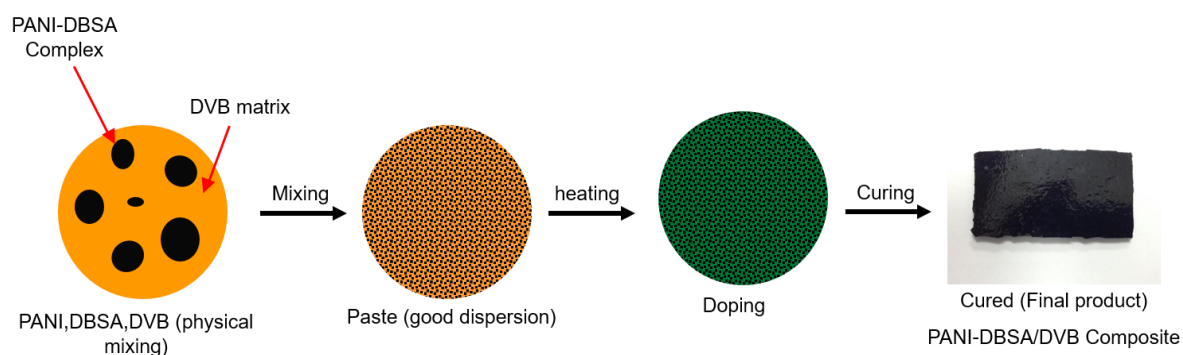
Figure 1.9 Scheme of single-step synthesis process of PANI-DBSA/DVB composite.

Divinylbenzene (DVB) has been used as a polymer matrix with PANI-DBSA mixture for the first time to prepare a conductive polymer composite[24]. Centrifugal mixing technique and roll-milling process have been used to prepare all mixtures. In the matrix system, DBSA acts both as a dopant and a curing agent, and therefore doping of PANI-DBSA and curing of the composite takes place simultaneously. A highly stable & densely cross-linked network of DVB matrix was formed when DBSA reacts with DVB. A cationic polymerization takes place between DBSA and DVB. Mixture of PANI-DBSA/DVB was cast molded to prepare composite samples. Finally, the electrical conductivity, mechanical properties and morphology of the prepared composites have been investigated.

1.6   Objective of the research

Objective of this research is to develop an environmentally stable conductive thermosetting matrix system which gives good electrical and mechanical properties after curing.

1. Optimization of PANI-DBSA molar ratio.
2. Parametric study of curing time and curing temperature.
3. Explaining doping and dedoping phenomenon.
4. Characterization of the PANI-DBSA/DVB composites using different techniques (UV-vis-NIR, FT-IR, SEM, Thermal Microscope, TGA, DSC).
5. Preparation of PANI-based thermosetting polymer composites.

Use this matrix to prepare conductive FRPs, which can be used for various structural applications. Two main application have been listed in the present thesis.

1. Preparation of CFRP and GFRP using PANI-DBSA/DVB matrix.
2. Application as EMI shielding material.

1.7   Discussion

The importance of the need of a highly conductive thermosetting composite was highlighted in this chapter. Brief introduction to literature was presented. PANI, DBSA and DVB were introduced and their individual properties were explained. Vast pools of ICPs, dopants and different matrices are available. The choice of these material was not mere a chance. Properties and reasons of choice of each component of the proposed system were explained.

DBSA is the main multifunctional material in our conductive system. It acts as a dopant for PANI, surfactant for the complex and curing initiator for the DVB matrix. Optimum DBSA content in the system is very critical for the overall improved properties of the composite. Ability to dissolve PANI-DBSA complex and polymerized by a protonic acid were the main factors to choose DVB as matrix.

Doping of PANI-DBSA and curing of DVB were explained using chemical reactions. Cationic polymerization of DVB was presented, however radical polymerization of DVB is also a known fact. Therefore, it can be inferred that in this system both types of polymerization could exist. Unique one-step synthesis of PANI-DBSA/DVB composite was explained. The hypothesis of this one-step synthesis process is unique in this research and opens up new opportunities of PANI related research.

We have used thermal doping technique in this work. However, PANI has shown much higher electrical conductivity with in-setu polymerization technique with other dopant. Therefore, a small compromise was made to make the manufacturing technique fast and simple. Objective of this research was also explained briefly in this chapter in which high electrical conductivity, mechanical properties and applicability of the matrix were targeted.

Chapter 2   Characterization of material

In this work, different material characterization techniques have been used extensively. Therefore before going to the experimental section, it is important to understand the materials and their characterization techniques.

2.1   Materials

PANI in emeraldine base (EB) form was procured from Regulus Co. Ltd. DBSA was supplied by Kanto Chemical Co. Ltd. and DVB was obtained from Sigma-Aldrich Co. All of the materials were used as received without any further purification or modification. VGCF-H was supplied by Showa Denko, Japan and used as received. Conductive adhesive silver paste DOTITE used for electrical conductivity measurement was procured from Fujikura Kasei Co. Ltd.

2.2   Measurements

The most common measurements in this research were electrical and flexural properties measurement of the composite samples. DC electrical conductivity of the samples were measured and reported unless specified. For PANI related researches, UV-vis-NIR and FT-IR spectroscopy plays an important role. Similarly for studying the morphology of the PANI-based conductive system, SEM and optical microscope were used. In this work, images were also obtained w.r.t the thermal treatment using an optical microscope. Thermal stability of the prepared polymer composites was investigated by TGA analysis.

2.2.1 Electrical Conductivity

DC electrical conductivity of the samples was measured using LCR meter (3522-50 LCR HiTESTER, Hioki E.E. Corporation) by four probe method as shown in **Figure 2.1**.

4-probes method to measure electrical conductivity is more accurate and simple compared to usual two-terminal measurement. In 4-probe method two separate pairs of current-carrying and voltage-sensing electrodes are used. In this method, constant voltage of 1 Volt was applied and drop of current and voltage were measured using highly precise ammeter and voltmeter respectively to calculate the resistance of the samples by Ohm's law ($R = V / I$) using LCR meter. The resistivity ρ, of uniform cross section can be computed as $\rho = RA/l$, while $\sigma = 1/\rho$, where l is the length of the sample, A is the cross-section area of the sample, σ (sigma) is the electrical conductivity and ρ (rho) is the electrical resistivity of the material.[47] Following procedure was employed to measure the electrical conductivity.

Procedure:

1. Use abrasive to clean the surface of the sample.
2. Clean the sample properly using ethanol.
3. Measure the dimensions of the sample using screw gauge.
4. Apply DOTITE conductive adhesive paste on the measuring sides with proper care.
5. Attach conductive tape on both sides to measure the resistance using 3522-50 LCR HiTESTER machine.
6. Dry DOTITE completely using furnace (by keeping sample for 15 min. at 45ºC).
7. Ensure proper connection of the conductive tape with the sample & probes of 3522-50 LCR HiTESTER machine.
8. Note the value of resistance appeared on the screen.
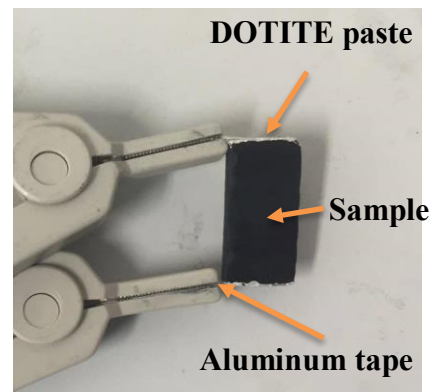
(a)   (b)

Figure 2.1 (a) 3522-50 LCR HiTESTER machine (b) Electrical conductivity measurement.

2.2.2 Mechanical properties

The flexural properties of the samples were measured using Universal Testing Machine (Instron-5582) by three-point bending method as shown in **Figure 2.2**. ASTM D790-02 standard test method for flexural properties of unreinforced plastics and electrical insulating material was followed. Three-point bending test was performed using a load cell of 5 kN and crosshead speed of 1 mm/min. The radii of loading nose and supports were kept at 5 mm. The total length, width and thickness of samples were taken as length 50 mm, width 12.5 mm and thickness 2mm, respectively. While the span distance was taken as 32 mm. If there was any change in the thickness of the sample due to manufacturing process, the thickness to span ratio of 1:16 was kept constant in case of unreinforced samples. For FRPs specimen testing, size of the samples were taken as length 100 mm, width 15 mm and thickness 2.5 mm, respectively. Span distance was taken as 80 mm. If there was any change in the thickness of the sample due to manufacturing process, the thickness to span ratio of 1:32 was kept constant in case of FRPs.

(a)   (b)
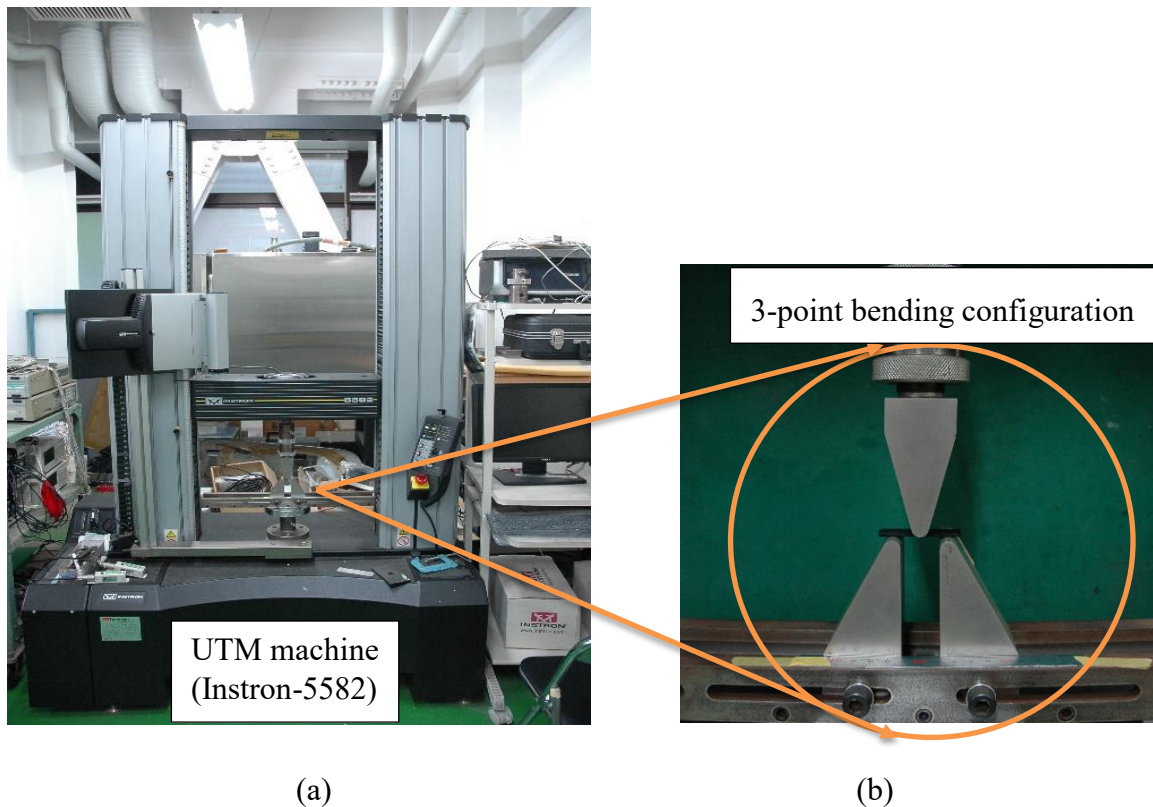
Figure 2.2 (a) UTM machine (Instron-5582) (b) 3-point bending configuration for flexural testing.

2.3   Material characterization

2.3.1 UV-vis-NIR spectroscopy

UV-vis-NIR is one of the most important tool to understand the behaviour of PANI-based composites[54]. Doping level, conductivity behaviour, chain conformation (coiled or stretched) and many other such properties can be studied and analyzed using UV-vis-NIR spectroscopy[55]. UV-vis-NIR analyzer (U-4100, Hitachi High Technologies Corporation) was used in this work. Sample preparation, sample holder and the UV-vis-NIR analyzer are shown in **Figure 2.3**.
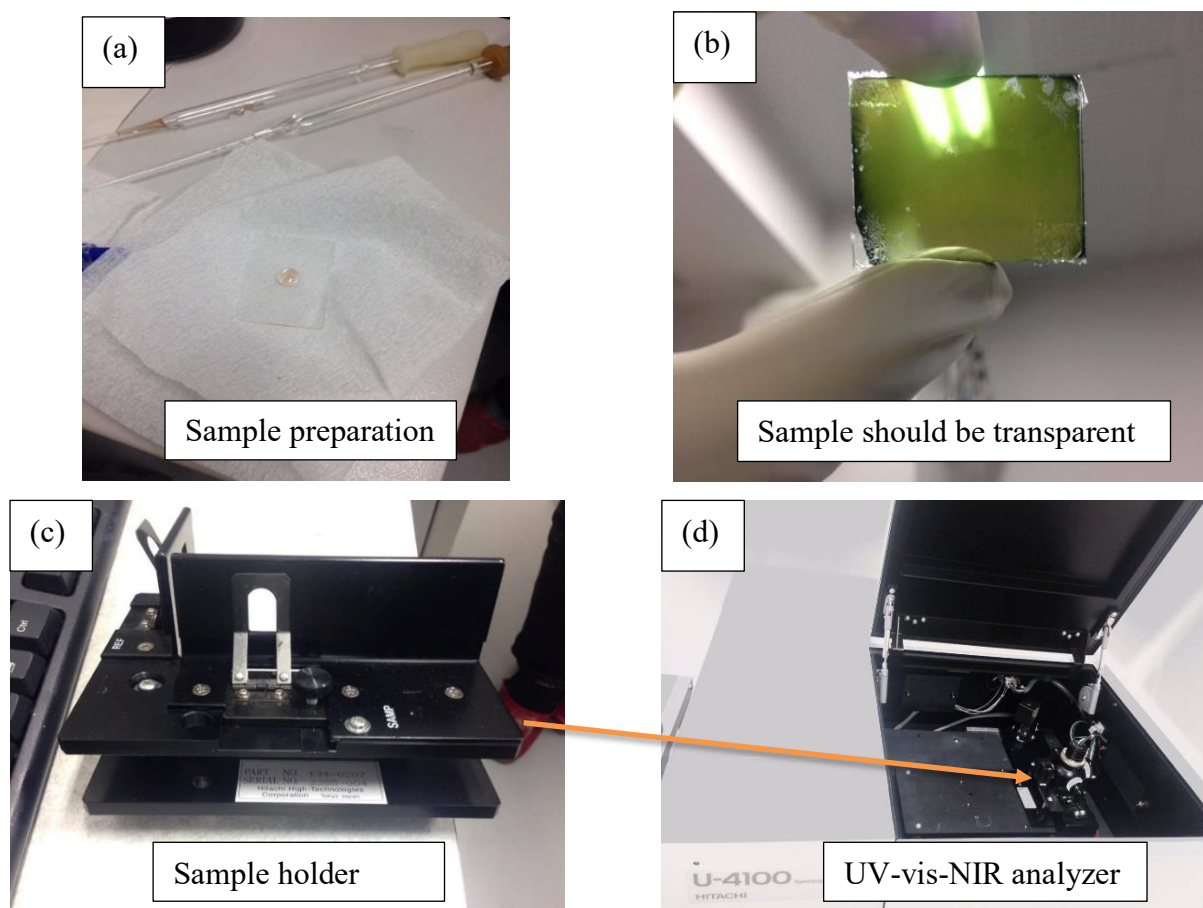
Figure 2.3 (a), (b) Sample preparation (c) sample holder (d) UV-vis-NIR analyzer (U-4100, Hitachi High Technologies Corporation).

UV-vis-NIR spectroscopy refers to the absorbance or reflectance spectroscopy of the samples in the UV, visible and near infra-red region. Perceived color of the chemical involved affect

the reflection and absorption in the visible range. A standard spectroscope measure the transmittance of the incident wave in percentage (%T). Calculated transmittance can be used to obtain absorbance.

Sample to be measured was put between glass substrates. Viscosity of the measuring sample should be low enough to allow incident wave to transmit through it. Additional solvent (toluene) was added in case of very viscous samples like PANI-DBSA complex. It was then put into the sample holder. The UV-vis-NIR spectra from 350 nm to 2600 nm range was recorded.

2.3.2 FT-IR spectroscopy

FT-IR spectroscopy is usually used to understand the molecular structures of materials and therefore FT-IR spectroscopy analysis is essential for a new material system. FTIR is also very helpful in the study of conducting polymers because of the ability to measure the FT-IR spectra of a material in any of the following forms, liquid, paste or solid. FT-IR can also be used to obtain the degree of doping and determining any change in the molecular structure of PANI after doping[56]. FT-IR analyzer and ATR sample holder is shown in **Figure 2.4**.

(a) FT-IR analyzer
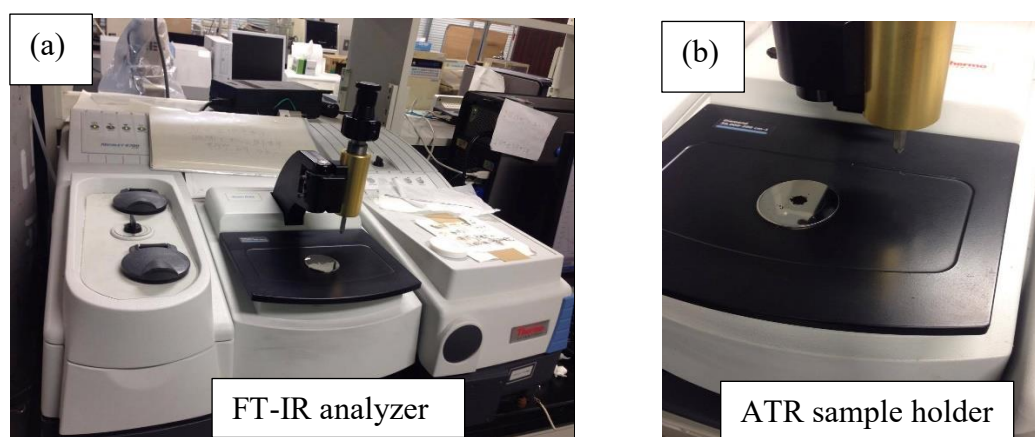
(b) ATR sample holder

Figure 2.4 (a) FT-IR analyzer (NICOLET 6700, Thermo Scientific Corporation) (b) ATR sample holder with diamond prism.

FT-IR is a vibrational spectroscopy technique which takes advantage of asymmetric stretching, vibrations and rotation of chemical bonds as they are subjected to different wavelength of light. Absorption peaks in an infrared absorption spectrum arise from molecular vibration. Pattern of

vibration is unique for a given molecule. FT-IR spectra was investigated using FT-IR analyzer (NICOLET 6700, Thermo Scientific Corporation) in this work. The spectra were measured in the range of 600-4000 wavenumber (cm^{-1}).

2.3.3 Thermal optical microscopy

The morphology of the samples w.r.t increasing temperature was studied using optical microscope (Olympus-BX50) connected to heating plate system. The heating plate temperature could be controlled using a temperature control device and the heating rate could also be varied according to the requirement.
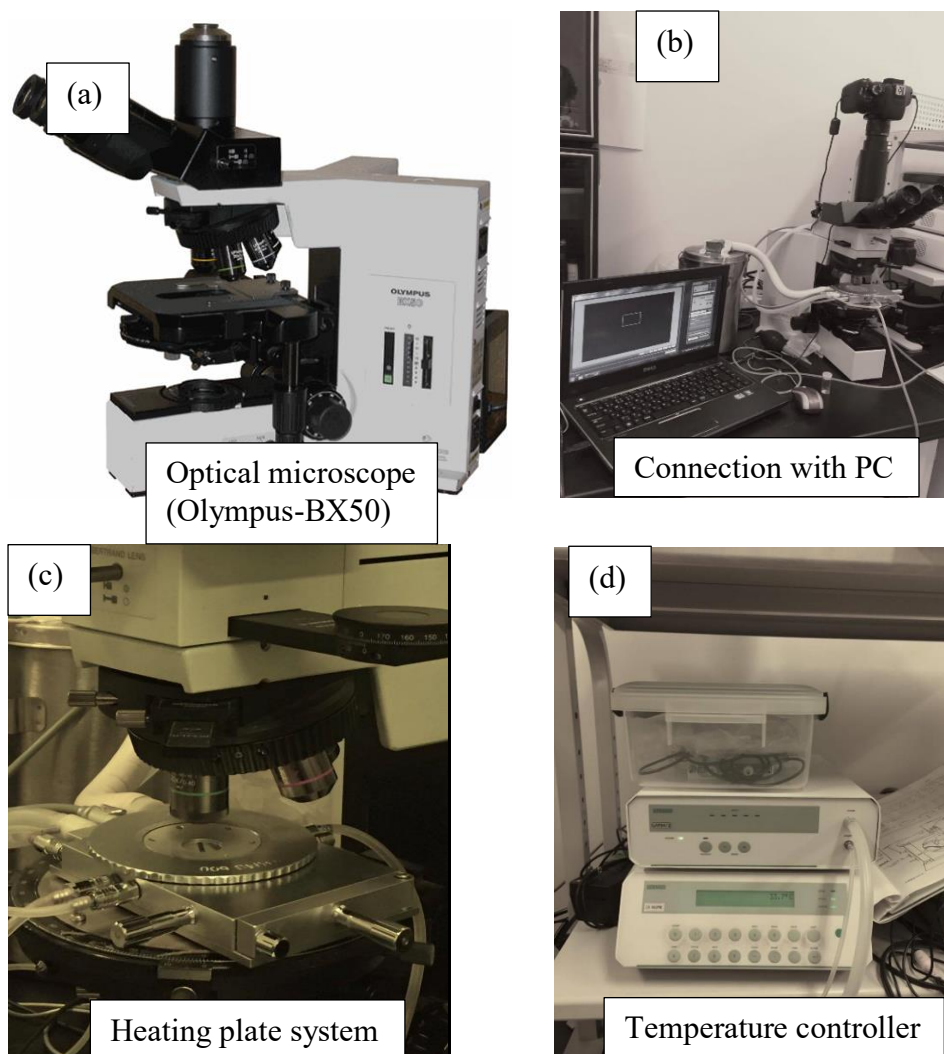
Figure 2.5 (a), (b) Optical microscope (Olympus-BX50) connected with PC (c) Heating plate system (d) temperature controller.

To observe the optical images, a small amount of sample was placed on the glass slide, and a cover slip was pressed firmly on top. Prepared glass slides with sample was further placed on the hot plate, having a small hole for transmitting light. We used temperature increment of 10 °C/min up to 180 °C and images were obtained during the heating process. With the images obtained from thermal optical microscope, doping and curing temperature of PANI-DBSA/DVB system were analyzed. Different components of the system are shown in **Figure 2.5**.

2.3.4 SEM analysis

It is well known that the morphology of PANI structure plays a significant role in its overall behaviour. We have used several different techniques to make PANI-based samples with different amount of DVB and different molar ratios of PANI and DBSA. Therefore, morphological study of PANI-based composite is very important to understand its conductive and structural behaviour. Microstructure of PANI has been studied using scanning electron microscope (SEM) images and correlation between mechanical properties, electrical properties etc. were investigated. A scanning electron microscope scans a focused electron beam over a surface to create an image. Secondary electrons emitted by atoms excited by the electron beam are detected and processed to obtain the surface topology of the sample. In this work, morphology of the samples were studied using the SEM (JSM-6700F, JEOL Ltd.). Other components of the machine are shown in **Figure 2.6**.

(a)

SEM (JSM-6700F, JEOL Ltd.)
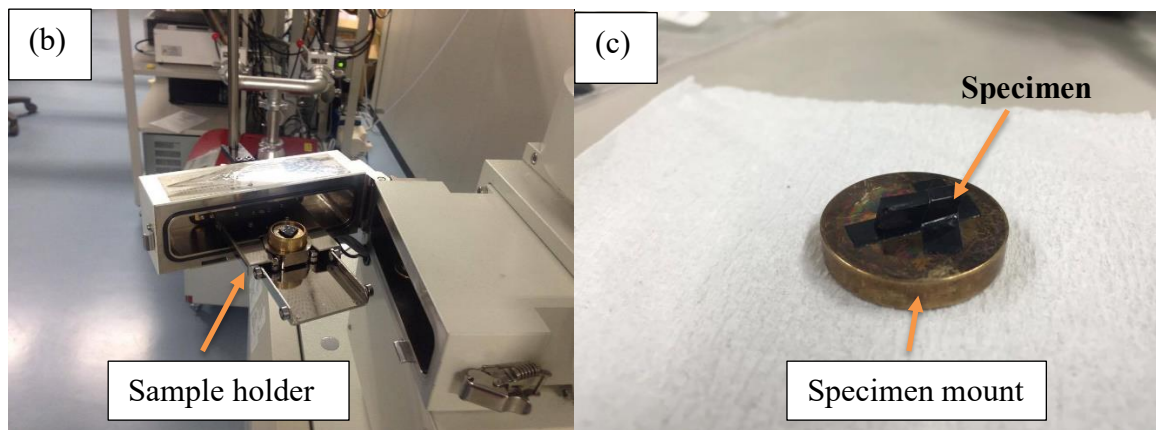
Figure 2.6 (a) SEM analyzer (JSM-6700F, JEOL Ltd.) (b) Sample holder (c) specimen mount.

2.3.5 TGA analysis

Thermal stability analysis of materials in aerospace industry is really important due to change in temperature during flight and taxing. In order to test the ability of PANI-DBSA/DVB matrix system to prepare FRPs for aerospace applications, it becomes necessary to know the thermal behaviour of this material system. Thermogravimetric analysis is the technique to measure change in weight of the material as a function of temperature. Thermogravimetric analysis can be used to determine the thermal stability of polymers, its moisture content, and volatiles or other impurities present in the material. The basic principle of TGA is the measurement of weight change in the sample compared to reference weight. TGA analysis operates on null balancing principle with a sensitive balance maintaining a reference weight for comparison. Thermal stability of PANI-DBSA/DVB cured composite with different DVB concentrations was studied using TGA analysis (SDTQ600, TGA Instrument) up-to 600°C with heating rate of 10°C/min in nitrogen atmosphere. However, PANI is highly thermally stable, therefore in case of pure PANI sample heating was done up to 800 °C. The effect on the change in the thermal stability of the composite system with the addition of DVB was determined and the effect of doping ratio on thermal stability and some other parameters were investigated and analyzed. Symbolic images of TGA analyser and its sample holder are shown in **Figure 2.7**.
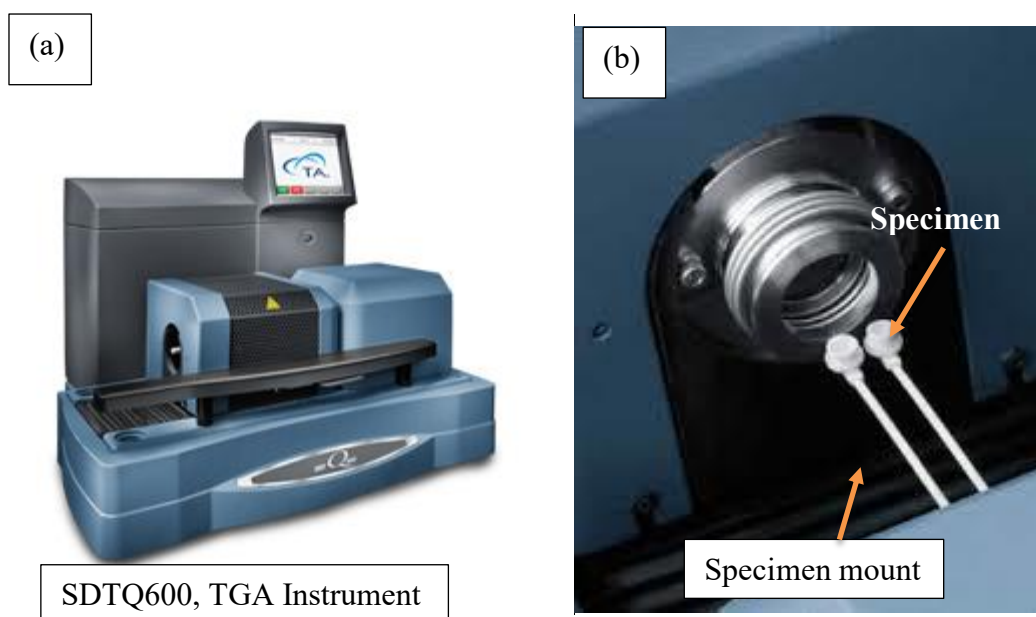
Figure 2.7 (a) TGA analyzer (SDTQ600, TGA Instrument) (b) Specimen mount.

2.4   Discussions

Since the discovery of polyaniline, they have been under development phase. Many industries are trying to manufacture different and heavy molecular polyaniline. With these constant phase of development, PANI available today has better quality compared to past. Therefore, for a new material system it was utmost important task to characterize it with different analytical techniques. In this chapter materials used in this research are listed. Different characterization techniques are explained with working principles. Electrical and mechanical property measurement procedures are the most used experiments in present work and therefore a detailed explanation has been provided. Sample preparation techniques are also explained in brief.

Chapter 3   Optimization of PANI-DBSA

Manufacturing the PANI-DBSA/DVB composite was optimized and therefore a thorough parametric study was required to obtain the best results. PANI-DBSA complex cannot be directly added to the DVB due to the fact that DBSA reacts with DVB immediately to start an uncontrollable exothermic reaction. **Figure 3.1** shows a real-time curing upon simply mixing PANI-DBSA and DVB.
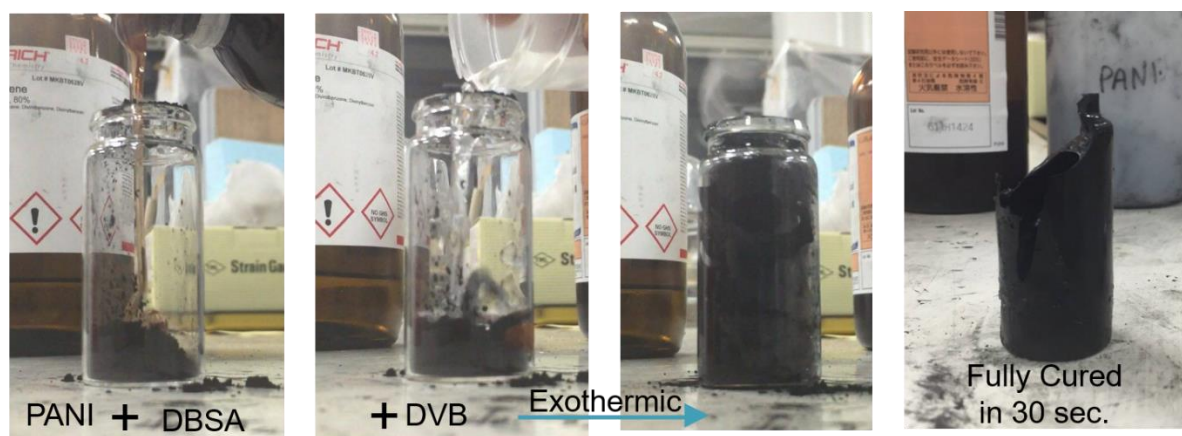
Figure 3.1 Real time exothermic reaction between DBSA and DVB.

As shown in the figure the mixture of PANI-DBSA/DVB stayed in liquid form for a very short time, for approximately 30-60 sec before curing of DVB started. Due to this problem preparation of any polymer composite sample or using this mixture for impregnating FRPs was impossible. The content of DBSA in the system is the most critical for both electrical and mechanical properties. The ideal molar ratio for PANI and DBSA to achieve maximum conductivity has been studied in literature. Different molar and weight ratios were suggested[57]. The molar ratio of PANI: DBSA also depends on the type of doping. For thermal doping Zheng et al.[58] proposed 1:3 wt. % ratio of PANI: DBSA. However, there have been immense improvements in the manufacturing of PANI from aniline monomer since then. At present much better quality of PANI is available. Therefore, it was the first important task to determine the best doping temperature, doping time and doping ratio for PANI: DBSA again.

3.1 PANI: DBSA doping temperature

To know the best thermal doping temperature of PANI, experimental and analytical method has been used. Three doping temperatures were used (80°C, 100°C and 120°C). Electrical conductivity value w.r.t doping time has been shown in **Figure 3.2**.
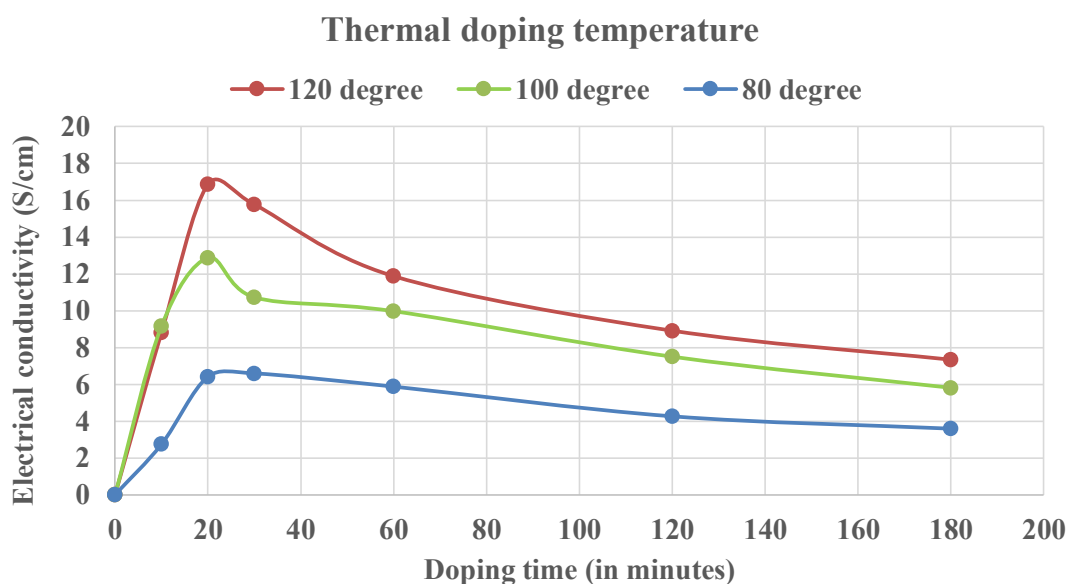
Figure 3.2 Effect of thermal doping temperature on electrical conductivity.

It can be observed from the plot that in all case PANI-DBSA achieved its highest conductivity values after some time after which there was reduction in the conductivity values. This phenomenon could be assigned to the doping and dedoping of PANI-DBSA after being subjected to thermal treatment w.r.t. time. However, it can be seen from the plot that PANI doped at 120 °C reached highest conductivity which can be attributed to the complete thermal doping of PANI-DBSA. At lower temperature, complete doping of PANI couldn't be achieved even after prolonged heating at the same temperature. On the other hand it is also observed that the reduction in electrical conductivity is sharper at 120°C than those with lower temperatures. Therefore, we can confirm that dedoping effect is more prominent at higher temperature but even after dedoping the conductivity value is higher than the highest conductivity values at lower temperature. Therefore, it can be understood from the results that 120°C is optimum

temperature for quick and best conductivity. However, dedoping phenomenon needs be addressed to achieve best electrical conductivity at elevated temperature.

3.2 PANI: DBSA molar ratio

DBSA used in this research is supplied by the KANTO CHEMICAL CO. INC. We used it as received. Formula weight of the DBSA is 326.49. Similarly PANI in emeraldine base form was procured from REGULUS CO. LTD. Formula weight of Aniline is 93.6.

PANI EB was mixed with different amount of DBSA in a centrifugal mixer to form 1:0.4, 1:0.5, 1:0.6, 1:0.7 and 1:0.8 molar ratios of PANI: DBSA. All the complexes were put in mould of size thickness 2 mm, width 12.5 mm and length 25 mm. Mould was further put in a hot press machine for thermal treatment. PANI: DBSA complexes with different molar ratios were prepared and heated for 20 min or longer at 120 °C. The electrical conductivity of the prepared complexes were measured at DC frequency using LCR meter. Highest conductivity of each sample was recorded and shown in figure 3.3. Same samples were further subjected to thermal treatment at 120°C for different time intervals (20, 30, 45, 60,160 and 120 minutes) as shown in figure 3.4.
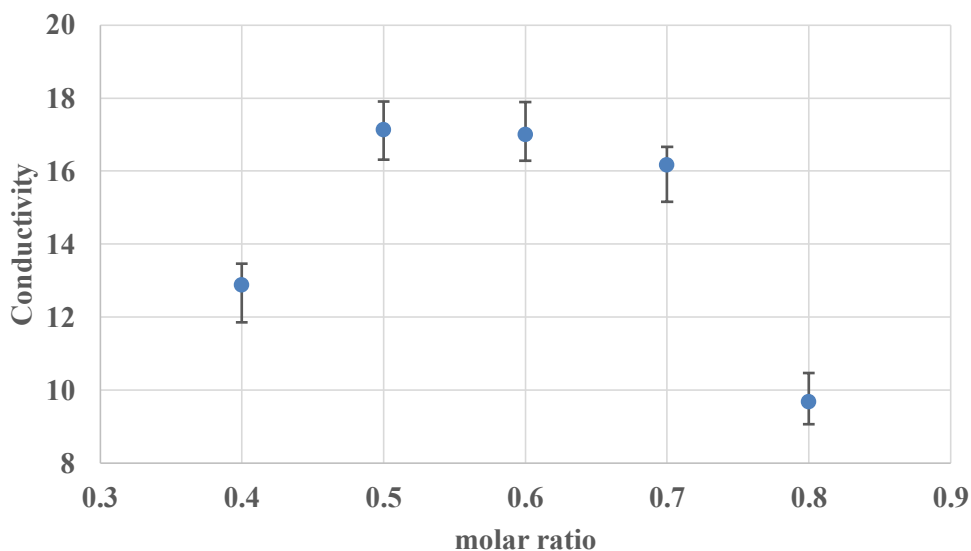
Figure 3.3 Highest electrical conductivity with different PANI-DBSA molar ratios.
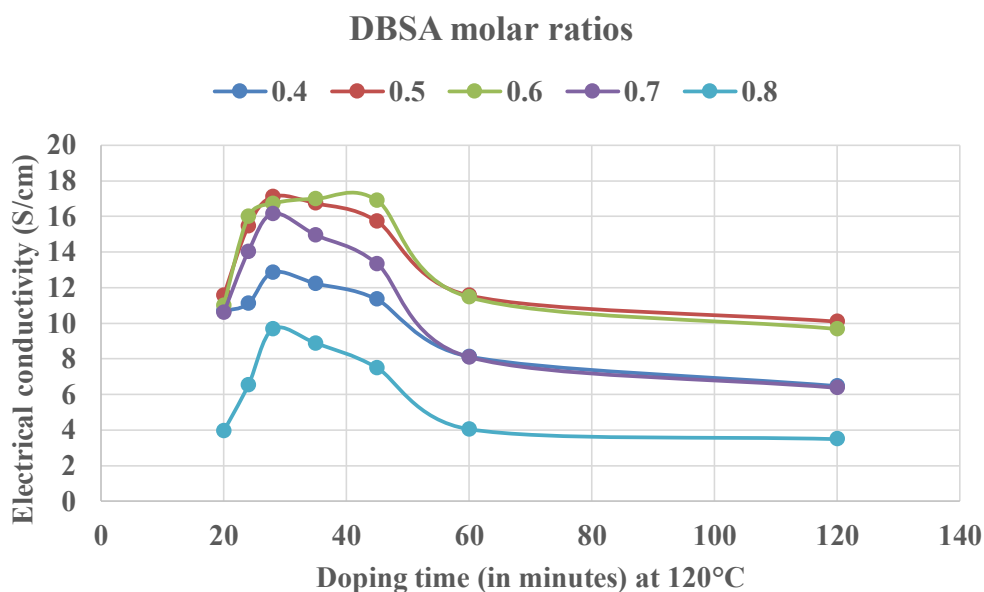
Figure 3.4 Electrical conductivity of different PANI-DBSA molar ratios w.r.t doping time.

Maximum conductivity between 20 minutes and 30 minutes was achieved in most of the cases. A sharp decrement in electrical conductivity was observed after 40 minutes of thermal treatment at 120°C. From this study we could confirm that PANI DBSA ratio 1:0.5 is the least requirement for the complete doping of PANI. DBSA with molar ratio 0.8 showed very low electrical conductivity. Excessive DBSA in the system is not good for the following reasons.

1. It can be seen from the plots that the excess DBSA does not contribute to the conductivity of the system and therefore, acts as an impurity in the system.
2. As mentioned earlier, free DBSA protons are responsible for the fast exothermic reaction and curing of DVB. Hence, more the amount of DBSA proton in the system lower would be the liquid state duration of the PANI-DBSA/DVB matrix.

3.2.1 Effect of excessive free DBSA protons

As explained in the section 1.4.2 (Mechanism of DVB polymerization), the initial step of cross linking polymerization of DVB is the protonation of β-carbon of DVB in presence of an initiator (Strong protonic acid DBSA), subsequently α-carbon of DVB forms a carbocation in the cationic polymerization. The carbocation attacks the β-carbon of another DVB monomer,

and hence the reaction continues. The repetition of such protonation and propagation mechanism leads to the complete poly-DVB. Therefore, free DBSA protons are required for initiation of DVB polymerization.

The more the number of free DBSA protons available in the system, more would be the chain initiation sites of DVB polymerization. More initiation sites will result in fast exothermic reaction of DVB unless there's a restriction in the amount of free DBSA proton available to start such a reaction. Therefore, the manufacturing process of PANI-DBSA/DVB composite is to be considered very carefully.

3.2.2 UV-vis-NIR spectra of PANI-EB

UV-vis-NIR spectra is a very interesting technique to observer the electronic structure of PANI based systems. UV-vis-NIR spectra of pure PANI EB powder dissolved in NMP (0.1 wt. % of PANI in NMP solution) were observed over the wavelength of 350-2600 nm. Measurement methodology presented in section 2.3.1 (UV-vis-NIR spectroscopy) was followed.

Solution of PANI EB powder dissolved in NMP was poured in to a glass substrate and spectra were measured at room temperature. **Figure 3.5** shows the UV-vis-NIR spectra for undoped PANI EB powder dissolved in NMP.
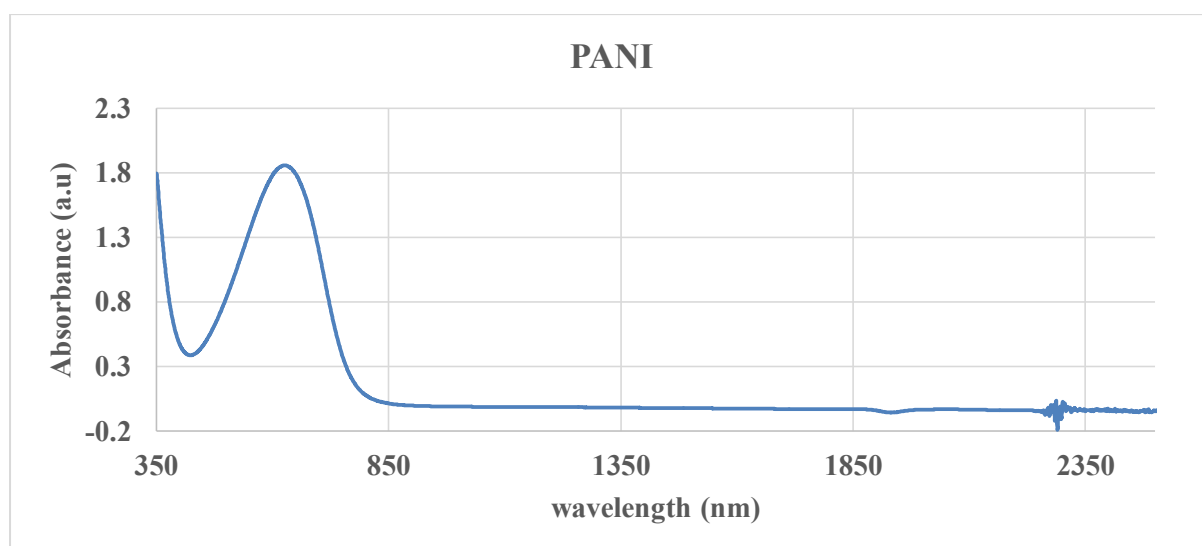
Figure 3.5 UV-vis-NIR spectra of PANI EB dissolved in NMP.

All the characteristic peaks of PANI EB form reported in literature can be observed in this plot[20]. To understand the behaviour of Emeraldine salt spectra, analyzing the spectra of Emeraldine base is important. From literature it is well known that two characteristic peaks of undoped PANI i.e. EB - Emeraldine base dissolved in NMP are present at around 325nm and around 629 nm. Due to the limitation of spectroscopy analyzer we could measure the spectra only in the range of 350-2600 nm. Usually, peak at 325 nm corresponds to the to the $\pi \rightarrow \pi^{*}$ transition of benzenoid amine ring. This peak is partially visible in the plots. The second peak at 629 nm is assigned to the $\pi_B \rightarrow \pi_Q$ excitation absorption in the quinoid imine ring. Both the characteristic peaks are present in our plots which confirm that the PANI was in its emeraldine base (undoped state) at room temperature.

3.2.3 UV-vis-NIR spectra of PANI-ES

For measuring the UV-vis-NIR spectra of doped PANI-DBSA complex, the sample was first put between two glass plates to make a sandwich-like structure at room temperature. These samples were subjected to heat for 0 min, 10 min, 1 hour and 2 hours. Spectra was taken after each thermal treatment. **Figure 3.6** shows the UV-vis-NIR spectra of roll-milled PANI-DBSA complex w.r.t. thermal doping time. It can be seen clearly from the plots that the characteristic peaks of undoped PANI vanished and new peaks at 380 nm and 800 nm appeared just after 10 minutes of thermal treatment. These peaks indicate the change in the electronic structure of PANI EB form into PANI ES form. First peak at 400 nm is attributed to the protonation of PANI backbone. When peak at 325 nm, that corresponds to the $\pi \rightarrow \pi^{*}$ transition of benzenoid amine ring overlaps with the characteristic peak of DBSA at 420 nm, it forms a flat and/or distorted single peak indicating high level of doping. Single flat peak attributed to the attachment of PANI and DBSA. Second peak in case of ES is present at 800 nm. This peak is attributed to the localized charge carriers or localized polarons. In its normal form PANI has a coiled structure which gets extended after doping. Absorption after 1000 nm can be assigned to the expanded coil-like structure of PANI after thermal doping[55]. UV-vis-NIR plots show that pure PANI-DBSA changes is electronic structure at 120 °C, but not completely and also do not lose its all electrical conductivity value up to 2 hrs of thermal treatment. Therefore, it second

our earlier assumption that 120 °C is an optimum temperature of thermal doping of PNAI-DBSA.
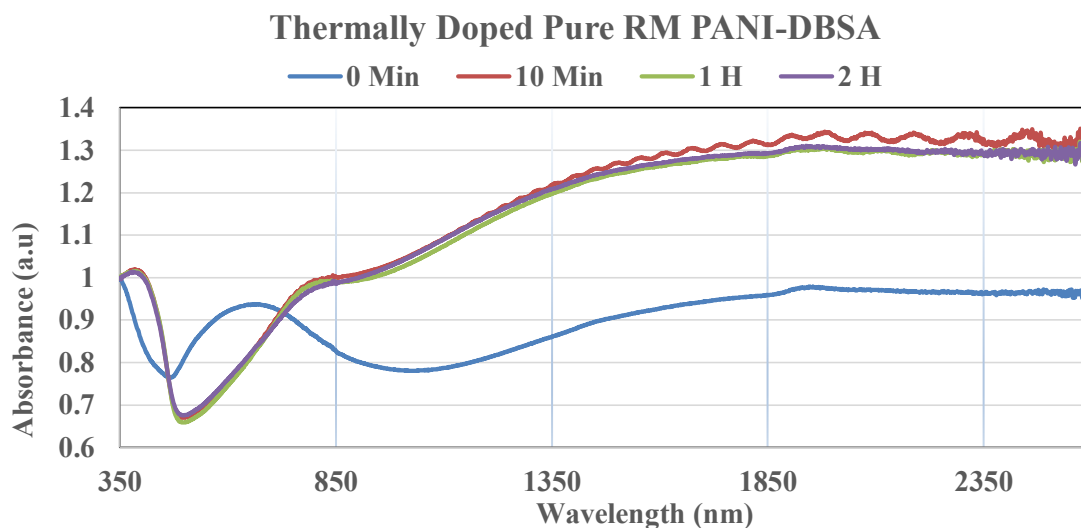
Figure 3.6 UV-vis-NIR spectra of RM PANI-DBSA complex at different thermal treatment time.

3.2.4 FI-IR spectra of PANI, DBSA and PANI-DBSA

FT-IR analysis is also an important tool to understand the change in chemical structure of a material. FT-IR spectra can be used to identify chemical bonds, functional groups and the components of unknown sample mixtures. As explained in the chapter 2, every single wavelength of light absorbed is characteristic of some specific chemical bonds. FT-IR spectra analysis of pure PANI EB powder, pure DBSA and PANI-DBSA complex were performed to determine any chemical structure changes after mixing and upon application of heat. Description of the main peaks related to PANI and DBSA are presented in **Table 3.1.** It can be seen that all the characteristic peaks of PANI-DBSA are present in the PANI-DBSA complex prior to the heat application and some new peaks are formed after doping. Therefore it can be confirmed that PANI and DBSA attached successfully to each other[47].

Figure 3.7 shows FT-IR spectra of pure PANI EB powder, pure DBSA and doped RM PANI-DBSA complex in one plot. Main characteristic peaks of PANI are C-C stretching of benzenoid and quinoid peaks at 1500 and 1590 cm^{-1}. Peaks at 1300 cm^{-1} can be assigned to the C-N stretching of 1,4 disubstituted benzene rings. Peaks at 1160 cm^{-1} is associated with (N=Q=N)

mode similar to the one reported in literature[15,56]. Peak at 829 cm^{-1} in spectra of DBSA is assigned to the C-H out of plane vibration of benzene ring. This peak is trademark peak of sulfonic acid group and is consistent in RM PANI-DBSA complex too. Broad peak at very high wavenumbers around 3200 cm^{-1} in PANI spectra is due to the N-H stretching in polyaniline. From the figure, it can be observed that DBSA has been attached to the PANI chain successfully. Amplitude of the absorbance unit have been modified for the comparison purpose within the same plot. Peak shifts and change in intensity ratio of benzenoid ring and quinoid ring are very useful techniques to quantify the doping extent and doping ratio. FT-IR has been used quite often in this research to find the most suitable doping extent to prepare PANI-DBSA/DVB composite with longer liquid state.
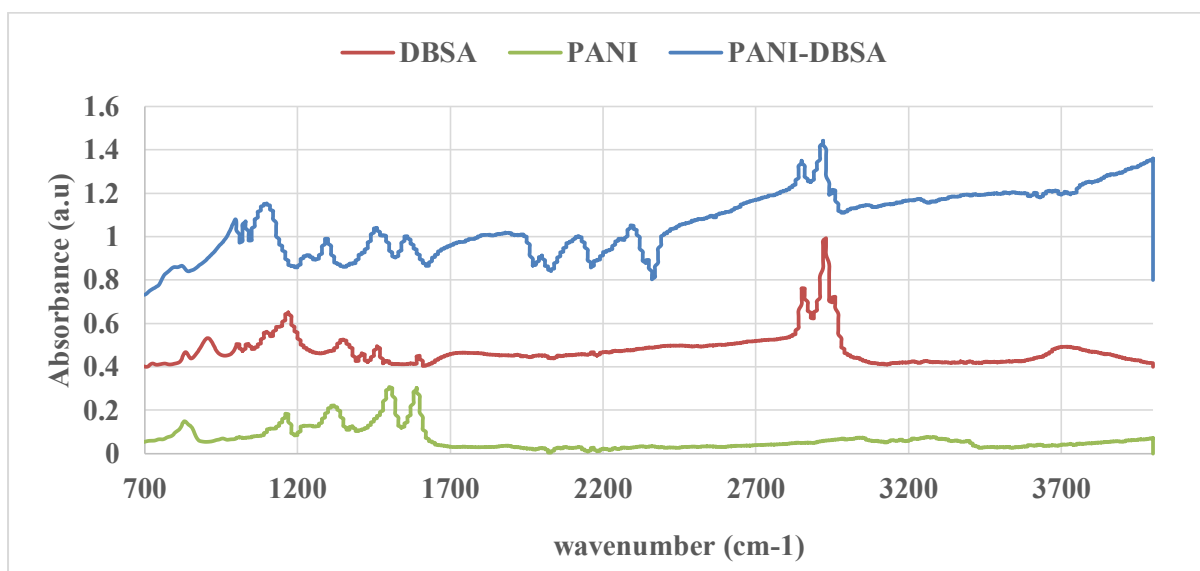
Figure 3.7 FT-IR spectra of PANI, DBSA and PANI-DBSA complex.

Table 3.1 The characteristics peaks of PANI, DBSA and PANI-DBSA complex[47].

Description	PANI	DBSA	PANI-DBSA
1. C–H Out of plane vibration of 1,4 disubstituted benzene ring	829	831	816
2. CH Stretching of Benzenoid rings of DBSA	-	1000	995

3. Peak for $NH_4^{+1}\ldots SO^{-3}$ interaction	-	1040		1030
4. N=Q=N mode	1160	-		1100
5. C–N Stretching of 1,4 disubstituted benzene ring	1320	-		1300
6. C=C Stretching vibration of benzenoid rings	1500	1460		1462
7. C=C Stretching vibration of quinoid rings	1590	-		1562
8. C–H Stretching of CH_2 and CH_3	-	2930 & 2850 respectively		2922 & 2850 respectively
9. N–H Stretching of PANI	3260			3200-3400

3.3   (PANI-DBSA)^{CM} complex preparation

Complex formed by mixing of PANI and DBSA using centrifugal mixer will be referred as (PANI-DBSA)^{CM} complex henceforth. To prepare this complex, PANI EB powder was put in the oven for 2 hours at 50°C to eliminate the moisture content present in it. Dried PANI and DBSA were mixed using a centrifugal mixer in the ratio of 30:70 by weight percentage, which is equivalent to the molar ratio of 1:0.69. As mentioned earlier DBSA molar ratios 0.5, 0.6 and 0.7 yielded the best conductivity result. Therefore, by considering the minimum DBSA required for complete doping, good process ability and curing of DVB, we choose 30:70 wt. % of PANI DBSA in our initial work. We changed this molar ratio to 1:0.60 in later part of work.

While mixing PANI-DBSA in centrifugal mixer, heat is generated which help PANI-DBSA complex to get thermally doped to some extent. Which means some of the DBSA protons are

already attached to the PANI chain. This semi-doping process of PANI-DBSA, reduces the number of free DBSA protons in the system therefore, enabling mixing of DVB without any sudden exothermic reaction between DBSA and DVB. Mixing time, mixing rotor speed and amount of PANI-DBSA used for mixing, all these factors affect the amount of heat generated during centrifugal mixing.

For this work following parameters were chosen, 4 gm PANI, 9.33 gm DBSA were mixed in a centrifugal mixer at 2000 r.p.m. for 5 min × 3 times. The prepared complex was stored in refrigerator for 1 night before use. These parameters were chosen on the basis of hit and trial basis and were modified in the later part of the research to obtain the stable PANI-DBSA/DVB matrix.

3.4 (PANI-DBSA)^{CM}/DVB matrix preparation

(PANI-DBSA)^{CM} complex was further mixed with different amount of DVB at room temperature to form a homogeneous PANI-DBSA/DVB mixture. Different weight percentage of DVB (30%, 50% and 70%) were used to determine the effect of DVB concentration on electrical conductivity and mechanical properties of the final composites.
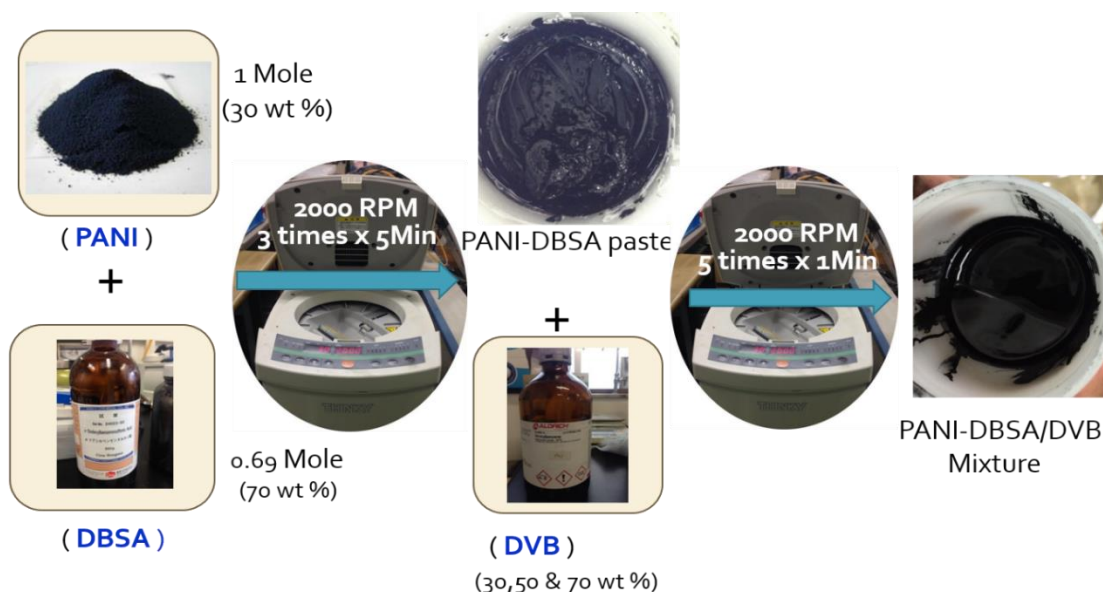
Figure 3.8 Scheme to prepare PANI-DBSA/DVB matrix using centrifugal mixing.

Centrifugal mixing was used to mix. As mentioned in earlier section, undoped PANI-DBSA complex cannot be added directly with DVB. Therefore PANI and DBSA were mixed first using centrifugal mixing. The heat generated during centrifugal mixing makes the PANI-DBSA doped to a very small extent. Semi-doped PANI-DBSA gives us an extra time before polymerization of DVB starts. However, after adding DVB the mixing speed and mixing time was monitored carefully to avoid immediate polymerization of DVB because DVB polymerization is usually assisted by high temperature. Therefore, mixing time and mixing speed were monitored carefully. Detailed manufacturing scheme is shown in **Figure 3.8**. Only the centrifugal mixing technique was used to prepare these composites, which will be, henceforth referred to as (PANI-DBSA)^{CM}/DVB composites.

3.5   Discussions

Problems faced in reality while making PANI-DBSA/DVB composite were explained in this chapter. It is shown that undoped PANI-DBSA reacts with DVB immediately and starts the exothermic curing of DVB matrix. Free DBSA proton available to start the DVB polymerization and absence of scavenging effect in undoped PANI-DBSA are assigned for this mechanism. Therefore a detailed parametric study was done to optimize the content and doping extent of PANI-DBSA to achieve the desired results. Thermal doping phenomenon of PANI-DBSA was studied. Best molar ratio between PANI and DBSA was investigated. 0.5, 0.6 and 0.7 Mole of DBSA with 1 Mole of PANI have shown the best results and therefore these ratios are recommended to prepare PANI-based polymer composite. 0.5 Mole DBSA found to be the least requirement for complete doping of DBSA, this finding is in well agreement with the literature[58]. Extra DBSA i.e. 0.8 Mole with 1 Mole PANI acts as an impurity in the system and therefore cause reduction in the electrical properties of PANI-DBSA complex after doping. Behaviour of electrical conductivity of PANI-DBSA w.r.t thermal treatment was explained also. First an increase in the electrical conductivity and thereafter a reduction in electrical conductivity was observed in all the cases. However, the rate of decrement was higher with higher doping temperature. This reduction in the electrical conductivity of PANI-DBSA complex after achieving its maximum value can be assigned to two factors. The first main reason is the deprotonation at higher temperature and second is the change in the conjugate

structure of PANI chain itself. This change in conjugate structure can be due to formation of new bonds within the PANI chain or rearranging of the bonds. Thermal degradation of polyaniline and also aging effect on polyaniline have been studied in past[59,60]. Ivana[61] et. al studied the structural change and degradation of PANI during treatment at 80 °C for three months. They found no change in the morphology but change in molecular structure of PANI corresponding to deprotonation, oxidation and chemical cross-linking reactions. Our result also predict the similar behaviour at higher temperature. Therefore, 120 °C temperature was found optimum for a quick and effective thermal doping. FT-IR, UV-vis-NIR spectra of PANI EB and PANI ES were explained to understand the electronic behaviour. Schematic representation to prepare centrifugally mixed PANI-DBSA/DVB matrix was shown.

Chapter 4   Preparation and characterization of (PANI-DBSA)$^{\text{CM}}$/DVB composite

As explained in section 3.2.1, free DBSA protons available in PANI-DBSA complex could initiate the curing process of DVB. Once the DVB curing starts it cannot be used to make any sample or for FRPs impregnation. However, by mixing PANI-DBSA for longer time at high speed, we could achieve enough longer liquid state duration of PANI-DBSA/DVB matrix at room temperature for preparation of few samples. However, the time before the start of curing was less than a few minutes. Liquid state stability was not taken into account while making centrifugally mixed (PANI-DBSA)$^{\text{CM}}$/DVB composite. In this chapter, only high electrical and mechanical properties were aimed for.

4.1   (PANI-DBSA)$^{\text{CM}}$/DVB composite preparation

(PANI-DBSA)$^{\text{CM}}$/DVB matrix was prepared using scheme explained in section 3.4. It was further poured in to moulds of size length 50 mm, width 12.5 mm and thickness 2 mm. The samples were cured using a hot-press machine (Toyoseiki, Mini test press. 10). Samples were subjected to initial heat in hot-press machine without applying any pressure. Initial slow heat helped to eliminate any volatile content if present. Pressure was applied after 10-15 minutes. 1-3 MPa pressure was applied. Samples were cured in hot-press machine for two hour at 120°C. Parametric study presented in section 3.1 suggested that curing time and curing temperature are the most important factors that determine the final electrical and mechanical properties of (PANI-DBSA)$^{\text{CM}}$/DVB composite. Therefore, it was tried to maintain same curing time and curing temperature for all the samples. Scheme to prepare (PANI-DBSA)$^{\text{CM}}$/DVB composite is shown in the **Figure 4.1.** Samples with different weight percentage of DVB (30%, 50% and 70%) were used. Electrical and mechanical properties of the prepared samples were measured. 3 samples for each measurement were taken. PANI, DBSA and DVB content were in the ratios as shown in **Table 4.1**

Figure 4.1 Manufacturing of (PANI-DBSA)[CM]/DVB composite.

Table 4.1 Relation between PANI, DBSA and DVB content in each composite[24].

Specimen Type	PANI		DBSA		DVB	
	(wt. %)	(mol)	(wt. %)	(mol)	(wt. %)	(mol)
A	9	1	21	0.69	70	5.8
B	15	1	35	0.69	50	2.5
C	21	1	49	0.69	30	1.1

The molar ratios have been normalized for comparison w.r.t PANI.

4.2 Electrical conductivity

Electrical properties of (PANI-DBSA)[CM]/DVB composite were measured using the 4-probe method as explained in section 2.2.1. Electrical conductivity results were compared as a function of DVB content in the composite. Effect of PANI content on electrical conductivity in the composite has been shown in the **Figure 4.2.**

It can be seen from the plots that the electrical conductivity is directly related to the PANI content in the composite. With an increment in the PANI content, there is a significant improvement in the electrical conductivity. Electrical conductivity of around 3.5 σ/cm has been recorded with 30 wt% DVB in the system. This result confirmed that PANI-DBSA complex is compatible with DVB matrix and can be used to prepare highly conductive thermosetting polymer composites. Electrical conductivity results of PANI-based thermosetting composites

prepared during this work has shown very good electrical conductivity than reported in literature[62].
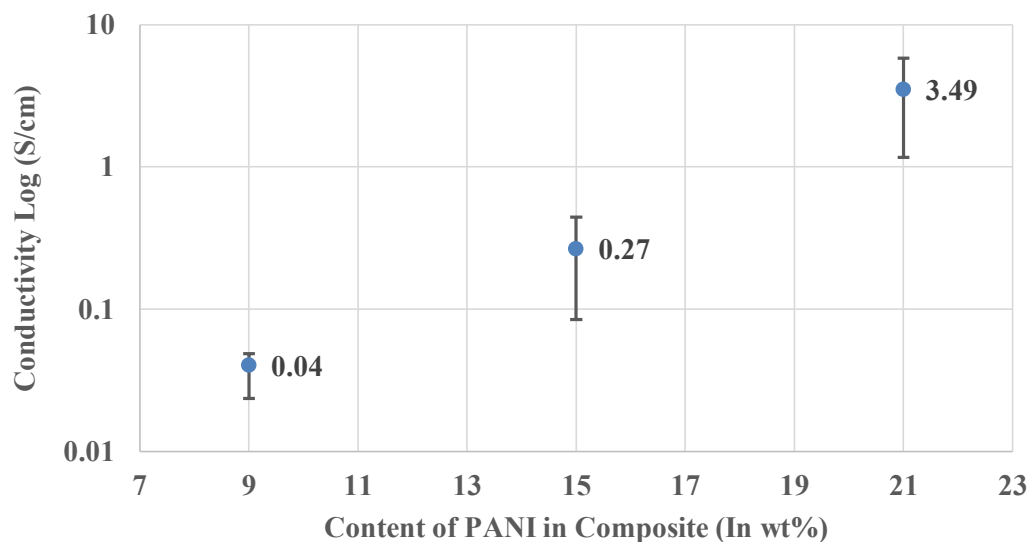
Figure 4.2 Electrical conductivity of (PANI-DBSA)[CM]/DVB composite w.r.t PANI content in the composite[24].

4.3 Mechanical properties

Flexural modulus, bending strength, load deflection curve and other mechanical properties of the composite were investigated. Mechanical properties with respect to the DVB content were presented. **Figure 4.3** and **Figure 4.4** show the flexural modulus and load deflection curve respectively. **Table 4.2** shows the bending strength of the composites. It is observed that over all mechanical properties of the composites increased with an increase in the content of DVB. Flexural modulus of composite with 30 wt. % DVB was found to be 0.54 GPa which was increased to 1.8 GPa with 70 wt. % of DVB. This increment can also be seen in other mechanical properties like bending strength. The value of pure DVB was difficult be measured due uncontrollable exothermic reaction between DVB and protonic acids. However, DVB with 70 wt. % DVB has shown very good mechanical properties, but still less than the commercial epoxy resins.

Although the mechanical properties of DVB matrix is not as good as epoxy based matrices, these results confirm that DVB can be used to prepare composites with high electrical and mechanical properties simultaneously. It is further evident that mechanical properties improve significantly with an increase in the DVB content. Maximum bending strength and strain is shown in **Table 4.2.** Improved mechanical properties can be associated with the presence of densely cross-linked DVB present in the system. In the present work, the main area to work upon is to improve the flexural strength of the matrix system. Strength needs to be improved a lot to replace epoxy system, in a few application areas where good strength necessary.
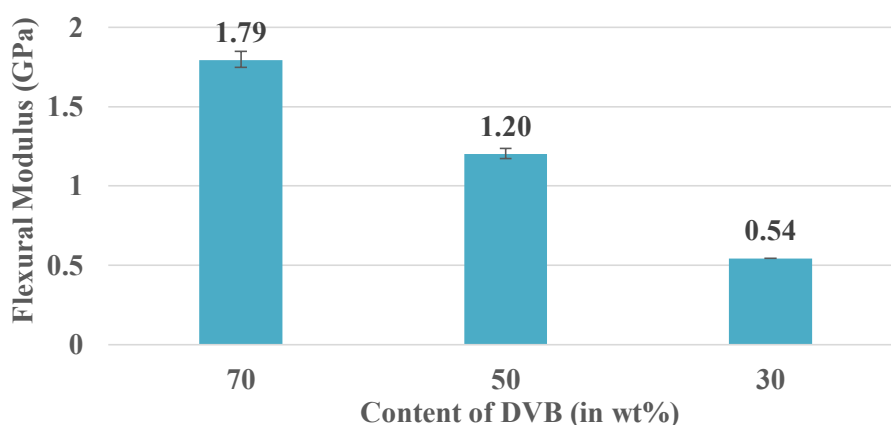
Figure 4.3 Flexural Modulus of (PANI-DBSA)[CM]/DVB composite w.r.t DVB content in the composite[24].
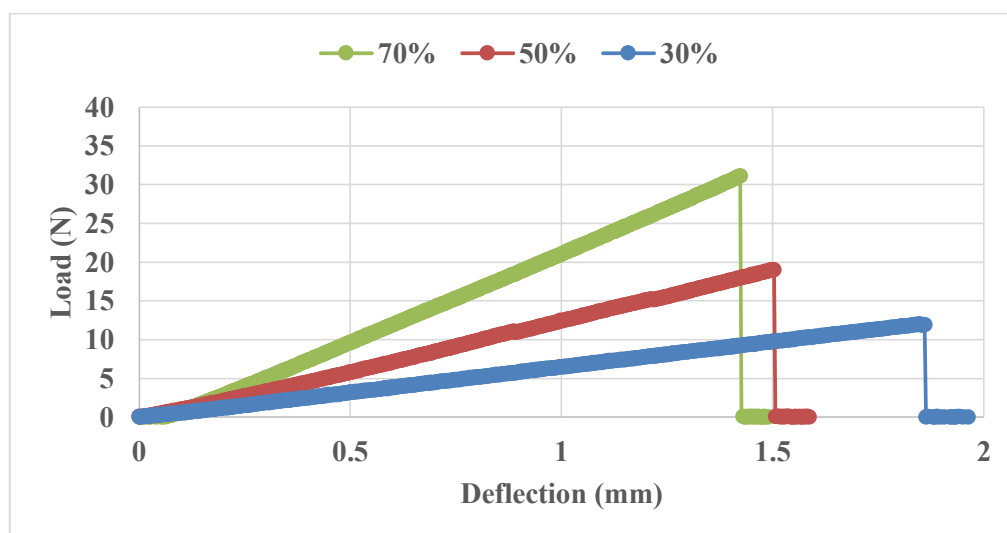
Figure 4.4 Load-deflection curve of (PANI-DBSA)[CM]/DVB composite w.r.t DVB content[24].

Table 4.2 Maximum bending stress and strain of the PANI-DBSA/DVB composite samples with different DVB content[24].

DVB wt. % in Composite	Maximum Bending Stress (MPa)	Maximum Bending Strain (in %)
30	9.17(0.84)	1.73(0.37)
50	18.09(1.77)	1.60(0.08)
70	26.73(3.88)	1.59(0.32)

4.4   Morphology

Morphology of prepared samples were studied using SEM technique. Cross section of the samples after fracture and sides of the samples were put into investigation to understand the electrical and mechanical behaviour of the composite. In **Figure 4.5** the cross section of (PANI-DBSA)^{CM}/DVB composites with 50 wt. % and 70 wt. % of DVB respectively have been shown. Dark black area is due to the insulating DVB matrix while bright grey area is because of conductive PANI-DBSA complex[10,63,64]. PANI-DBSA agglomeration of size around 1-10 μm can be seen clearly. In composite with 70 wt. % DVB, darker area is more visible due to excess amount of insulating DVB.
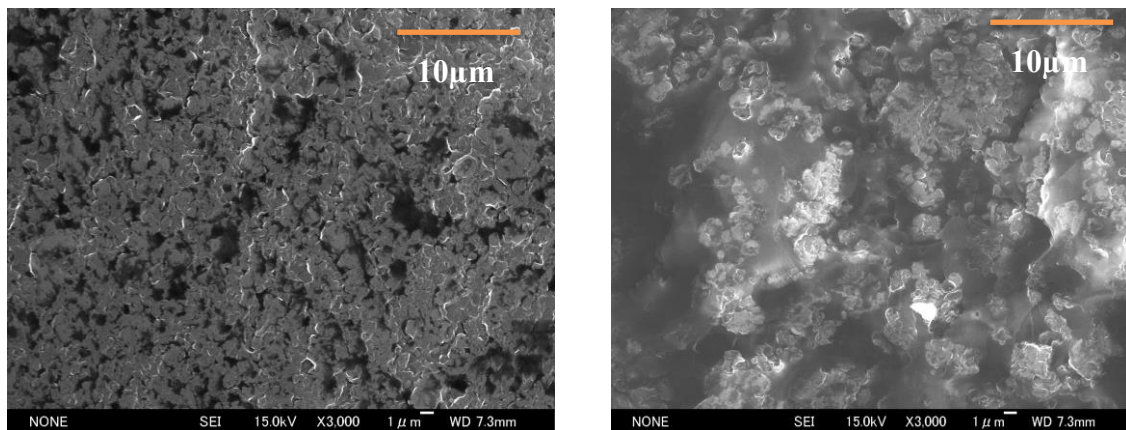
       (a) **(PANI-DBSA)^{CM}/DVB (50%)**   (b) **(PANI-DBSA)^{CM}/DVB (70%)**

Figure 4.5 (a) & (b) SEM micrographs of fracture surface of 50 wt. % and 70 wt. % of DVB in (PANI-DBSA)^{CM}/DVB composite respectively.

When we observed the side surfaces of the (PANI-DBSA)^{CM}/DVB composite with different amount of DVB one interesting phenomenon was consistent. From **Figure 4.6** it can be seen that the side walls of the composite has a layer of dark colour material, which could be DVB. Therefore from the micrographs, we can assume that during thermal treatment of the matrix, some uncured DVB monomers squeeze out to the external surfaces of the sample and are then cured. Therefore, one insulating layer of around 10 µm thickness was formed on the side walls. Therefore it is recommended to remove this insulating layer of DVB before measuring the electrical conductivity of the composite.
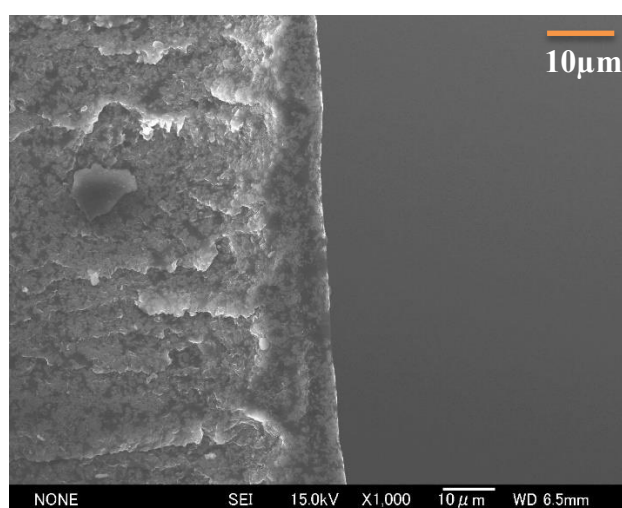
(PANI-DBSA)^{CM}/DVB (50%)

Figure 4.6 SEM micrographs of side surface of (PANI-DBSA)^{CM}/DVB composite with 50 wt. % DVB.

Pure doped PANI-DBSA complex has conductivity around 15~18 S/cm while, DVB is an insulator. Therefore, it is obvious that higher the amount of PANI-DBSA in the composite system higher would be the electrical conductivity. Similarly, DVB contributes to the mechanical properties of the composite and therefore, higher content of DVB and completely cured DVB will result in better mechanical properties of the system. These results were better understood with SEM micrographs.

4.5   Prediction of flexural modulus using Kerner-Nielsen model

With the increasing interest of researchers in nanocomposites, a big portion of research also being allocated to the prediction of mechanical properties of these nanocomposites. In nanocomposites a variety of fillers are being used like CNT, carbon black and graphene nanotubes. All these fillers have different geometries and therefore different models have been proposed to predict mechanical properties due to these fillers[65]. Also tensile modulus prediction models seem to be the most studied[66,67]. Halpin-Tsai model usually used to predict the tensile properties of fibered geometry fillers while taking their aspect ratios in to account i.e. CNT and CNF. Halpin-Tsai equation can also take care of the orientation of the fillers. However as can be seen from SEM micrograph shown in **Figure 4.7.** PANI-DBSA agglomerates are similar to spherical shapes.
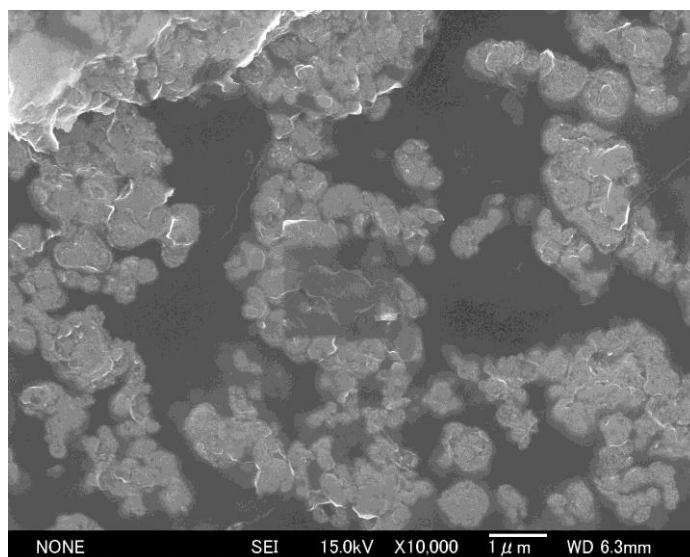
Figure 4.7 SEM image of PANI-DBSA agglomerates inside DVB matrix.

Tze Siong Chew et al.[68] and Mohamad Ayad et al.[69] studied the structure of doped PANI and reported surface area of 349 (m^2/g) and size of 20-100 nm of PANI agglomerates. However, it should be noted that PANI-DBSA agglomerates depends on the type of doping and mixing. Nevertheless, These results showed very close approximation of PANI-DBSA agglomerates with the carbon black, who has surface area of 1250 (m^2/g) and size of 30-100 nm of agglomerates. Both fillers have spherical shapes and conductive nature. Therefore, it would be

a fair approximation to use the same model as used in case of carbon black for PANI-DBSA fillers to predict the mechanical properties of the PANI-DBSA/DVB composite w.r.t. to the PANI-DBSA content.

To take care of aspect ratio of particulate, Shao-Yun Fu et al.[67] and Michael D. Via et al.[70] proposed to use Kerner-Nielsen Model for carbon black particulates. Kerner-Nielsen model do not require the specific knowledge of aspect ratio of the filler and can be used for spherical particulates. Kerner-Nielsen model has been shown in **Equation 4.1- 4.4**[65].

$$\frac{E_C}{E_M} = \frac{1+ABV_f}{1-\psi BV_f} \tag{4.1}$$

Where,

$$A = K_E - 1 \tag{4.2}$$

And,

$$B = \frac{\left(\frac{E_f}{E_M}\right)-1}{\left(\frac{E_f}{E_M}\right)+A} \tag{4.3}$$

Also,

$$\psi = 1 + \frac{1-\phi_m}{\phi_m}V_f^2 \tag{4.4}$$

E_C, E_M are the moduli of composite and matrix respectively. E_f is the modulus of filler and V_f is the volume fraction of the fillers in the composite. A and B can be calculated using equations mentioned above. Where, K_E is the Einstein coefficient and ϕ_m is the maximum packing factor. Constant A, depends on the Einstein coefficient, which is the function of aspect ratio and orientation of the fillers. Einstein coefficient K_E, and maximum packing factor ϕ_m for carbon black filler were chosen as 2.5 and 0.2 respectively in many literatures[70,71].

We also have used the same value of aforementioned constants in case of PANI-DBSA filler. The results obtained from the above model has been in a very good agreement with the experimental results. All the values needed for theoretical prediction of flexural modulus are shown in **Table 4.3**.

Table 4.3 – Values needed for theoretical prediction using Kerner-Nielsen model.

PANI-DBSA content	Einstein coefficient	Transfer Efficiency	Modulus of filler	Modulus of Matrix	Constant	Fitting factor	Volume Fraction
	K	A	E_f	E_M	B	ϕ_m	V_f
30 wt %	2.5	1.5	1100	3389	-0.37018	0.2	0.2843
40 wt %	2.5	1.5	1100	3389	-0.37018	0.2	0.3792
50 wt %	2.5	1.5	1100	3389	-0.37018	0.2	0.4742
60 wt %	2.5	1.5	1100	3389	-0.37018	0.2	0.5688
70 wt %	2.5	1.5	1100	3389	-0.37018	0.2	0.6636

However, in the present case we cured all the samples at 120°C for 8 hours just to achieve the maximum mechanical properties without taking care of electrical properties of the composites. It was obvious that the electrical properties of all the samples reduced drastically after exposed to high temperature for so long. **Figure 4.8** Shows the comparison between theoretical values predicted by using Kerner-Nielsen model and experimental values.
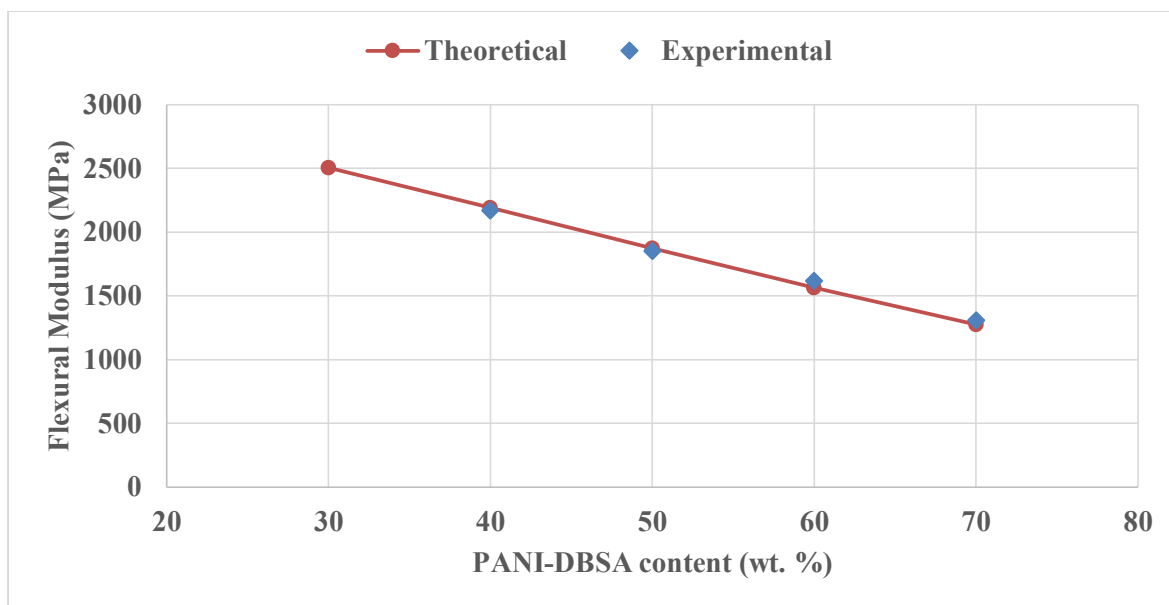
Figure 4.8 Theoretical values predicted by using Kerner-Nielsen model and experimental values of PANI-DBSA/DVB composite w.r.t PANI-DBSA content in composite.

4.6 Discussion

(PANI-DBSA)^{CM}/DVB composite was prepared using centrifugal mixing process and characterized in this chapter. Electrical and mechanical properties of prepared sample were measured. It was found that the electrical conductivity of this thermosetting composite system has a very high value compared to the results available in literature. The reason for such high electrical conductivity of PANI-based composite with DVB matrix is due to the compatibility of PANI-DBSA system with DVB. In literature, a lot work has been done to prepare PANI-epoxy composite but consistent high electrical conductivity was not realized. For such behaviour dedoping of PANI's imine in epoxy system could be assigned. Researchers also tried to change different hardener and found that the electrical conductivity is highly dependent on hardener type. In the present work, we have not used any additional hardener as well. These noble ideas made PANI-DBSA/DVB composite highly conductive with good mechanical properties. Electrical properties were found to be directly related to the content of PANI in the composite. Similarly mechanical properties were directly related to the DVB content and its cross-linking extent.

However, there were still some problems to be solved for example, liquid state duration of the PANI-DBSA/DVB mixture using centrifugal mixing manufacturing technique was low. With low liquid state duration it was impossible to use this matrix to impregnate fabrics or put in a mould.

Electrical and mechanical properties of the composite were explained using SEM analysis as well. PANI-DBSA agglomerates were dispersed properly within DVB matrix. After a particular concentration of PANI-DBSA, a conductive network seems to be formed, which accounts for the good electrical conductivity. In past, it was difficult to use higher content of conductive fillers due to their poor process ability. However, with PANI-DBSA system it is possible to use high content ratio of PANI-DBSA filler due to its good process ability. However, electrical conductivity and mechanical properties are the function of PANI-DBSA content in the system. Therefore, it was important to know the effect of PANI-DBSA concentration on mechanical properties. For this purpose, Kerner-Nielsen model was used to predict the flexural modulus of the composite w.r.t. PANI-DBSA content in the composite. We assumed few constant as similar to the a carbon-black filled epoxy system. We got very good agreement between theoretical and experimental values. However, K_E the Einstein coefficient and ϕ_m the maximum packing factor should be calculated specifically for the PANI-DBSA agglomerates and predict the composite mechanical properties again.

Chapter 5   Preparation and characterization of (PANI-DBSA)^{RM}/DVB composite

The problem of low liquid state duration in centrifugally mixed sample was a major problem to use this matrix for commercial applications. We could achieve very impressive results in terms of electrical and mechanical properties as listed in previous chapter, but the lack of environmental stability compelled us to change the manufacturing process. To achieve this goal of improving stability, we referred to literature that reported the scavenging properties of conducting polymers[50,51,72,73]. Radical scavenging antioxidants are often assessed by their ability to neutralise stable free radicals. P. A. Kilmartin et al.[50] reported that soluble PANI was found to be very efficient and rapid scavenger of free radicals. Therefore, stretched form of PANI could act as a radical scavenger, in addition to the lack of abundance of free DBSA protons that could prevent curing of DVB. There are two ways to achieve this semi-doped stage. First, is to break the big PANI agglomerations into smaller one while mixing in a roll-milling machine and second by temperature controlled semi doping of PANI. Completely doped PANI cannot be dispersed into solution. In this thesis, only the first way to obtain a highly environmentally stable PANI-DBSA/DVB mixture at room temperature has been mentioned.

5.1   (PANI-DBSA)^{RM} complex preparation

In this method PANI and DBSA were mixed in the wt. % ratio of 30 and 70 respectively. This ratio was chosen for proper viscosity while mixing using roll-milling process. This ratio is equivalent to the normalized ratio of 1:0.69 of PANI and DBSA. Basic structure of a roll-milling process has been shown in **Figure 5.1.** The parameter of the roll-milling process for example roller speed, space between rollers and number of rotations were decided after careful consideration of viscosity, doping level and agglomeration size of PANI-DBSA respectively.
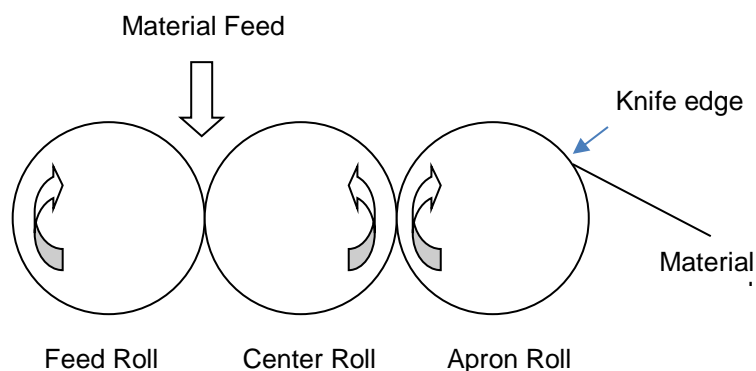
Figure 5.1 Schematic representation of three-roll mill process which is used to achieve a uniform homogenous paste of PANI and DBSA.

Roll-milled PANI-DBSA complex was further mixed with different amount of DVB wt. % and mixed using a centrifugal mixer. Henceforth the composite prepared using roll-milled PANI-DBSA complex will be referred as (PANI-DBSA)^{RM}/DVB composite. The same process explained in chapter 4 was followed to prepare (PANI-DBSA)^{RM}/DVB matrix. All the parameters were kept the same as for the (PANI-DBSA)^{CM}/DVB matrix.

Prepared (PANI-DBSA)^{RM}/DVB matrix was further poured in to the mold and put in hot press machine for curing for two hours at 120°C. Electrical properties, mechanical properties, morphological study and material characterization was done in the similar manner as explained in chapter 2.

5.2   Effect of roll milling on liquid state duration

As expected, the liquid state duration of PANI-DBSA complex after adding DVB was increased significantly as shown in **Table 5.1**[47]. This improved liquid state duration of the matrix can be attributed to the breaking of big PANI agglomerations into smaller one, semi-doping state of PANI-DBSA (less amount of free DBSA protons) and scavenger effect of extended polyaniline. Properties of (PANI-DBSA)^{RM}/DVB were studied and compared with the (PANI-DBSA)^{CM}/DVB composite presented in chapter 4.

Table 5.1 Relation between PANI, DBSA and DVB content in each composite and time taken before curing starts.

Matrix type	PANI (In wt.%)	DBSA (In wt.%)	DVB (In wt. %)	Curing starts (Centrifugally-mixed) samples (minutes)	Curing starts (Roll-milled) samples (minutes)
1	9	21	70	<1	>15
2	15	35	50	<1	>12
3	21	49	30	<1	>10

5.3 Electrical conductivity

The effect of PANI content on electrical conductivity of the (PANI-DBSA)[RM]/DVB composite and (PANI-DBSA)[CM]/DVB composite has been compared and shown in **Figure 5.2.** It can be clearly seen from the figure that the (PANI-DBSA)[CM]/DVB composite exhibits higher conductivity compared to (PANI-DBSA)[RM]/DVB composite with the same amount of DVB. Two main reason for less conductivity of roll-milled composite could be.

1. Small agglomerations of PANI-DBSA dispersed very well inside insulating DVB matrix and couldn't reach percolation threshold.

2. There is a trade-off between PANI and DVB for DBSA protons and at higher temperature it is easy for stretched PANI (semi doped) to dedope (detachment of PANI and DBSA).

As mentioned (PANI/DBSA)[RM]/DVB takes a longer time before the complete curing of DVB due to the scavenging effect of PANI as well as due to limited available free DBSA protons. Thermal treatment at higher temperature also assists in separating PANI and DBSA protons from each other, this phenomenon is called dedoping. Dedoping phenomenon due to curing time and curing temperature has been explained in detail in the chapter 7. Therefore, longer the time of DVB polymerization, higher would be the dedoping of PANI which attribute to lower conductivity. DVB gets cured very fast in case of centrifugally (PANI-DBSA)[CM]/DVB composite and hence, this composite shows higher conductivity. The electrical conductivity up

to 1.3 S/cm in case of (PANI-DBSA)[RM]/DVB composite and 3.49 S/cm in case of (PANI-DBSA)[CM]/DVB composite with 30 wt. % DVB was found.
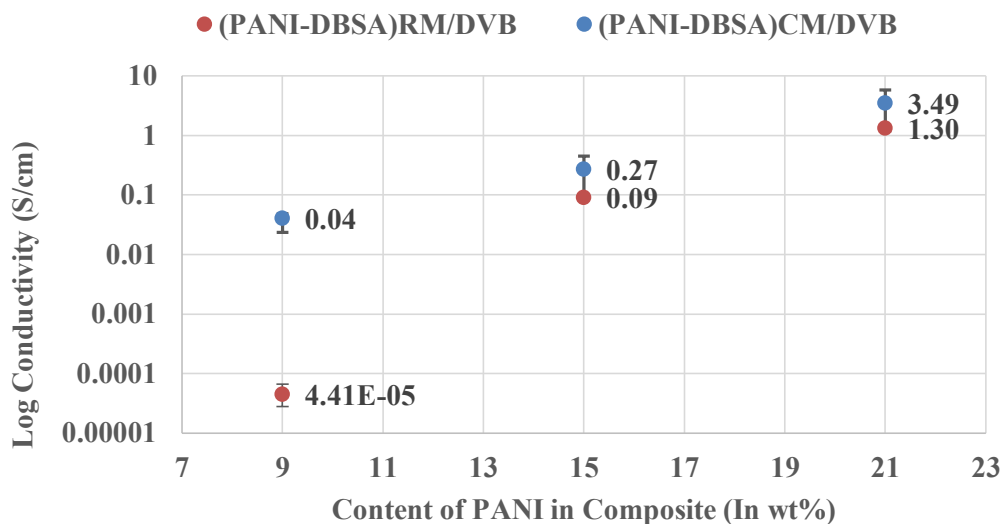
Figure 5.2. Electrical conductivity of (PANI-DBSA)[CM]/DVB composite and (PANI-DBSA)[RM]/DVB composite with different wt. % of PANI[47].

5.4   Mechanical properties

Mechanical properties of (PANI-DBSA)[RM]/DVB composite have been determined using 3-point flexural testing. It has been found that (PANI-DBSA)[RM]/DVB composite has lower overall mechanical properties as compared to (PANI-DBSA)[CM]/DVB composite at the same curing time and curing temperature. This behaviour can be attributed to the incomplete polymerization of DVB in roll-milled samples due to the scavenging effect of semi-doped PANI-DBSA complex. Also amount of free DBSA proton was limited in case of RM samples as compared to the CM samples and hence, longer time was needed for complete polymerization of DVB. However, roll-milled composite can also achieve its full strength on complete polymerization of DVB present in the matrix. It just needs longer curing time, but in that case conductivity decreases drastically due to the dedoping effect described earlier.

As shown in **Figure 5.3** flexural modulus up to 1.78 GPa with 70 wt. % of DVB was obtained in case of (PANI-DBSA)[CM]/DVB composite. On the other hand, flexural modulus up to 0.98

GPa with 70 wt. % of DVB was obtained in case of (PANI-DBSA)^{RM}/DVB composite. With lower content of DVB, i.e. 30 wt. %, it was expected to have low value of mechanical properties. Flexural modulus of 0.54 GPa for the (PANI-DBSA)^{CM}/DVB composite and 0.35 GPa for the (PANI-DBSA)^{RM}/DVB composite were obtained with 30 wt. % of DVB respectively[47]. It has been found that the electrical conductivity of PANI-DBSA/DVB composite and flexural modulus are inversely proportional to each other. It should be noted that these values were obtained with fixed curing profile. With different curing profile different values were obtained.

However, for comparison purpose curing for 2 hours at 120 °C was performed. It was expected that better mechanical properties should be obtained with higher DVB content in the composite. It can be confirmed from the plot that higher DVB content results into higher flexural properties. This work confirmed that a thermosetting strong polymer composite can be made with good electrical properties as well. Electrical and mechanical properties of this composite can be controlled by choosing adequate DVB content and curing profile. This work is the introductory work for PANI-DBSA/DVB composite and we want to use this matrix to impregnate FRPs. As, tensile properties of the FRP composites are determined by the fiber properties, only flexural properties have been included in this work, Flexural strain and flexural stress curves for (PANI-DBSA)^{CM}/DVB and (PANI-DBSA)^{RM}/DVB composite samples are also shown in the **Figure 5.4** and **5.5** respectively. Maximum bending strength for both type of composites have been shown in **Table 5.2**

Table 5.2 Maximum bending strength of (PANI-DBSA)^{CM}/DVB and (PANI-DBSA)^{RM}/DVB composites.

DVB wt. % in Composite	Maximum Bending Strength (MPa) for CM samples	Maximum Bending Strength (MPa) for RM samples
30	9.17(0.84)	7.05(0.94)
50	18.09(1.77)	16.07(0.72)
70	26.73(3.88)	16.93(2.18)

Note: Parentheses indicate the standard deviations.
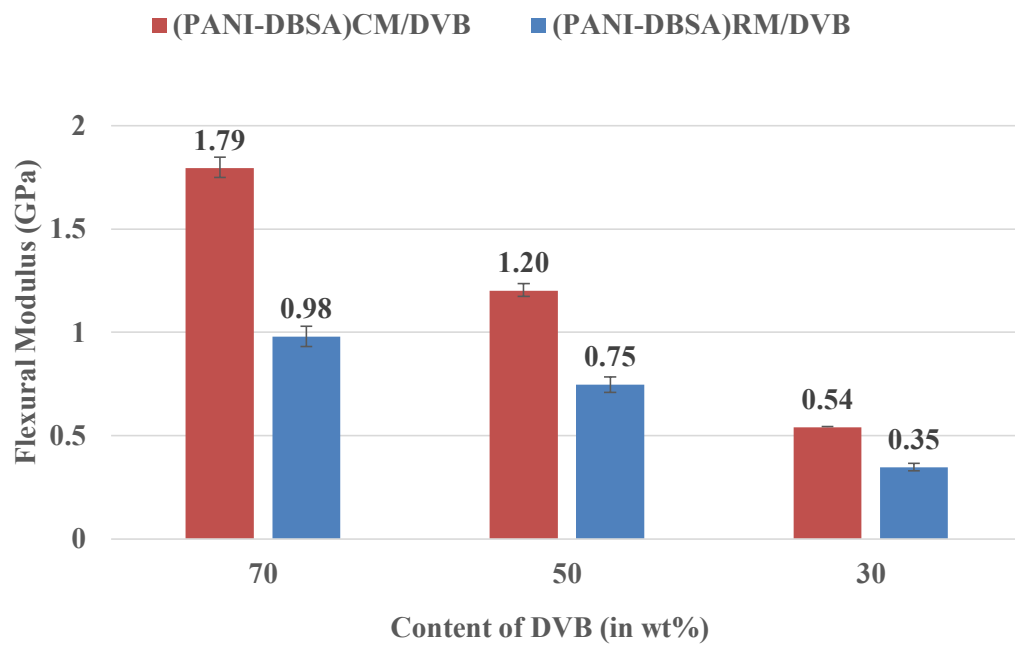
Figure 5.3 Flexural properties of (PANI-DBSA)^{CM}/DVB composite and (PANI-DBSA)^{RM}/DVB composite with different wt. % of DVB in composite[47].
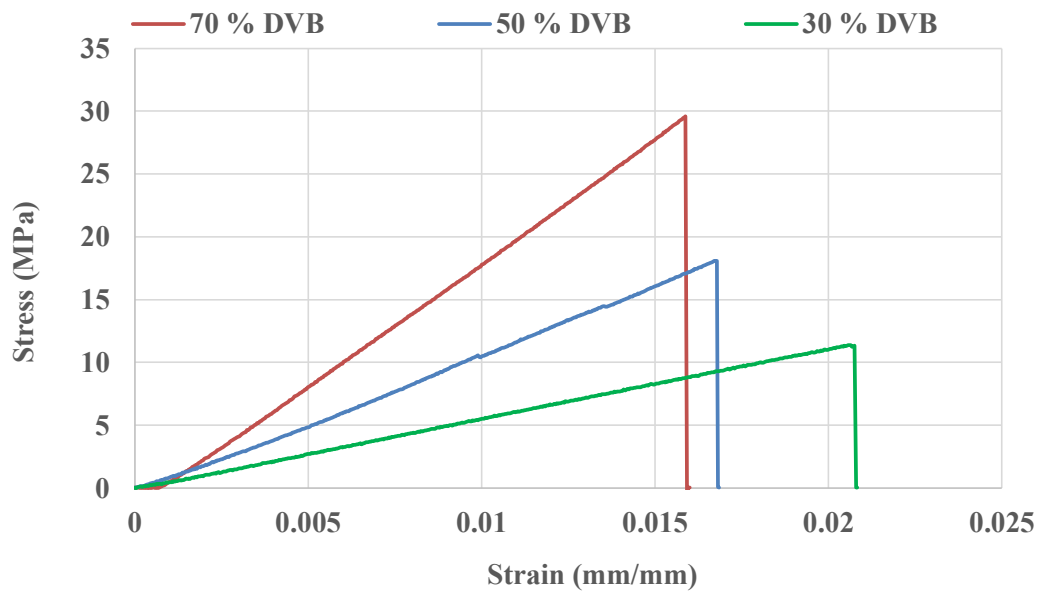
Figure 5.4 Stress Strain curve of (PANI-DBSA)^{CM}/DVB composite[47].
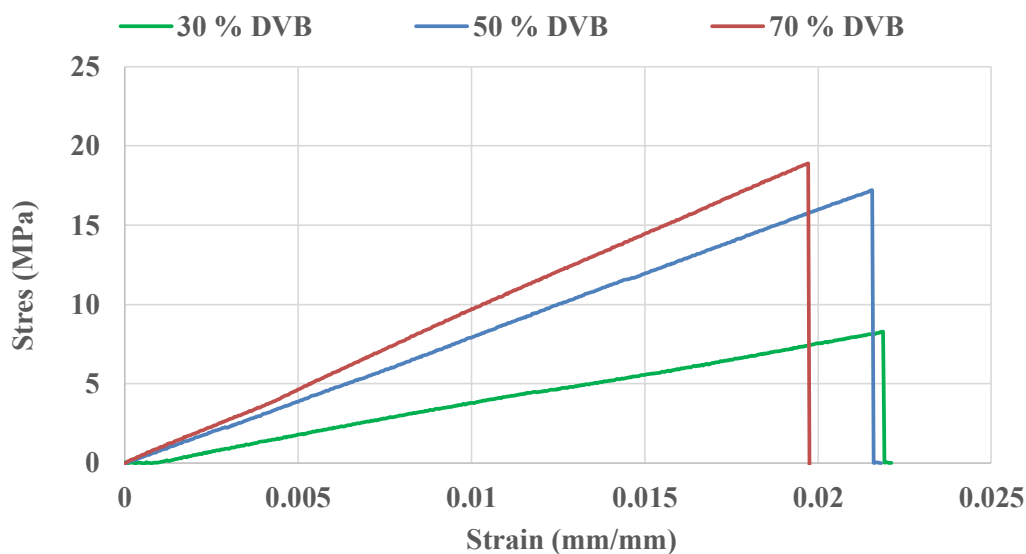
Figure 5.5 Stress Strain curve of (PANI-DBSA)[RM]/DVB composite with different wt. % of DVB in composite[47].

5.5   UV-vis-NIR spectra

A huge difference in the electrical and mechanical properties of (PANI-DBSA)[CM]/DVB composite and (PANI-DBSA)[RM]/DVB composite was found even with the same curing profile and same content. UV-vis-NIR analysis has been done to understand this difference in electrical and mechanical properties for both centrifugally mixed and roll-milled PANI-DBSA complex as shown in **Figure 5.6**. Characteristics peaks of undoped PANI i.e. EB - Emeraldine base dissolved in NMP are present at around 325 nm and around 629 nm as reported in literature[74]. First peak at 325 nm, can be assigned to the $\pi \rightarrow \pi^*$ transition of benzenoid amine ring and second peak 629 nm is associated with the $\pi_B \rightarrow \pi_Q$ excitation absorption in the quinoid imine ring[31]. These two peaks are the characteristic peaks of base form of PANI and change in these peaks signify the doping process in PANI. However, our experiment was carried out in 350-2600 nm range and therefore first peak at 325 nm cannot be seen in these plots.

It can be seen from the UV-vis-NIR spectra of CM PANI-DBSA and RM PANI-DBSA that the peak present in CM PANI-DBSA samples has been shifted to 660 nm in case of RM PANI-DBSA samples. This shifting of quinoid imine peak can be attributed to the beginning of the

formation of polaron band. Peak at 660 nm is also broader as compared to the CM PANI-DBSA samples. Mcdiarmid et al.[75] reported that a free carrier tail in UV-vis-NIR spectra of doped PANI is due to the extended conformation of PANI chain. PANI is found in coiled structure in its undoped stage. This free carrier tail can only be seen after 1000 nm in RM PANI-DBSA sample while missing in CM PANI-DBSA samples. This confirms that PANI has smaller agglomeration and extended conformation after roll-milling process. This free carrier tail can also be assigned to presence of some electrical conductivity in the RM PANI-DBSA complex.

However, complete PANI-DBSA usually has the second peak at around 780 nm. But the presence of the peak at 660 nm but not at 780 nm shows that the complex is in semi-doped state.
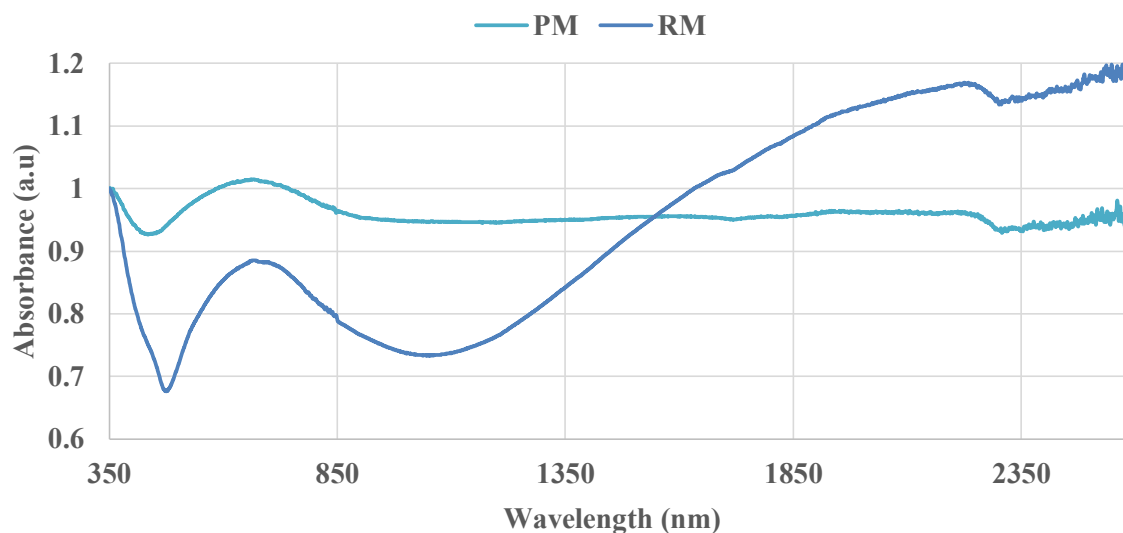
Figure 5.6. UV-vis-NIR analysis of CM PANI-DBSA and RM PANI-DBSA complexes[47].

5.6   SEM analysis

Scanning electron microscopy is an important tool to study the morphology of PANI-based composites. The cross section of (PANI-DBSA)RM/DVB composite and (PANI-DBSA)CM/DVB composite after fracture has been studied using SEM and shown in **Figure 5.7**. Composites with 50 and 70 wt.% of DVB content of both the composites were chosen for comparison. Morphological study w.r.t DVB content has been done. Also effect of PANI-

DBSA complex preparation on final composite was also studied. With different DVB content, a huge difference between the microstructures of the samples can be seen. Higher DVB content helped to obtain a better dispersion of PANI-DBSA in to the matrix. Good homogenous mixture is important to achieve uniform results throughout the composite. From these SEM images, it can be assumed that PANI-DBSA agglomerations are the conductive islands in DVB matrix.
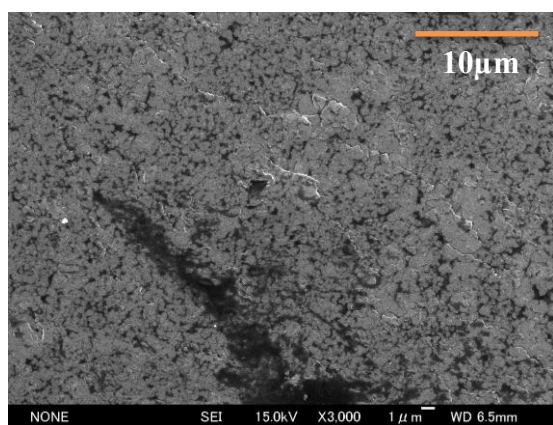
(a) (PANI-DBSA)^{RM}/DVB (50%)
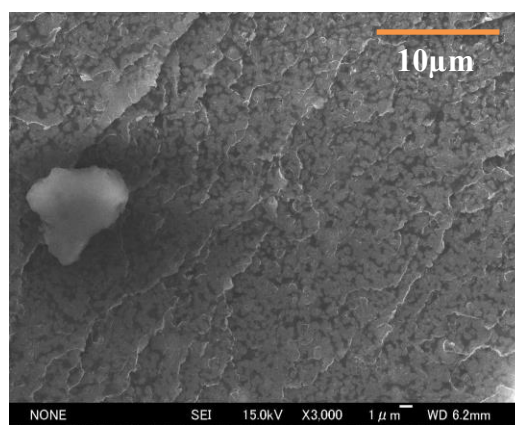
(b) (PANI-DBSA)^{RM}/DVB (70%)
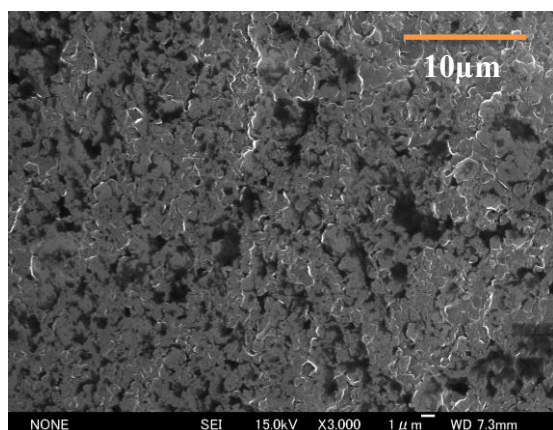
(c) (PANI-DBSA)^{CM}/DVB (50%)
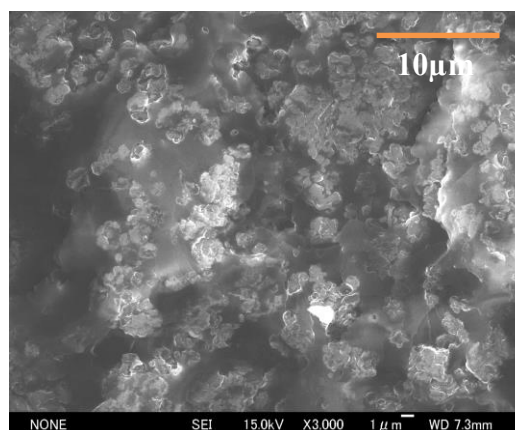
(d) (PANI-DBSA)^{CM}/DVB (70%)

Figure 5.7 (a) & (b) SEM micrographs of 50 wt. % and 70 wt. % of DVB in (PANI-DBSA)^{RM}/DVB composite. (c) & (d) (PANI-DBSA)^{CM}/DVB composite with 50 wt. % and 70 wt. % of DVB.

Similarly, low concentration of DVB results in a poor dispersion of PANI-DBSA complex into the matrix due to insufficient matrix. These big agglomeration of PANI-DBSA complex in composite can be assigned for the low mechanical properties of the composite. Usual PANI-

DBSA agglomeration sizes are in the range of 10-50 μm. However after roll-milling process agglomerates reduced to size of 1 μm. Due to these small agglomerations RM samples dispersed more homogenously. **Figure 5.7** (a) & (b) shows the SEM image of RM composite and (c) & (d) shows SEM image of CM composite respectively.

We already showed in the previous section that higher DVB content accounts for better mechanical properties and good surface finish. These results can be verified from the SEM images shown in **Figure 5.7**. Morphological study by SEM analysis helped understand electrical and mechanical properties more clearly. The higher content of PANI-DBSA agglomerates in to the system account for better electrical conductivity at low DVB concentration and good dispersion, while high cross-linked network of DVB account for better mechanical properties.

5.7 Thermal stability

TGA analysis has been done to understand the thermal stability of pure PANI, DBSA, DVB and PANI-DBSA/DVB composite. Weight change of the samples w.r.t to thermal treatment is attributed to the degradation of samples. In aerospace industry temperature change is a very frequent phenomenon. Therefore, TGA analysis of pure PANI, DBSA, DVB and PANI-DBSA/DVB composite with different DVB ratios have shown in **Figure 5.8, Figure 5.9, Figure 5.10 and Figure 5.11** respectively.
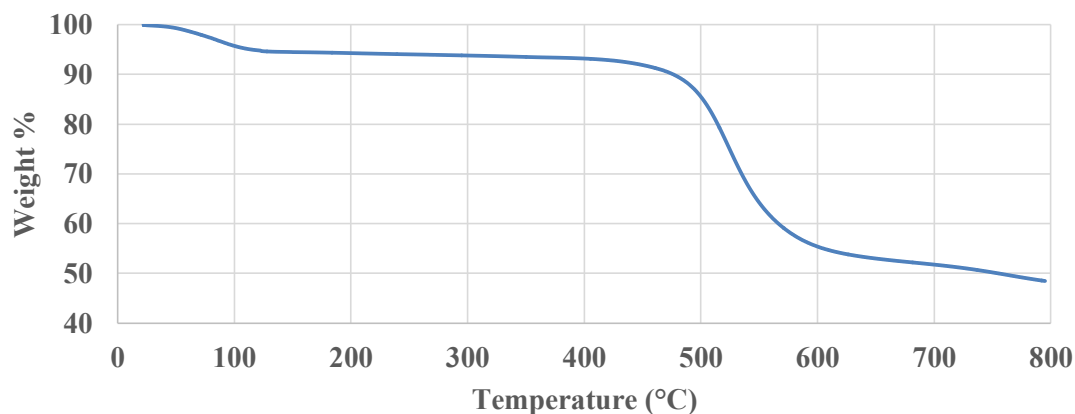
Figure 5.8. TGA analysis of pure PANI

It can be seen from the plot that weight loss in PANI occurs in two main stages. The first stage of weight loss is below 125°C, corresponding to the weight loss due to evaporation of moisture and other volatile content and oligomers. PANI shows high moisture content because of its hygroscopic nature and powdery form. Therefore, it is recommended to dry PANI powder before use. The second main stage is between 450-650°C, which corresponds to the decomposition of the PANI backbone itself. The backbone gradually decomposes at higher temperature. Even at 800°C, significant weight of undecomposed PANI can be observed. Following reasons can explain this behaviour. In nitrogen atmosphere carbonization of polymer takes place leaving some residue. Complete burning didn't occur, while only heat decomposition of PANI occurred in N_2 atmosphere. Also, most part of PANI structure is benzene, which is very stable.
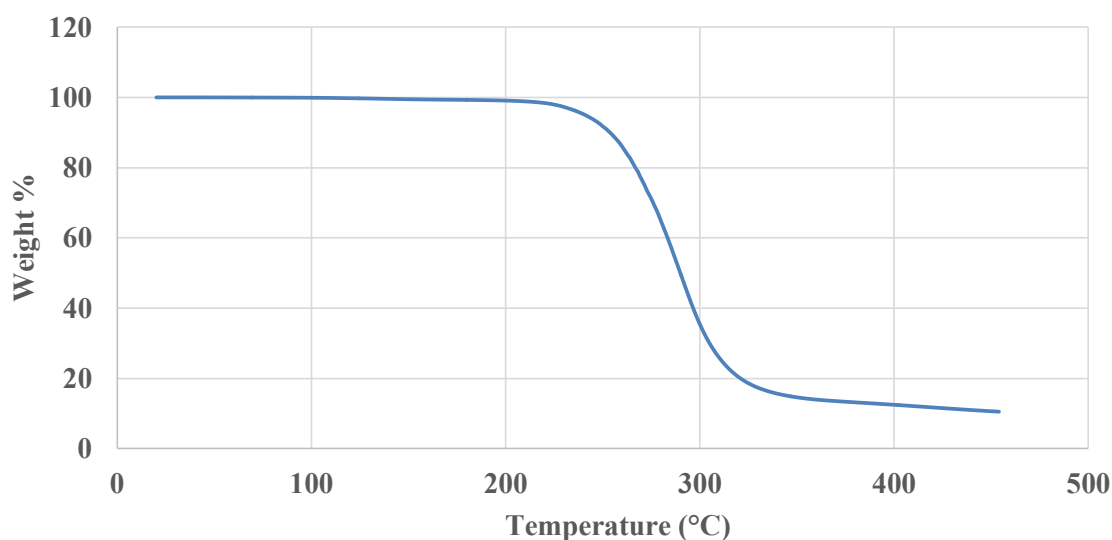
Figure 5.9. TGA analysis of pure DBSA.

Figure 5.9 corresponds to the TGA analysis of pure DBSA. The first stage of weight loss is below 220°C, corresponds to the weight loss due to moister and other volatile content. As it can be seen very small amount of such substances were present in DBSA. The second main stage is between 220-330°C, which corresponds to the decomposition of the DBSA polymer. Even at 450°C, around 10% weight of undecomposed DBSA can be observed, which could be attributed to the carbonization of polymer in nitrogen atmosphere leaving some residue.
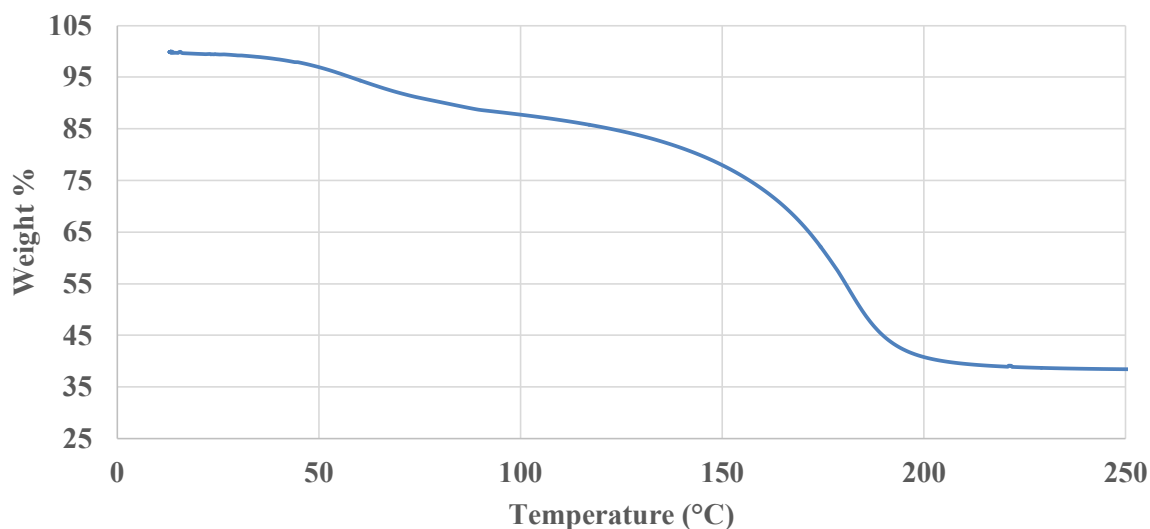
Figure 5.10. TGA analysis of pure DVB.

Due to the volatile nature of DVB, the main weight losses stages are difficult to distinguish as shown in **Figure 5.10**. However, we can still divide the weight loss in three main stages. The first stage of weight loss is below 100°C, which corresponds to the weight loss due to moisture and other volatile DVB monomers. The second main stage is between 100-200°C, which corresponds to the decomposition and evaporation of the DVB monomer. After 200°C, there is a constant weight residue of more than 35% weight of undecomposed DVB. This TGA shows that DVB can be self-polymerized at high temperature even without any initiator. A white rubbery form of poly-DVB has been observed after heat treatment of DVB at 120°C for some time. This white colour poly-DVB is the self-polymerized form of DVB.

No significant difference was found in TGA analysis of composite prepared by centrifugal mixing and roll-milling process. Therefore only TGA analysis of (PANI-DBSA)RM/DVB composite has been shown in **Figure 5.11**. As can be seen from the plot, weight loss stages of all the samples can be divided into two main stages. First degradation before 200 °C can be due to the moisture or oligomers present in the samples. Other volatile content present in the samples could also be the reason for this weight loss before 200 °C. Evaporation of non-polymerized DVB monomers also contribute to this change of weight. The second stage after 300°C, can be assigned to the decomposition of DBSA present in the system. It is known that DBSA starts degradation around 320°C.
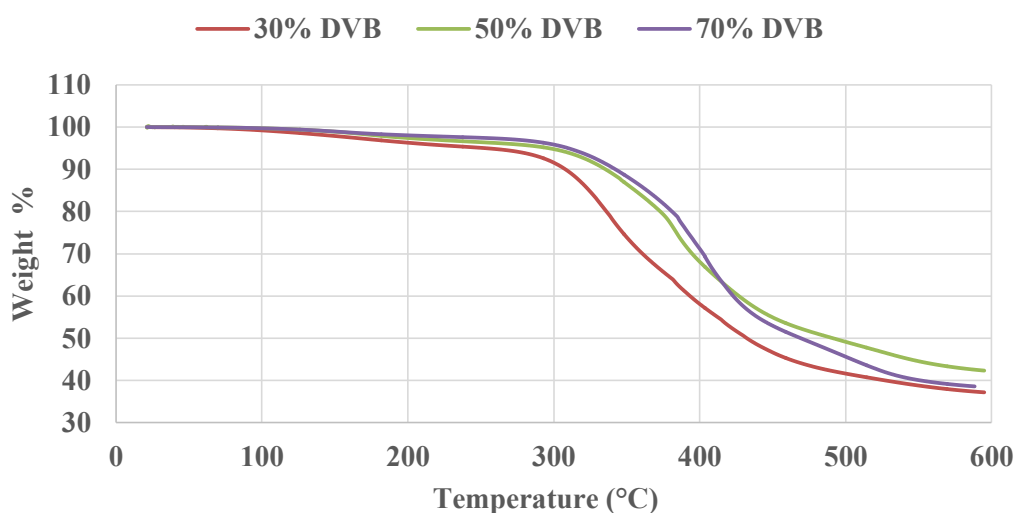
Figure 5.11 TGA analysis of (PANI-DBSA)[RM]/DVB composite with different wt. % of DVB[47].

Higher the amount of Poly-DVB present, higher the stability until 400°C, which shows that poly-DVB is much stable than uncured DVB. However, the loss after 400°C is higher in the composite with higher concentration of the DVB, indicating that the poly-DVB start degrading after 400°C. The sharp decrement from 400-600 °C is due to the degradation of bound poly-DVB and therefore steeper slope of weight loss in case of higher DVB ratio can be seen. The later part of weight loss can be attributed to the decomposition of PANI and also undecomposed poly-DVB.

5.8   Discussion

(PANI-DBSA)[RM]/DVB composite has been prepared using roll-milling process. Using this manufacturing technique we prepared semi-doped PANI-DBSA complex to achieve longer liquid state of PANI-DBSA/DVB matrix before its polymerization starts. Finally, very good liquid state duration was achieved. However, electrical and mechanical properties of (PANI-DBSA)[RM]/DVB composite are lower than (PANI-DBSA)[CM]/DVB composite. The reason for low electrical conductivity of roll-milled composite can be explained in following two reasons.

1.   Small agglomerations of PANI-DBSA dispersed very well inside insulating DVB matrix and couldn't reach percolation threshold.

2.   There is a trade-off between PANI and DVB for DBSA protons and at higher temperature it is easy for stretched PANI (semi doped) to dedope (detachment of PANI and DBSA). Therefore, deprotonation of PANI in the presence of uncured DVB is the main reason for such behaviour.

In the starting of the chapter we introduced the scavenging effect of doped PANI, which hinder the radical polymerization of DVB. In roll-milling process PANI-DBSA is found to be in semi doped stage as verified with UV-vis-NIR spectra. This semi-doped PANI slow down the polymerization of DVB and hence at the same curing profile of (PANI-DBSA)^{RM}/DVB composite exhibit lower mechanical properties than (PANI-DBSA)^{CM}/DVB composite. And also account for the longer liquid state duration. These behaviours were investigated using different characterization techniques.

Semi-doped PANI-DBSA complex obtained after roll-milling process have shown better miscibility as well. The reason for better dispersion of PANI-DBSA into DVB matrix can be attributed to the attachment between PANI and DBSA molecules and surfactant properties of DBSA.

Thermal stability of all the component and composites were investigated using TGA analysis and it was shown that PANI-DBSA/DVB composite is thermally stable up to 300 °C.

Chapter 6   VGCF as additional filler with PANI

Polyaniline (PANI) based electrically conductive thermosetting hybrid nanocomposite has been prepared by incorporating high apparent-density type vapour grown carbon fibers (VGCF-H) as additional conductive filler. The main conducting component of the matrix is still PANI, protonated with a protonic acid, dodecylbenzenesulfonic acid (DBSA). Divinylbenzene (DVB) is used as a cross-linked thermosetting polymer as explained in chapter 4 and 5. With addition of VGCF-H higher electrical conductivity and better mechanical properties have been achieved. Different weight percentages of VGCF-H in the PANI-DBSA/DVB matrix, were used and their effect on composite's properties have been investigated. Electromagnetic interference (EMI) shielding properties of composite with and without VGCF-H are measured in X-band frequencies and compared in following chapters. The effect of dispersion on electrical and mechanical properties also has been explained using SEM micrographs. The results of this study confirmed that a polymer thermoset conductive composite with improved electrical, mechanical and EMI shielding effectiveness has been successfully prepared.

6.1   PANI-VGCF nanocomposite

We demonstrated a unique one-step synthesis process of PANI-DBSA/DVB composite in previous chapters while choosing divinylbenzene (DVB) as the resin system. It was demonstrated that a PANI-DBSA/DVB composite has very high electrical and good mechanical properties. However, we struggled to get a longer liquid state duration. We found that roll-milling process is very effective to achieve longer liquid state duration but electrical and mechanical properties reduced in that case. Therefore we wanted to retain longer liquid state duration with good electrical and mechanical properties as well. Xiuyan et al.[76] from our group tried to improve the properties by adding additional graphene oxide (GO) in to PANI-DBSA/DVB system. She found that electrical and mechanical properties could be improved by adding GO in to the system.

In the present work I tried to improve the electrical and mechanical properties of the PANI-DBSA/DVB system by adding additional filler namely vapour grown carbon fibers (VGCF-H). VGCF-H has been chosen due to its high electrical properties, easy handling, availability and ability to disperse easily. The idea of using VGCF-H is inspired by the hypothesis that PANI-DBSA agglomerates are the conductive islands in the insulating DVB matrix. Therefore, VGCF-H can be used as the connective conductive bridge between those islands and also improve the mechanical properties.

A highly conductive composite material with good mechanical properties is the demand of present industrial and academic fields. Therefore, I tried to prepare a thermoset conductive composite with high mechanical and electrical properties with longer liquid state duration. The same composite also has shown remarkable EMI shielding behaviour attributable to its conductive nature presented in chapter 9.

6.2   Preparation of PANI-DBSA-VGCF/DVB composite

It has been reported in previous chapter that undoped PANI-DBSA complex is very difficult to use directly to obtain an longer liquid state of matrix (longer curing time at room temperature) using DVB cross-linked polymer due to the exothermic reaction between DBSA and DVB. Therefore we suggested to use semi-doped PANI-DBSA complex to obtain an environmentally stable matrix by using roll-milling process. In addition to that, we propose that we can obtain a semi-doped PANI-DBSA complex even by mixing in centrifugal mixer by utilizing the heat generated during mixing.

In this chapter we have used centrifugal mixing again and optimized the mixing parameters to get a semi-doped PANI-DBSA complex due to heat generated after mixing VGCF-H. VGCF-H has high aspect ratio therefore, more heat is generated during centrifugal mixing with the addition of more amount of VGCF-H. To obtain a good dispersion of VGCF-H into the final composite, VGCF-H was first mixed with DBSA to obtain a good homogenous DBSA-VGCF-H complex. PANI was further added to the DBSA-VGCF-H complex and mixed in a centrifugal mixer. Due to the heat generated during the centrifugal mixing, PANI got semi-doped and hence PANI-DBSA-VGCF/DVB matrix with longer liquid state could be prepared.

The matrix was further poured into a mould and put in a hot-press machine for 2.5 hours at 120°C. In all of the samples, PANI-DBSA was maintained at 1:0.6 Molar ratio. Please note the change in curing profile here, we found in previous chapter that 2hrs curing time was not sufficient with semi-doped PANI-DBSA complex to cure DVB completely. Also to use centrifugal mixing we choose 1:0.6 Molar ratio of PANI and DBSA to limit the excessive free DBSA protons. DVB wt. % was fixed as 50 wt. % of the total composite. 1, 3 and 5 wt % of VGCF-H were added to prepare different samples. Hypothesis and scheme to use VGCF and manufacturing scheme has been shown in the **Figure 6.1**.
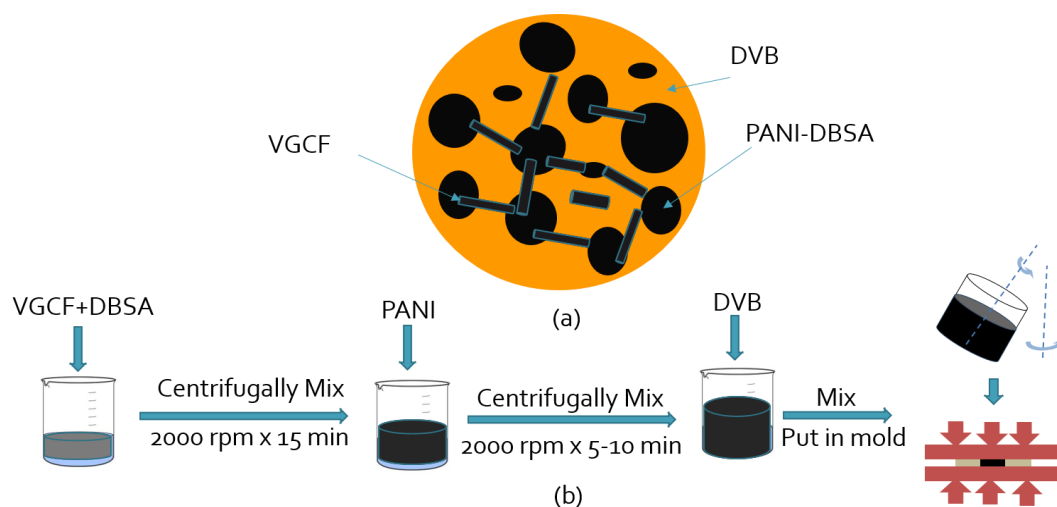
Figure 6.1 (a) Hypothesis (b) Scheme to prepare PANI-DBSA-VGCF/DVB composite.

6.3   PANI-VGCF nanocomposite

6.3.1 Electrical Conductivity

Electrical properties of the composites w.r.t. the VGCF-H content was measured and compared with the neat PANI-DBSA/DVB composite. For comparison purpose 50% DVB was fixed and the VGCF-H amount was varied while making the composite samples. It has been found that with the increase in VGCF weight percentage in the composite there is a significant improvement in the electrical properties. With the 5 wt. % of the VGCF, electrical conductivity

was 1.97 S/cm as compared to 0.27 S/cm in the composite without VGCF.

6.3.2 Mechanical properties

Similarly, Flexural Modulus was also improved with the addition of VGCF in to the matrix. Increase in the flexural modulus was observed with the increase of VGCF-H content in the composite up to 3%. However, the modulus of the composite with 5 wt. % VGCF was decreased. This behavior could be attributed to the poor dispersion of the VGCF in the matrix. Agglomeration of VGCF-H could be another reason for the decrement in the flexural modulus of the composite, which is also supported by the SEM investigation. Electrical and mechanical properties of the composites are shown in **Figure 6.2.**

PANI-DBSA-VGCF/DVB (50% DVB)
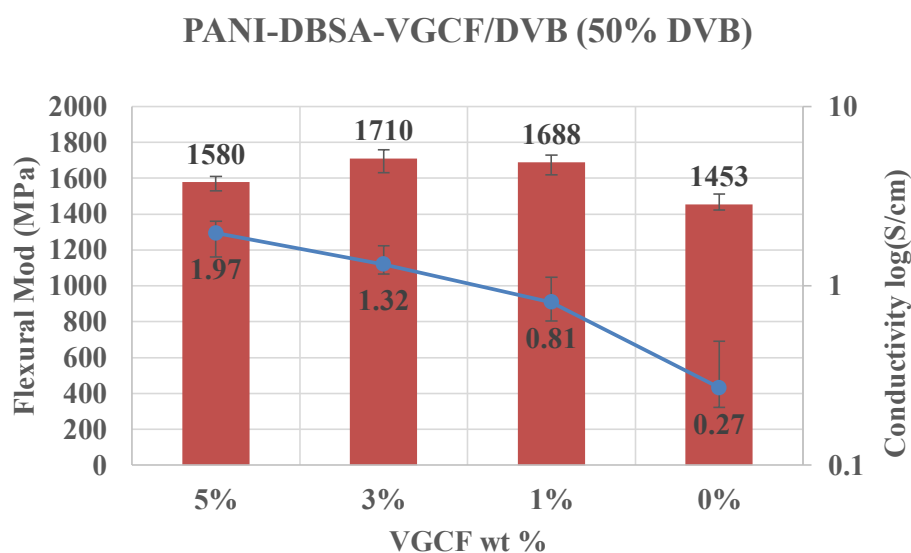
Figure 6.2 Flexural modulus and electrical conductivity of PANI-DBSA-VGCF/DVB composite w.r.t VGCF wt. %.

6.3.3 SEM analysis

The morphologies of the PANI-DBSA-VGCF/DVB composite were studied and compared using SEM as shown in **Figure 6.3**. Connecting conductive networks can be seen clearly from the micrographs with the increase in the VGCF weight percentage, contributing to the improved electrical properties.

(a)

(b)

Agglomerations

(c)

(d)

(e)
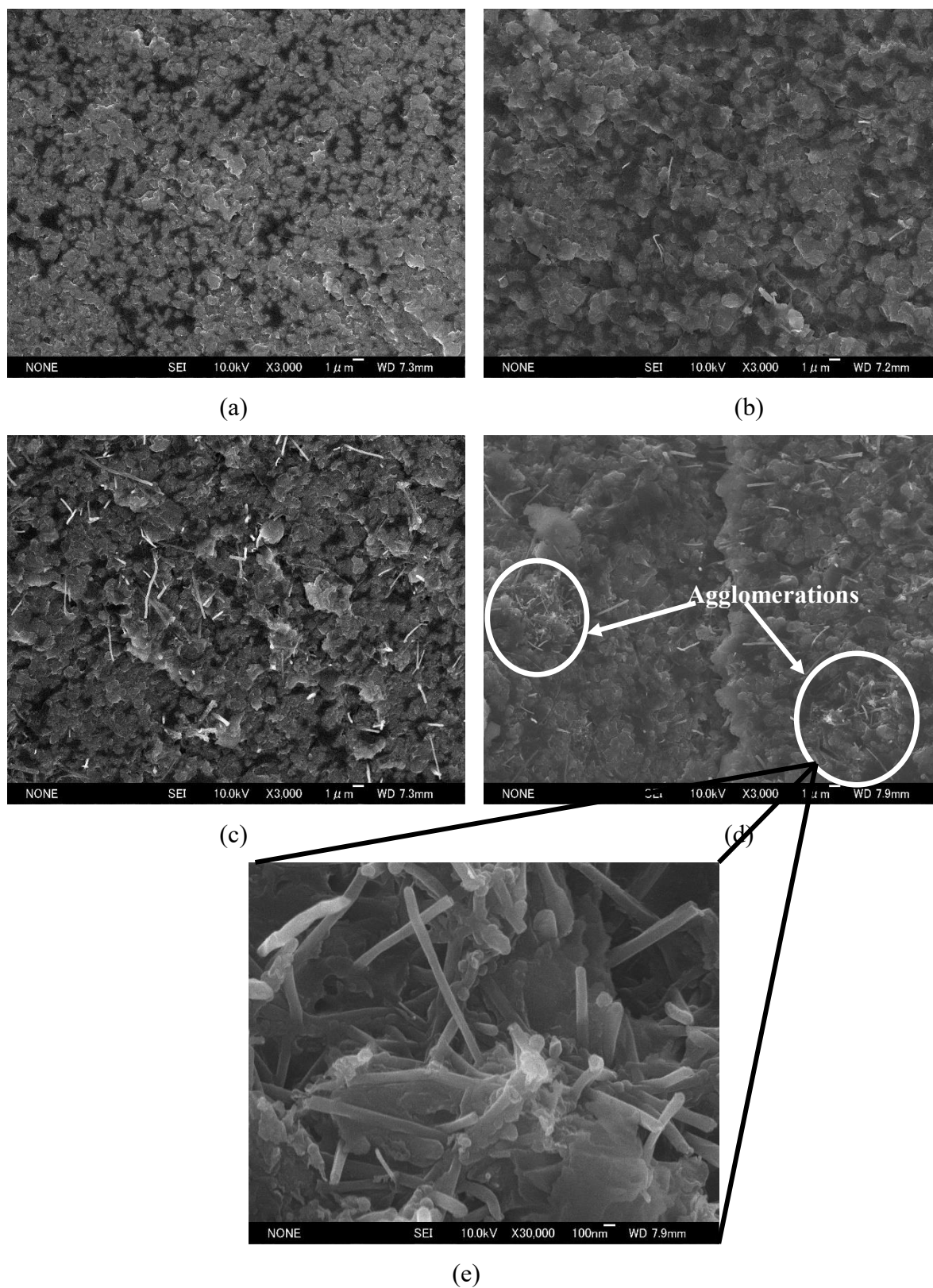
Figure 6.3 SEM micrographs of PANI-DBSA-VGCF/DVB composite w.r.t VGCF wt. % in the composite (a) 0% (b) 1 % (c) 3% (d) 5% (e) VGCF agglomeration.

VGCF agglomerates are also very much visible in the composite with 5 wt. % of VGCF. As we have seen a decrement in the mechanical properties of the composite with 5 wt. % of VGCF-H, the SEM micrographs confirm our hypothesis that this reduction could be due to the formations of VGCF agglomerations. VGCF-H dispersion is one of the most important factor to improve overall properties of the composite. With the higher VGCF-H wt. % in the composite, the viscosity of the matrix increases substantially. Therefore composite with 3 wt. % of VGCF-H is optimum for better electrical and mechanical properties.

6.4   Discussion

A highly conductive PANI-DBSA-VGCF/DVB hybrid nanocomposite was prepared and analysed in this chapter. It was shown that the electrical and mechanical properties of the composites improved significantly with the addition of the VGCF in PANI-DBSA/DVB composite. Improved electrical conductivity can be explained by the highly conductive nature of VGCF-H and formation of a 3-D electrical conductive network, as can be seen using SEM. However, change in flexural modulus with the addition is complicated due to increment up to 3 wt% and then reduction at 5 wt% of VGCF-H. It was found that the flexural modulus of PANI-DBSA-VGCF/DVB hybrid nanocomposite is improved to 1.71 GPa at 3 wt. % loading of VGCF-H in to the composite with 50wt% DVB. Beyond 3 wt. % of loading, slight decrease in the flexural modulus is observed due to agglomerations, but it is still higher than the pure PANI-DBSA/DVB composite. Similar behaviour was reported in case of MWCNT filled epoxy in flexural strength[77]. But reduction in flexural modulus could be due to the change in curing behaviour due to the addition of additional filler. It has been reported in literature that at higher loading of filler, curing process slows down[78]. The reduction in flexural modulus with higher loading of VGCF-H in to the system, might be due to the incomplete curing of DVB. Detailed DSC analysis should be done to find the answer of this problem, however at the time of writing this thesis due to the unavailability of DSC analyzer and time, this work will be completed in future. The micrographs obtain by SEM has confirmed that VGCF-H acts as a connecting bridge between the conductive PANI-DBSA islands in insulating DVB matrix. This 3-D electric conducting network can be assigned for the improved electrical conductivity in the composite.

Chapter 7   Dedoping phenomenon

A significant difference in the conductivity and mechanical properties of PANI-DBSA/DVB composite has been found with different curing time and curing temperature. To investigate this problem, a thorough parametric study has been carried out and the reason for such behaviour was sought out. Incomplete polymerization of DVB and dedoping phenomenon of PANI was found to be the main reason for low mechanical and electrical properties respectively. In this chapter, effect of curing time and curing temperature has been reported. Experimental results were verified by analytical study as well.

7.1   Effect of curing time

It was observed that electrical conductivity of PANI-DBSA/DVB composite samples mainly depends on curing time. This phenomenon was consistent in both manufacturing techniques i.e. centrifugal and roll-milling. To understand this behaviour we cured the samples for different time duration. We prepared samples using both the methods as explained in chapter 4 and chapter 5 respectively. For comparison, composite with 50 wt. % of DVB were taken in both the cases. All other parameters were kept constant with curing time being the only variable. It has been found that electrical conductivity is inversely proportional to the curing time of the composites as shown in **Figure 7.1.** However, (PANI-DBSA)^{RM}/DVB composite has shown rapid decrement in the electrical conductivity w.r.t curing time. This could be attributed to the fact that in roll-milled samples DVB takes longer time to cure and due to trade-off between PANI and DVB for DBSA protons, electrical conductivity decreases at a faster rate as compared to (PANI-DBSA)^{CM}/DVB composite. (PANI-DBSA)^{CM}/DVB composite cures faster, therefore there's no more competition between PANI and DBSA for free protons. However separation of PANI and DBSA protons due to thermal treatment is also another reason. This phenomenon becomes even more prominent when PANI is in its stretched conformation (semi-doped state). Therefore rate of separation of DBSA protons from PANI chain at high temperature is high due to extended conformation of PANI in roll-milled samples.

The change in molecular structure of PANI at high temperature is also has been reported in past and therefore could be another reason of reduction in electrical conductivity of PANI-DBSA at higher temperature. Thermal degradation of PANI has been reported in literature[59,61,79].
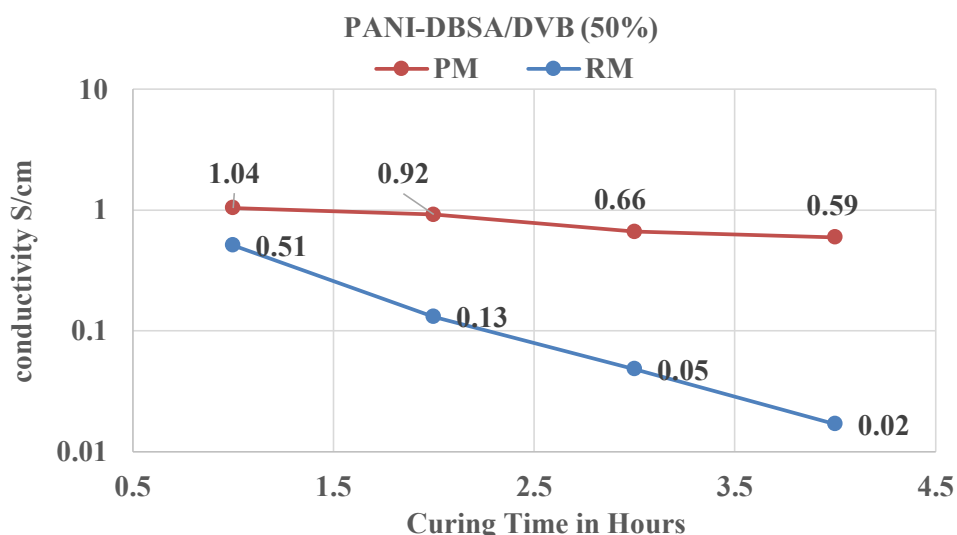
Figure 7.1 Effect of curing time on electrical conductivity of PANI-DBSA/DVB composites prepared by centrifugal mixing and roll-milling method.

To verify curing time based dedoping, UV-vis-NIR spectra have been conducted and analyzed. It has been shown in our previous work that UV-vis-NIR spectra does not change w.r.t to curing time in case of (PANI-DBSA)^{CM}/DVB[24]. In present work, to understand the dedoping process in the system, we measured the UV-vis-NIR spectra of (PANI-DBSA)^{RM}/DVB composite with 70 wt.% DVB composition. The sample was subjected to thermal treatment of 120°C for two hours and UV-vis-NIR spectra were measured after 0, 10, 60 and 120 minutes of heating as shown in **Figure 7.2**.

UV-vis-NIR spectra can be used very effectively to know the extent of doping of PANI. It is known that after doping imine peak of PANI changes its location and the ratio of imine peak (at 800 nm) to the amine peak (at 320 nm) can be used to find the degree of doping. We observe that the peak at 780 nm continued to reduce w.r.t curing time. Therefore, by analyzing **Figure 7.2** we can infer that degree of doping of (PANI-DBSA)^{RM}/DVB composite reduces w.r.t curing time due to deprotonation of PANI. Also in literature it has been mentioned that

overlapping of $\pi \rightarrow \pi^*$ at 320 nm peak with that 420 nm peak of DBSA to form a flat and/or distorted single peak indicates a high level of doping[80]. This peak also gets divided into two peaks after longer thermal treatment clearly showing the detached PANI and DBSA, thus confirming the dedoping of PANI.
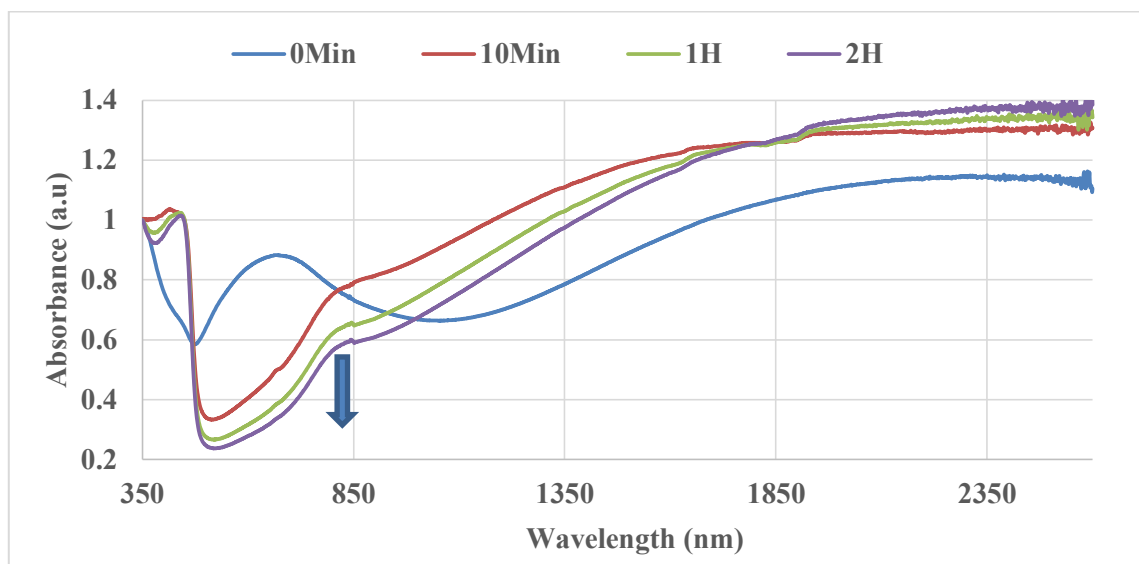
Figure 7.2 UV-vis-NIR spectra of (PANI-DBSA)[RM]/DVB composite w.r.t curing time.

7.2 Effect of curing temperature

To understand the effect of curing temperature two similar samples of (PANI-DBSA)[RM]/DVB composite were chosen and subjected to two different curing temperatures. It was found that the rate of electrical conductivity decrement was higher with high curing temperature as shown in **Figure 7.3.** Sample cured at 100 °C shows very high electrical conductivity compared to the sample cured at 120 ° C. Rapid decrement in the electrical conductivity with higher curing temperature can be assigned to the dedoping of PANI at high temperature. Higher the temperature higher the dedoping rate. **Figure 7.3** represents the experimental values of electrical conductivity w.r.t two different curing temperatures.

To confirm the experimental results UV-vis-NIR spectra were obtained for the similar samples with similar conditions as shown in **Figure 7.4**. Two samples of (PANI-DBSA)[RM]/DVB composite were chosen and subjected to 120°C and 150°C for 1 hour and analysed using UV-

vis-NIR spectroscopy. In case of sample cured at 150°C the peak after 850 nm decreased drastically as compared to the sample cured at 120°C. Peak at 350 nm also got more distorted. Suppression of free tail after 1000 nm, suggested the reduced electrical conductivity. These results confirm the aforementioned experimental results.
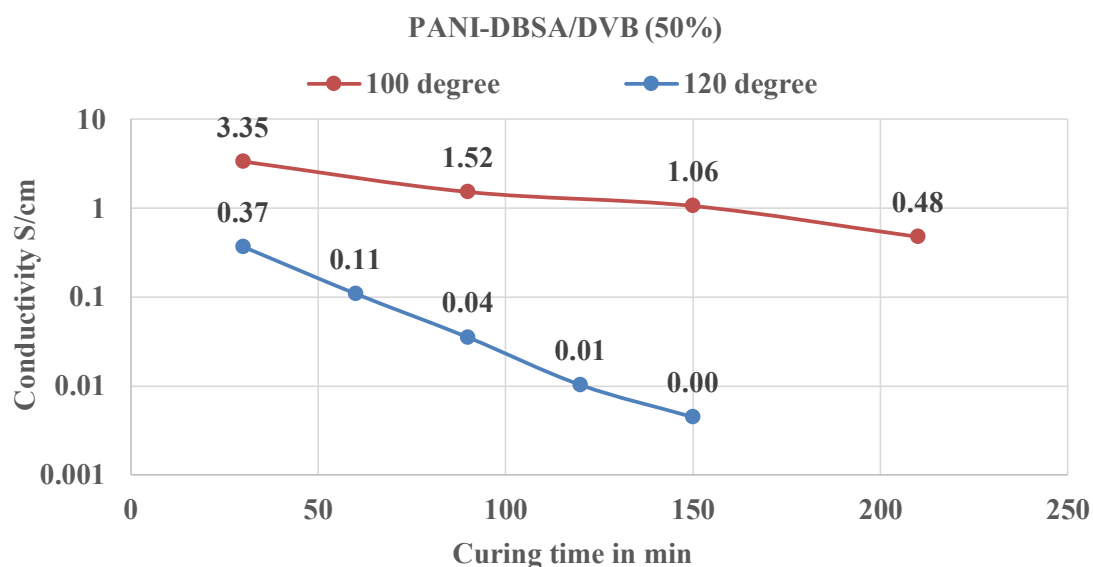
Figure 7.3 Effect of curing temperature on electrical conductivity of PANI-DBSA/DVB composites.
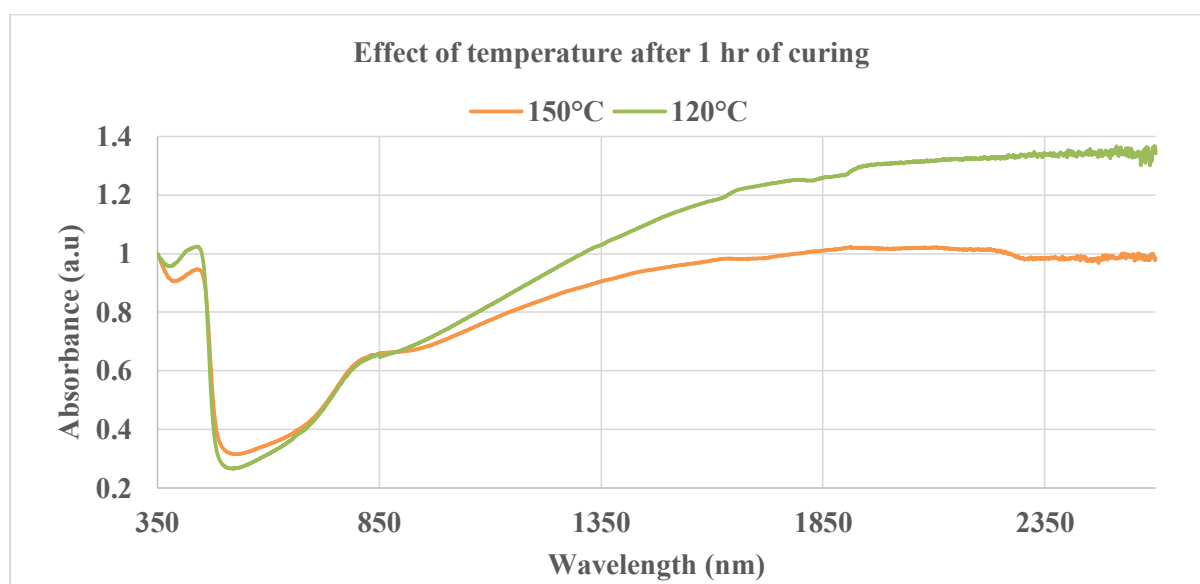
Figure 7.4 UV-vis-NIR spectra of (PANI-DBSA)[RM]/DVB composite with different curing temperature.

7.3   Thermal optical microscopy

Another technique of thermal optical microscopy was also used to understand the temperature based doping and dedoping phenomena of PANI-DBSA/DVB composite. (PANI-DBSA)^{CM}/DVB complex was observed in thermal optical microscope while increasing the temperature at the rate of 10 °C/min. (PANI-DBSA)^{CM}/DVB mixture with higher DVB content was chosen to reduce the viscosity of the PANI-DBSA complex. Pictures were taken at regular interval of time & temperature as shown in **Figure 7.5**. As discussed in section 1.1.1 upon complete doping emeraldine base form of PANI (characterize by the dark blue colour) changes in to emeraldine salt form (characterized by the green colour). The colour of PANI-DBSA complex can be used to characterize the doping extent. As seen from the figure below, until 80 °C there is little change in the color of the complex. Complex turn completely green at 120°C confirming the doping process. After 120°C the color began to change again pointing towards the dedoping phenomenon. Results obtained from thermal micrographs confirm the experimental results. It should be mentioned that DSC would be a better technique to determine the exact doping temperature.
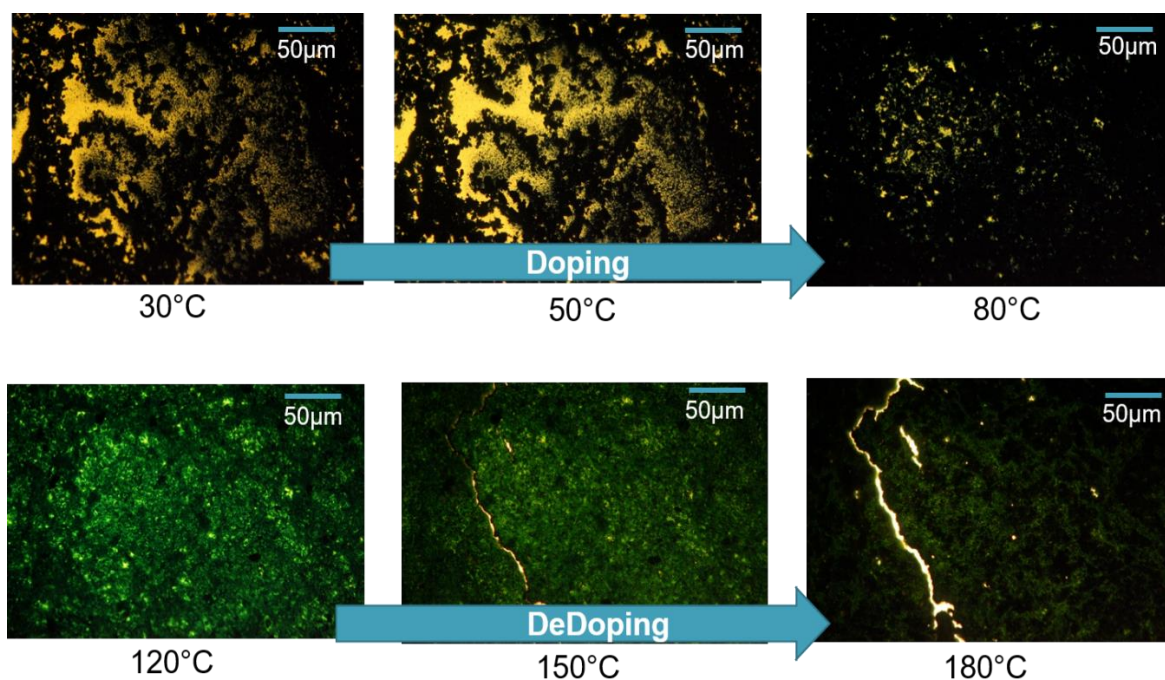
Figure 7.5 Thermal optical images of (PANI-DBSA)^{RM}/DVB composite w.r.t curing time and curing temperature.

7.4   Discussion

Electrical and mechanical properties of PANI-DBSA/DVB composite depend on curing time and curing temperature. Therefore, fixed curing profile is necessary to obtain the repeatability of the samples. In this chapter dedoping effect in (PANI-DBSA)^{RM}/DVB composite was explained using different techniques. It is shown that dedoping is higher at high temperature and in chapter 3 we showed that 120 °C is the optimum temperature and is re-established here.

The difference in values of electrical conductivity of PANI-DBSA/DVB composite with different wt % of DVB is due to the different manufacturing process and different curing profiles. However, rather than the exact numbers, a pattern or trend was tried to find in this chapter. Therefore, it is possible to have little different values of electrical conductivity values as compared to the one presented before. But this change is very little and can be overlooked.

PART II – Structural applications of FRPs prepared by using conductive thermosetting matrix

Chapter 8   PANI-based conductive FRPs

In the past, the mixture of PANI-DBSA has been used as conductive fillers with different insulating polymers like polystyrene (PS), polyamides and epoxy resin to prepare conductive polymer composites. Electrically conductive FRPs composites also have been prepared using conventional fillers such as CNT and carbon black etc[81–83]. For example, Vavouliotis A. et al.[84] used the MWCNT to prepare the conductive CFRP and used electrical change method to determine the fatigue life prediction of the CFRP laminates. Similarly Song D.Y. et al.[85] utilized the correlation between mechanical damage behavior and electrical resistance change in the CFRP composites as a health monitoring sensor. They conducted experiments and confirmed the results that the value of residual electrical resistance was dependent on the maximum strain applied. Yokozeki et al.[86] and Hirano et al.[87] showed the effectiveness of conductive composite in supressing the effect of thunder lightning strikes.

The problems related to low conductivity value and complicated manufacturing process to prepare thermoset conductive FRP composite have been addressed in this work using conductive thermosetting matrix explained in previous chapters. In most of the cases epoxy with different conductive filler have been used in the past. However, this is the first time when is used DVB as cross-linking thermoset polymer to prepare the FRPs. Very limited work has been done to enhance the through thickness conductivity of FRPs in literature. We have tried to obtained high electrical conductivity in through thickness direction of CFRPs and GFRPs.

8.1   Sample preparation

It was observed that, polymerization of DVB starts immediately in case of centrifugally mixed (PANI-DBSA)^{CM}/DVB matrix as explained in chapter 4 and hence it could not be used to impregnate FRPs. In chapter 5, we explained that (PANI-DBSA)^{RM}/DVB matrix has longer liquid state duration. Therefore (PANI-DBSA)^{RM}/DVB matrix has been used to impregnate carbon fabric and glass fabric cloths in the present work. Roll-milled PANI-DBSA complex with fixed molar ratio has been used with different weight percentage of DVB (30%, 50% and

70%) with corresponding weight percentage of PANI content (21%, 15% and 9%) and DBSA content (49%, 35% and 21%) respectively, to prepare 3 sets of PANI-DBSA/DVB matrices. The mixture of PANI-DBSA/DVB was further used as matrix to impregnate the carbon fabric cloth and glass fabric cloth using hand lay-up process as shown in **Figure 8.1**. The impregnated stacks of CFRP and GFRP were cured using hot-press machine for 2 hours at 120°C to prepare the final composites samples. 3 samples of each PANI-CFRP and PANI-GFRP have been prepared and samples of different dimensions were cut for various measurements (electrical & mechanical properties). Three samples for electrical conductivity measurement and three samples for mechanical properties measurement were used. Same samples have been used for morphological study. At higher DVB content, the viscosity of the solution became too low and the matrix drained down through the fabric. On contrary, lower DVB content results into highly viscous matrix which was very difficult to apply onto the fabrics with a shorter curing, leaving a very small window of time to apply the matrix to the fabric.
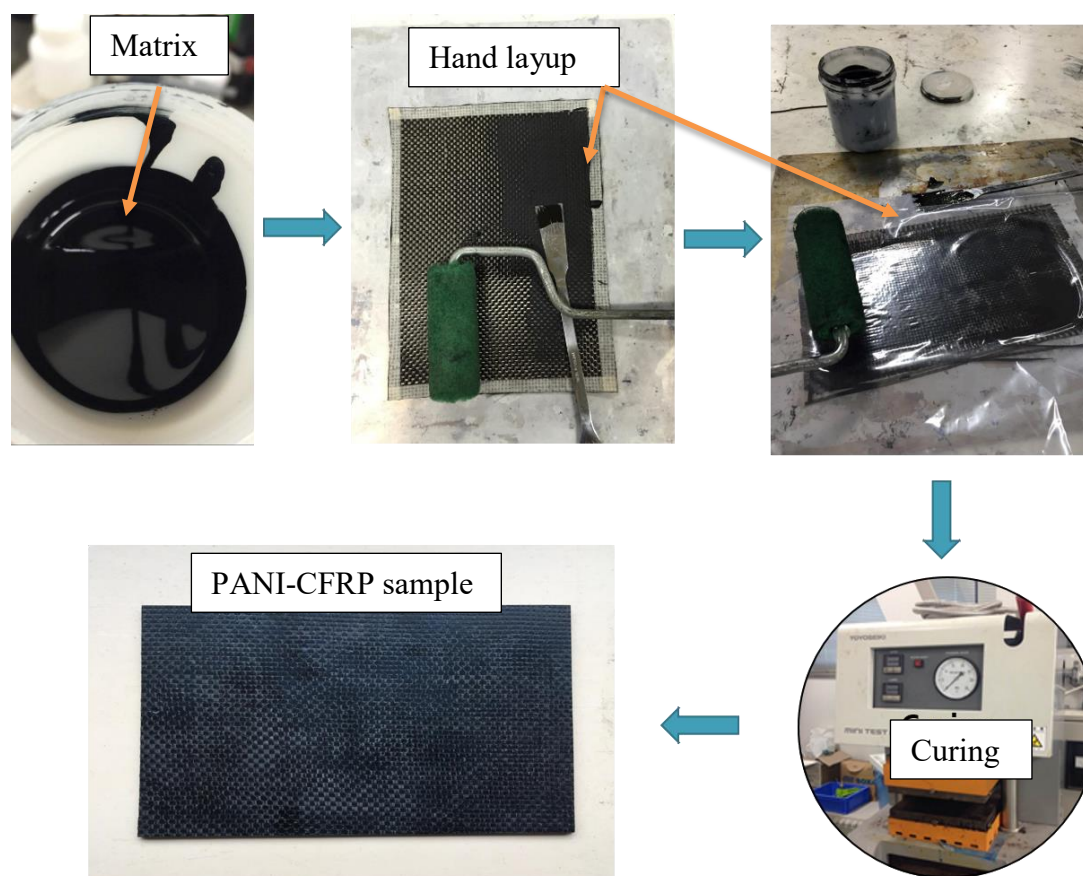
Figure 8.1 Hand layup process to prepare PANI-CFRP.

8.2   Electrical conductivity

Electrical conductivity of the PANI-CFRP composite samples and PANI-GFRP composite samples were measured and analyzed as a function of PANI content. The effect of PANI content on the electrical conductivity of the PANI-CFRP composite and PANI-GFRP composite has been shown in **Figure 8.2**. It can be clearly seen from the figure that the PANI-CFRP composite with 9 wt % of PANI exhibits a conductivity value of 0.80 S/cm, which is much higher than the conductivity reported in epoxy based conductive composites with different polyaniline morphology mentioned in the literature[82]. The value of conductivity of the conductive thermoset CFRP composites has been found to be higher than other thermoset conductive composites mentioned in literature[82,88]. Electrical conductivity of PANI-CFRP obtained in this work is almost 36 times higher compared to epoxy based CFRP in thickness direction. Similarly, 6 times higher in fiber direction as well. It has been observed that with the same amount of PANI content, PANI-GFRP composites samples show low electrical conductivity as compared to PANI-CFRP composite samples. Conductive nature of carbon cloth and non-conductive behavior of glass cloth can be attributed for such behavior. These promising results widen the scope of conductive composites for super capacitor, sensors and EMI shielding applications using strong conductive FRP composites.
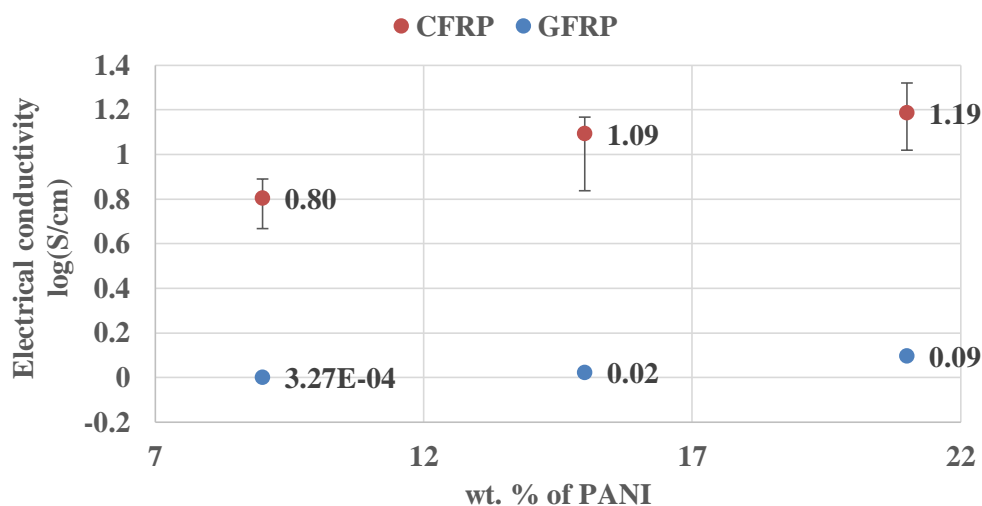
Figure 8.2 Electrical conductivity of CFRP & GFRP w.r.t PANI content.

It is evident from the plot that with the increase of the wt% of PANI-DBSA in both the composites, there is significant increase in the electrical conductivity. The effect of thickness

on the conductivity also has been studied. CFRP samples with different thickness i.e. 2.5 mm and 1 mm have been prepared and their electrical conductivity was compared as shown in **Figure 8.3**.
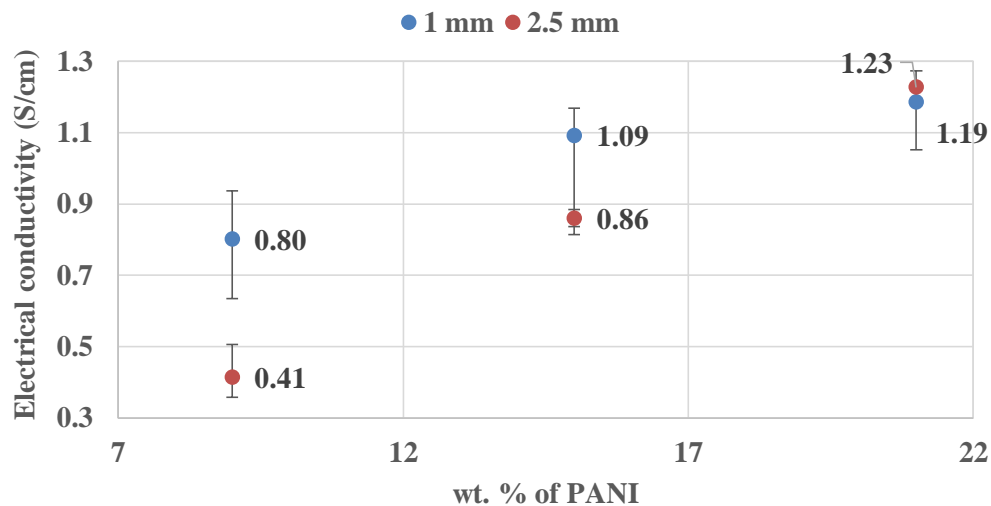
Figure 8.3 Electrical conductivity of CFRP with 1 mm and 2.5 mm thickness w.r.t PANI content.

It can be seen from the plot that with 30% of DVB content there is not any significant change in the conductivity. On the other hand, with the increase in the DVB content the electrical conductivity reduced in the 2.5 mm thick sample as compared to 1 mm thick samples. The reason for such behavior could be the low viscosity of the PANI-DBSA/DVB mixture at higher content of DVB, and hence the matrix might have drained down to the bottom of the 2.5 mm thick CFRP samples, creating a non-uniform distribution of the matrix in the samples. Therefore, it should be noted that the manufacturing process and controlled parameters like curing temperature and curing time are also very important factor to have consistent electrical conductivity results. 50-60 wt% DVB is the most suitable for conductive structural applications.

8.3 Mechanical properties

The flexural properties of the composites have been determined using 3-point flexural testing as explained in section 2.2.2. **Figure 8.4** and **Figure 8.5** show the load-deflection curve for

PANI-CFRP composite and PANI-GFRP composite, respectively. As it can be seen from the plots that both the composite samples do not demonstrate brittle failure and fail more gradually as compared to epoxy based CFRP composites. The failure in both the cases is not catastrophic or brittle as is the case with epoxy based composites. This behavior can be assigned to the incomplete curing of matrix. The failure mainly occurs due to the delamination between the layers on the application of the load on composite or matrix failure.

It has also been observed that PANI-CFRP composite with the composition of 30 wt. % of DVB, shows a flexural modulus of 33.45 GPa which increases up to 43.06 GPa with the 50 wt. % of DVB. Similarly, PANI-GFRP composite with the composition of 30 wt % of DVB, shows a flexural modulus of 11.12 GPa which increases up to 14.50 GPa with the 50 wt. % of DVB as shown in the **Figure 8.6**. The value of flexural modulus of the PANI-CFRP composite with 50 wt % of DVB is quite comparable to flexural modulus value of epoxy resin based CFRPs. As expected, the flexural modulus of PANI-GFRP composite is very low as compared to PANI-CFRP composite. These results show that a CFRP & GFRP can be made conductive with good mechanical properties, by using PANI-DBSA/DVB conductive thermoset mixture as a matrix. The decrement in the flexural modulus with 70% DVB also confirms that due to the low viscosity of the mixture at high DVB content, the distribution of PANI-DBSA/DVB matrix is not uniform in the composite at higher concentration of DVB.
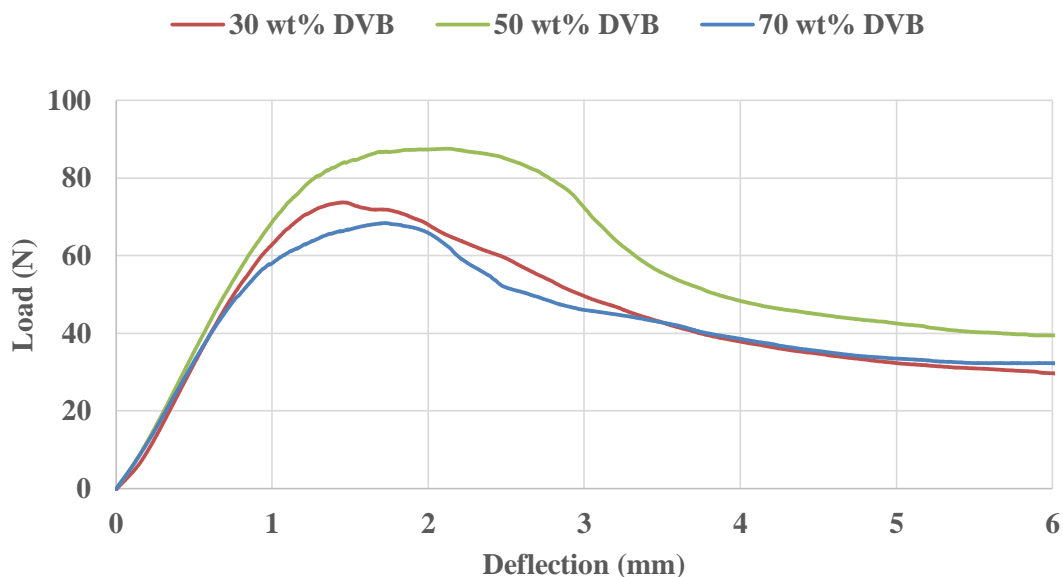
Figure 8.4 Load-deflection curve of PANI-CFRP composite with different wt % of DVB.
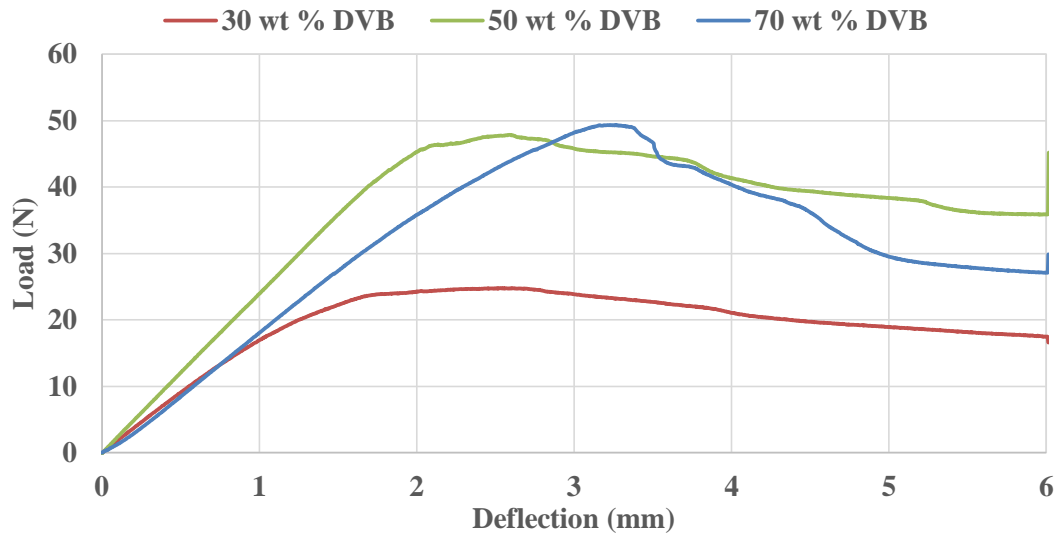
Figure 8.5 Load-deflection curve of PANI-GFRP composite with different wt. % of DVB.
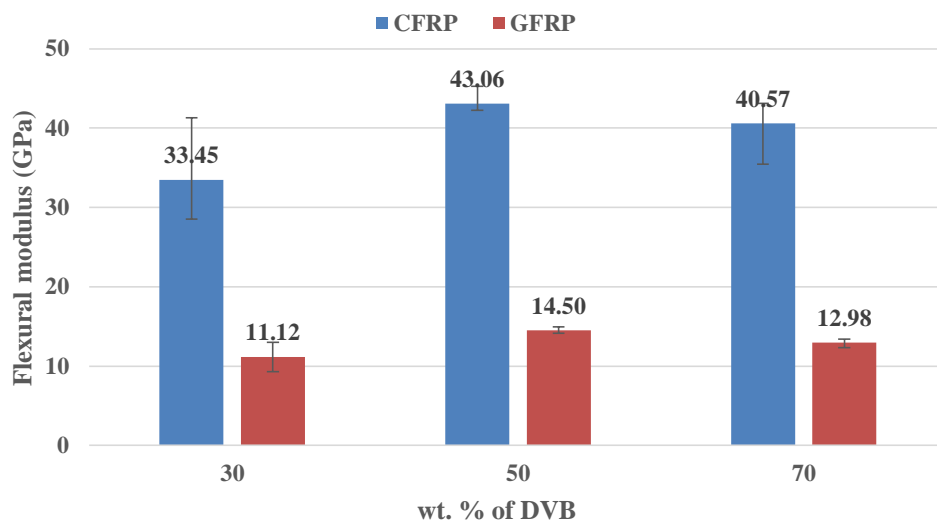
Figure 8.6 Flexural modulus of CFRP with 2.5 mm thickness & GFRP with 1.5 mm thickness w.r.t DVB content

8.4 ILSS test

To understand the interlaminar strength and properties, interlaminar shear strength test was conducted. Short beam three point bending test has been used to evaluate ILSS. JLS K7078

standard was followed. **Figure 8.7** shows the scheme of the ILSS test and equation 8.1 gives the ILSS value.
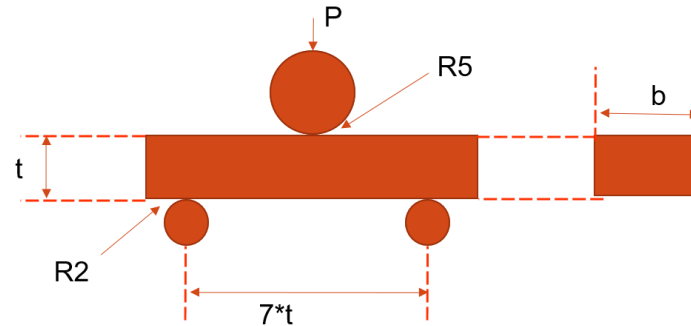
Figure 8.7 Scheme of the ILSS test.

$$ILSS = \frac{3}{4} \cdot \frac{P_{max}}{b.t}$$

(8.1)

Three-point bending test was performed using a load cell of 5 kN and crosshead speed of 1 mm/min. The radii of loading nose was kept at 5 mm and supports were kept at 2 mm. The total length, width and thickness of samples were taken as length 20 mm, width 10 mm and thickness 1.8 mm, respectively. While the span distance was taken as 13 mm. If there was any change in the thickness of the sample due to manufacturing process, the thickness to span ratio of 1:7 was kept constant.

ILSS value of CF/PANI was found to be 15.57 MPa. This value is good enough to use CF/PANI composites for structural application. However, the ILSS value lower than the CF/epoxy composites.

8.5   Morphological study

The surface and cross section of PANI-CFRP composite and PANI-GFRP composite have been studied using optical microscope. In **Figure 8.7**, the surfaces and the cross section (after failure) of PANI-CFRP composites with 30, 50 and 70 wt% of DVB content have been compared. For different DVB content, a great difference between the microstructures of the samples can be seen. At higher content of DVB, more homogenous surface can be obtained due to proper

dispersion of PANI-DBSA mixture in DVB. On the other hand, a low concentration of DVB results into a poor dispersion and hence agglomeration of PANI-DBSA blend in composite can be seen clearly in the images. **Figure 8.7** consist of two columns, first column shows the morphology of PANI-CFRP composite's surfaces with different DVB content and second column shows the PANI-CFRP composites cross section after failure after bending test. Images (a) and (b) in first column clearly identifies the PANI-DBSA and DVB phases in the composite samples.

It has been further observed that the surface properties of the composites improve significantly with the increase of DVB content in the composite. The electrical and mechanical properties can be well understood with the help of morphology. Higher concentration of conductive PANI-DBSA mixture account for the high conductivity at low DVB concentration, while good dispersion and dense cross-linking network at high concentration of DVB accounts for better mechanical properties. As can be seen from the figures that the phases between PANI-DBSA and DVB can be seen more clearly at low DVB concentration as compared to higher concentration of DVB. It can also be observed from the right column that the failure in PANI-CFRP with 30 wt% DVB and 50 wt% DVB is due to the crack formation in the matrix, while for PANI-CFRP with 70 wt% DVB, the failure occurred at the interface of matrix and carbon fabric. A more detailed study about the interface properties between matrix and fabric will be conducted in future.

PANI-CFRP surface

PANI-CFRP cross section

(a)

(a)
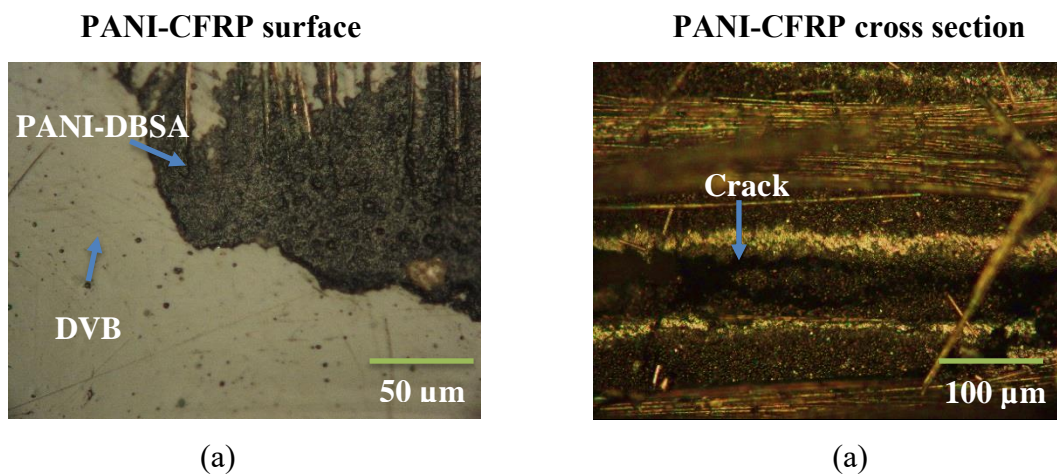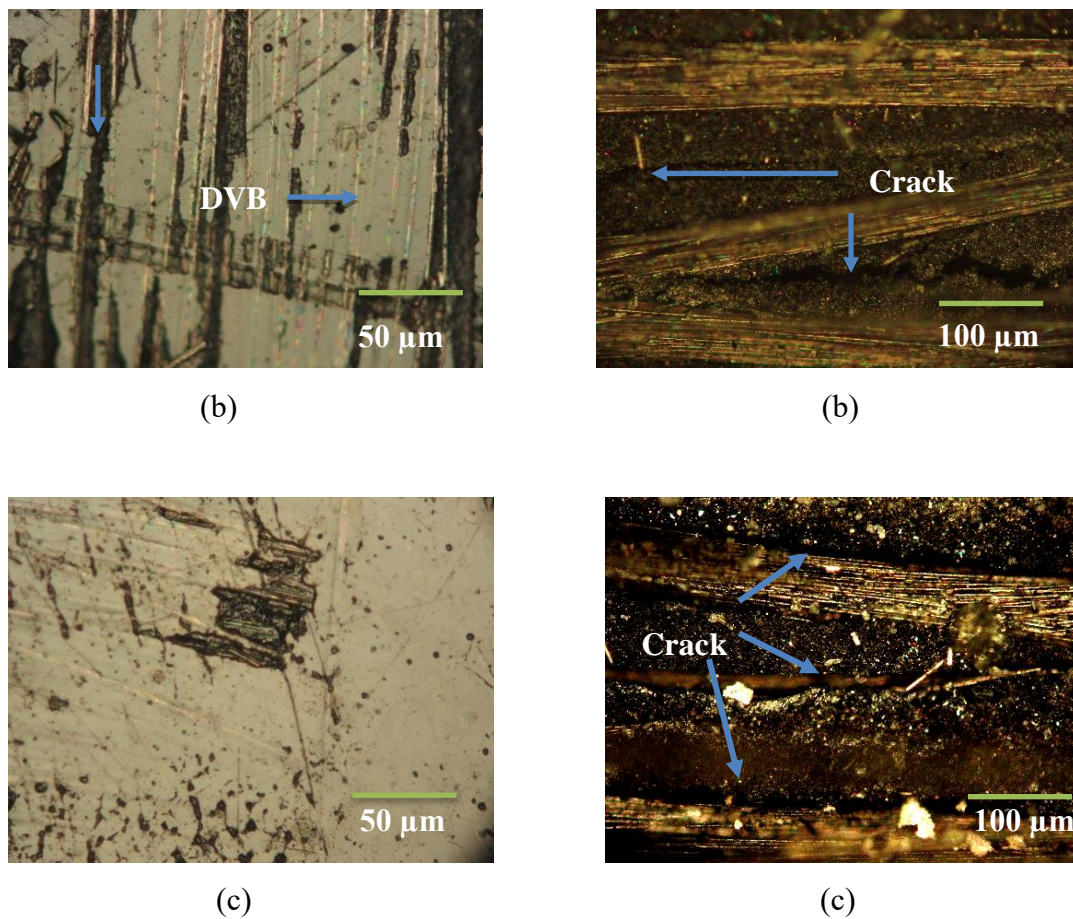
Figure 8.8 Optical microscope micrographs of PANI-CFRP composite surface and cross section with (a) 30 wt% of DVB content (b) 50 wt% of DVB content (c) 70 wt% of DVB content.

8.6   Discussion

In present chapter preparation of thermoset CFRP and GFRP composites with good electrical conductivity in thickness direction as well as good mechanical properties has been reported. This conductivity is much higher than the Epoxy based conductive composite mentioned in available literature. 36 times more in thickness direction and 6 time more in fiber direction. The change in electrical conductivity w.r.t DVB content was also presented and found that with higher PANI-DBSA content higher conductivity was obtained. However, the change in conductivity values in CFRP with different PANI-DBSA content is not so big. This could be due to the fact that even small amount of PANI-DBSA act as an electrical pass between

different carbon fabric layers. Means, the major electrical conductivity of the CF/PANI comes from the carbon fiber itself. In case of GFRP, the electrically conductivity is purely due to the conductive nature of matrix. Hence a huge difference w.r.t DVB content can be seen.

CFRP with 50 wt.% of DVB content shows flexural modulus of 43.058 GPa and then some reduction in CFRP with 70 wt.% of DVB content. This reduction in flexural modulus can be attributed to the low viscosity at higher DVB content and incomplete impregnation of fabrics. **Table 8.1** show the Comparison between PANI-based CFRP and epoxy based CFRP.

Table 8.1 Comparison between PANI-based CFRP and epoxy-based CFRP.

	CF/PANI	**CF/Epoxy**
Electrical Conductivity (Thickness direction)	~>1 S/cm	~0.027 S/cm
Electrical Conductivity (Fiber directions)	~150 S/cm	~25 S/cm
Flexural Modulus	49 GPa	54 GPa
Flexural Strength	250 MPa	600 MPa
ILSS	15.57 MPa	49.75 MPa

It is clear from the results that CF/PANI has shown remarkable improvement in electrical properties in both directions, longitudinal and transverse. However, lower mechanical properties of CF/PANI compared to CF/epoxy limits is application. To improve mechanical properties, a thorough study needs to be done in future. It is well known that carbon fiber are coated with special sizing for better compatibility with epoxy system. Same fabric were used to prepare CF/PANI samples and hence the compatibility of present sizing on carbon fabric and PANI-DBSA/DVB matrix could be the reason for such lower mechanical properties. The morphological study showed that the crack in CF/PANI was observed at interface and within matrix as well. Therefore, at this point of time it is very difficult to predict the exact interface properties of PANI-DBSA/DVB matrix with carbon fabrics. By desizing the carbon fabric, I could achieve some improvement in the mechanical properties of CF/PANI. This work is

intended to publish soon. Another reason for lower mechanical properties could be due to the inclusion of air voids during hand lay-up process. Improved manufacturing technique will be required in future to prepare high quality CF/PANI composites. From the results obtained in this chapter, it can be inferred that the PANI-based conductive thermoset CFRP and GFRP of the desired electrical and mechanical properties can be prepared by altering the content of PANI, DBSA and DVB. These PANI-FRPs can be used for conductive structural application in the field of thunder lightning strike protection and EMI shielding.

Chapter 9   EMI SE of PANI-based composites

The ability of a material to limit the amount of harmful EMI radiation from external environment is known as EMI shielding effectiveness. EMI is very common problems with the electronic components in daily life. EMI radiation from external environment can damage or malfunction the electronic properties of the concerned electric circuits. In general, radiation from outside of the product may couple with the electronics of the material and cause interference. The most common example is the weird sound from radio when a mobile rings near it. EMI SE material have a great demand in electronic market as well as in aerospace industry[89,90]. Usually metal based material are considered to be most effective for EMI shielding. We can say that the EMI shielding effectiveness of a material is its ability to stop the incoming EMI waves. EMI SE can be defined as the ratio of magnitude of incident EMI field to the magnitude of transmitted EMI field[91].

Theoretically, when a conductive material is placed inside an electromagnetic field, a counter filed is set up in the material. This electric field is setup due to the fact the opposite charge inside the conductive material align themselves in way to create electromagnetic field of their own. This electromagnetic field is opposite in polarity of applied field. Hence, total effect of external electric field get cancelled up to some extent. The thickness of the conductive material can vary according to the requirement. A conductive material with low permeability can be used for magnetic field shielding. Because eddy current generated in the conducting material will create alternating magnetic field with opposite orientation and therefore can as used for magnetic field shielding applications. Usually at higher frequencies high shielding properties are observed.

Shielding effectiveness (SE_T) can be expressed mathematically as shown below in **Equation 9.1**,

$$SE_T(dB) = 10\log_{10}\left(\frac{P_T}{P_I}\right) = 20\log_{10}\left(\frac{E_T}{E_I}\right) = 20\log_{10}\left(\frac{H_T}{H_I}\right) \qquad (9.1)$$

Where, P, E and H are the power, electric and magnetic waves respectively and subscript I and T denotes the incident and transmitted waves respectively. Usually shielding effectiveness is measured in (dB). Some of the common values are -20, -30 and -40, which represent attenuation of 99%, 99.9% and 99.999% respectively.

9.1   Shielding effectiveness: principle

Shielding effectiveness of a material is a combination of three mechanisms, called effectiveness due to absorption (A), reflection (R) and multiple internal reflections (M). Overall effectiveness is the sum of all these three parameters as shown in **Equation 9.2.**

$$SE_T(dB) = SE_A(dB) + SE_R(dB) + SE_M(dB)$$

(9.2)

These parameters are related to the intrinsic property of individual materials. In case when, shielding due to absorption is more than 10 dB, in that case shielding due to multiple reflection can be ignored. Materials with high shielding due to absorptions are considered to be very important in the field of stealth technology.

Graphical representation of shielding effectiveness of a material due to all aforementioned parameters is shown in **Figure 9.1.**
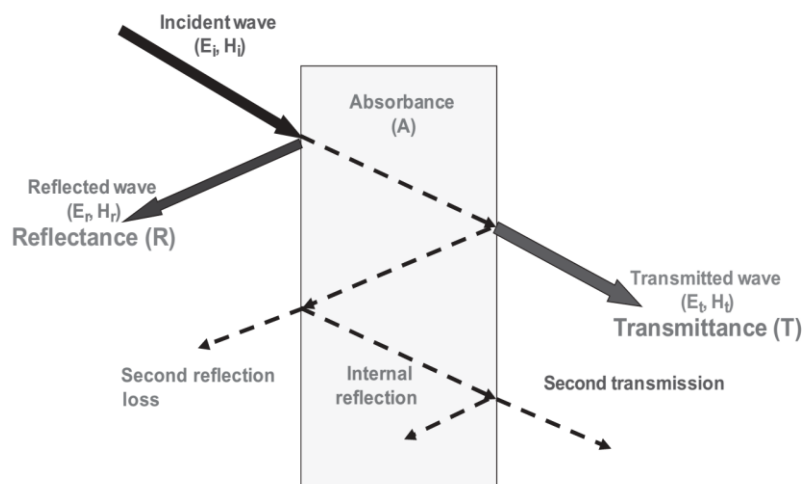
Figure 9.1. Scheme of total shielding effectiveness[91].

9.2 Shielding effectiveness: experiment

Shielding effectives was experimentally measured using an instrument called vector network analyser (VNA) as shown in **Figure 9.2**. VNA has two ports for incident and transmitted waves, it express the complex parameters using S parameters, which are S_{11}, S_{22}, S_{12} and S_{21}. First digit of the subscript number of S parameter represent incoming port and the second digit represent measuring port. For example S_{12} represent incident from port 1 and measuring at port 2.
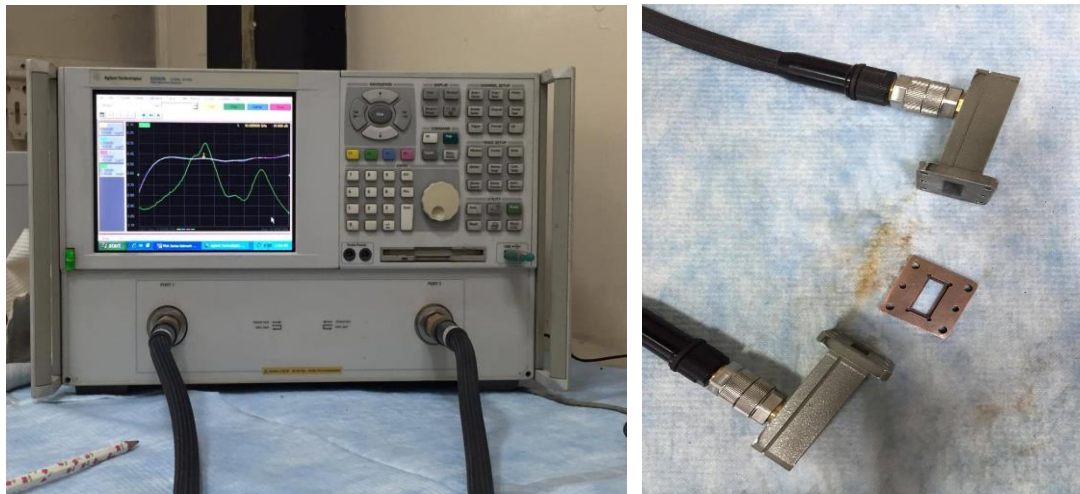
Figure 9.2. (a) Vector network analyser (VNA) (b) Sample holder (between 2 ports).

S parameters can be used to determine the reflectance (R) and transmittance (T) using simple equations as shown below.

$$R = \left|\frac{E_R}{E_I}\right|^2 = |S_{11}|^2 = |S_{22}|^2 \tag{9.3}$$

$$T = \left|\frac{E_T}{E_I}\right|^2 = |S_{12}|^2 = |S_{21}|^2 \tag{9.4}$$

Which gives the absorbance using following equation,

$$A = (1 - R - T) \tag{9.5}$$

However, after primary reflection from the surface of the material, effective EM wave enters inside the material is $(1 - R)$, hence effective absorbance can be expressed as,

$$A_{eff} = \frac{(1-R-T)}{(1-R)} \tag{9.6}$$

SE due to absorption and reflection can be expresses as

$$SE_R(dB) = 10\log_{10}(1-R) \tag{9.7}$$

$$SE_A(dB) = 10\log_{10}(1-A_{eff}) = 10\log_{10}\left[\frac{T}{(1-R)}\right] \tag{9.8}$$

Therefore, by measuring S parameters using VNA, we can calculate attenuation due to absorption$SE_A(dB)$ and reflection $SE_R(dB)$ respectively.

9.3   Shielding effectiveness: results

EMI shielding effectiveness (SE) of (PANI-DBSA)^{CM}/DVB composite, PANI-based CFRP & GFRP and PANI-DBSA/DVB composite with or without VGCF-H have been investigated in KU-band i.e. 12.4 GHz-18 GHz and also in X-band 8 GHz-12.4 GHz. **Figure 9.3** show the EMI SE of (PANI-DBSA)^{CM}/DVB composite samples prepared in chapter 4. Similarly **Figure 9.4** & **Figure 9.5** show the EMI SE of PANI-based CFRP and GFRP composite samples respectively prepared in chapter 8. Also EMI SE of composites with additional 5 wt. % of VGCF-H filler with PANI-DBSA/DVB is presented in **Figure 9.6.** EMI SE was found to be increasing with the PANI-DBSA content in the composite and reducing with the increase in DVB content. This behavior confirm the basic hypothesis that better electrical conductive materials exhibit better EMI SE properties.

We have shown in these results that PANI-based CFRP can be effective for EMI SE and therefore could be used as future stealth material. Maximum total EMI shielding effectiveness (SE$_T$) of pure PANI-DBSA/DVB composite, PANI-CFRP, PANI-GFRP and PANI-DBSA-VGCF/DVB composite were found to be 32(dB), 28(dB), 16(dB) and 73 (dB) respectively in KU-band.
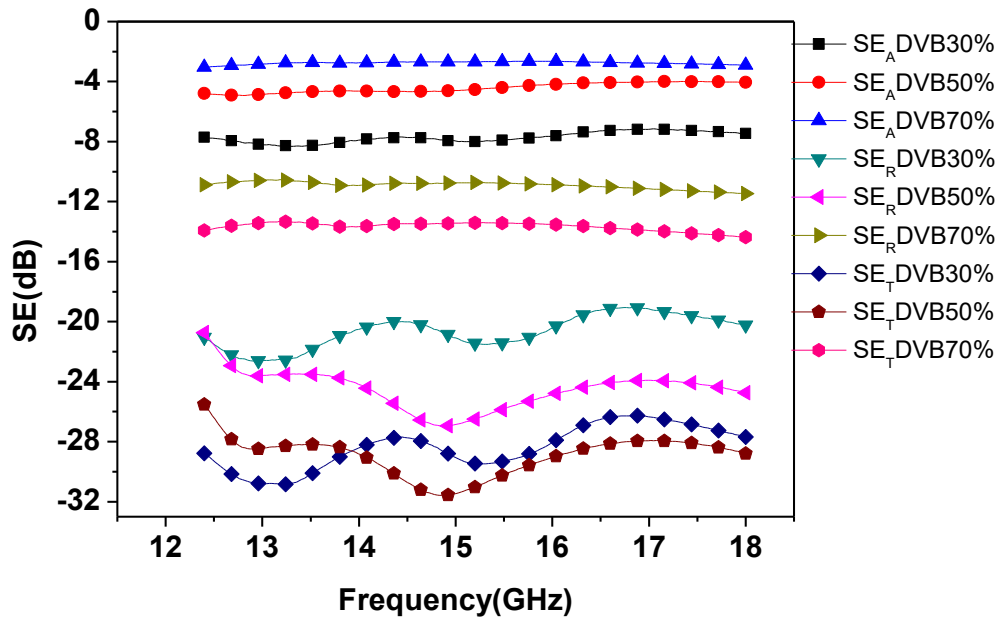
Figure 9.3 Shielding effectiveness of (PANI-DBSA)^{CM}/DVB composites with different DVB content in Ku-band.
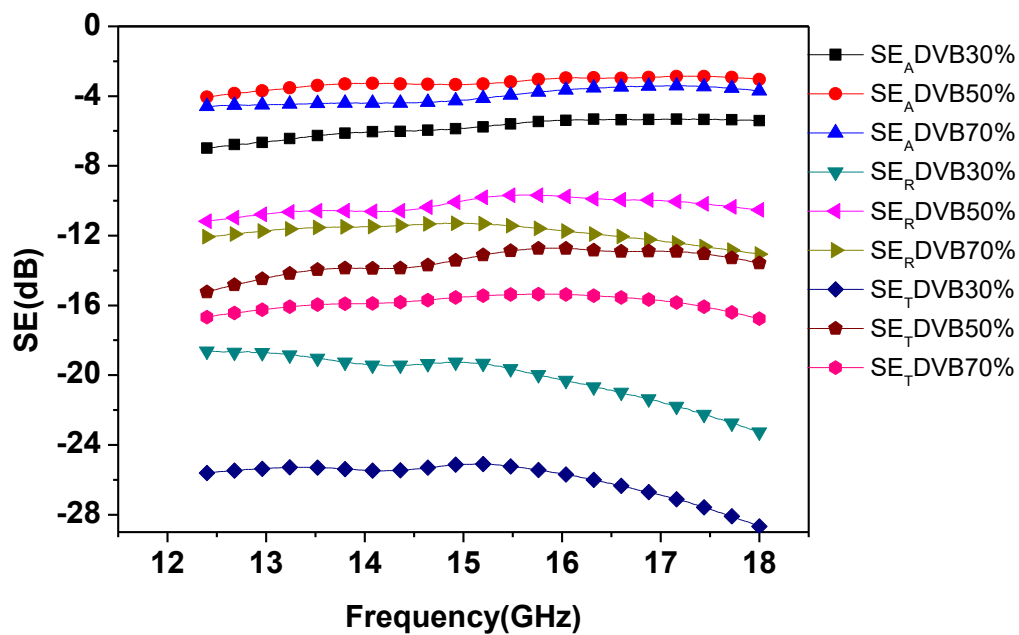
Figure 9.4 Shielding effectiveness of RM PANI-CFRP with different DVB content in Ku-band.
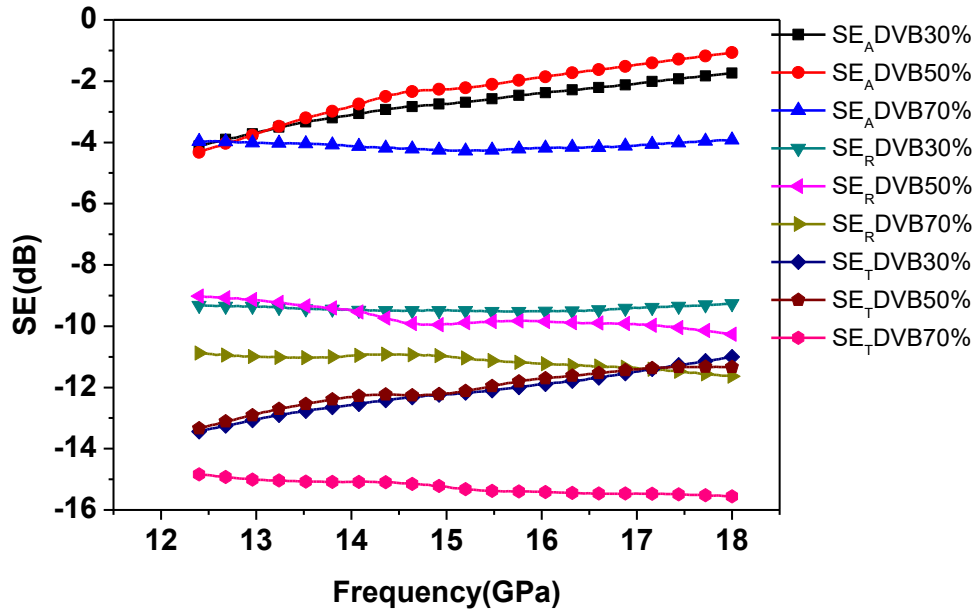
Figure 9.5 Shielding effectiveness of RM PANI-GFRP with different DVB content in Ku-band.
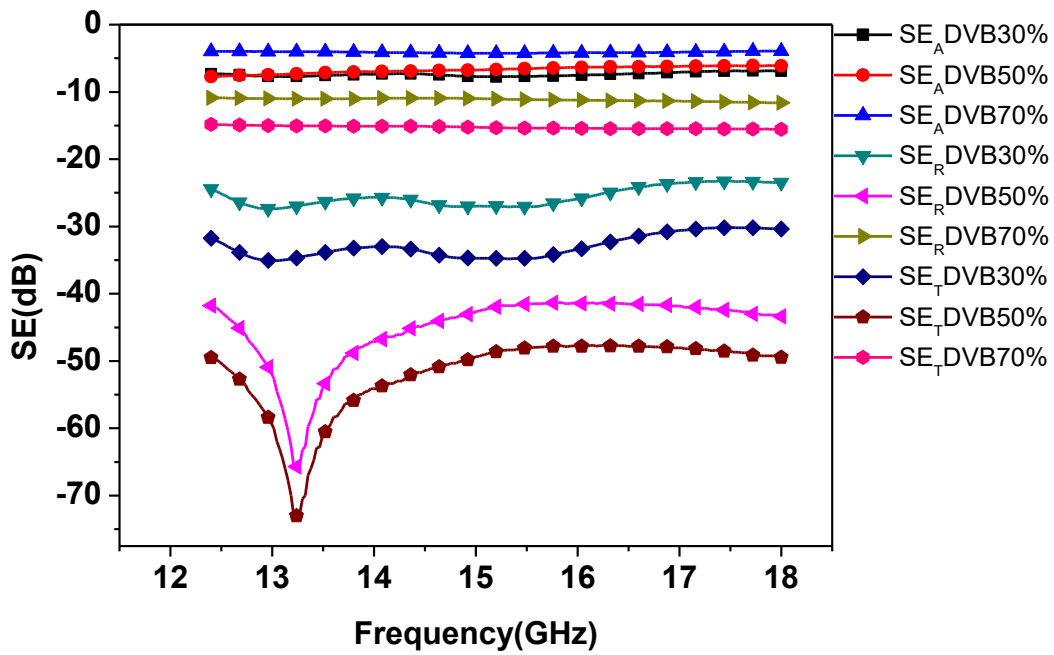
Figure 9.6 Shielding effectiveness of PANI-VGCF with different DVB content in Ku-band.
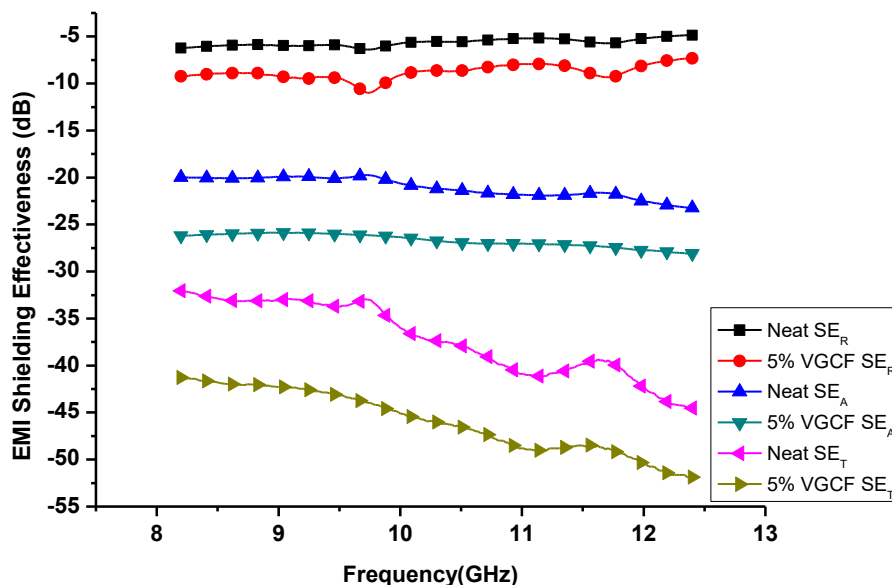
Figure 9.7 Shielding effectiveness of PANI-DBSA/DVB and PANI-DBSA-VGCF/DVB nanocomposites in X-band (8.2–12.4 GHz).

To understand the effect of additional VGCF-H filler on the EMI properties of the samples, we also presented a comparison of PANI-DBSA/DVB composite with and without VGCF-H in 50 wt. % DVB in X-band i.e. 8.2 GHz – 12.4 GHz as shown in **Figure 9.7**. It has been found that composite with 5 wt. % of VGCF-H has shown remarkable improvement in the EMI SE of the composite compared to the composite without VGCF-H. Total EMI shielding effectiveness (SE_T) improved to 51 dB for PANI-DBSA-VGCF/DVB composite from 28 dB for PANI-DBSA/DVB composite (23 dB) at 12.4 GHz frequency. SE due to reflection (SE_R) and absorption (SE_A) were improved by 2.46 dB and 21.32 dB respectively at 12.4 GHz. This means that these samples are capable to attenuate more than 99.99% of the incident electromagnetic waves.

The increase in the EMI SE can be attributed to the improved electrical conductivity of the composite by adding VGCF-H. The electrical conductivity of the composite with VGCF is more than ~ 7 times of the composite without VGCF-H. The intrinsic behavior of VGCF to absorb electromagnetic waves is also responsible for such remarkable improvement of EMI SE in the material.

9.4 Discussion

Principle of EMI shielding was explained in this chapter and EMI SE of different PANI-based composites were investigated. It was found that composite with higher content of PANI-DBSA has shown better EMI SE properties. Which can be attribute to the improved electrical conductivity of the system. A direct correlation between electrical conductivity and EMI SE is presented in **Table 9.1.**

Table 9.1 Relation between electrical conductivity and EMI-SE in PANI-based composites.

Sample name	Electrical conductivity (S/cm)	EMI SE at 18 GHz
PM DVB 30	2.68	29
PM DVB 50	0.226	27
PM DVB 70	0.023	13.8
VGCF DVB 30	2.02	33
VGCF DVB 50	0.74	55
VGCF DVB 70	0.027	15

Composite with VGCF-H has shown great improvement in the EMI SE of the composite. This behaviour can be assigned to the improved overall electrical conductivity of the PANI-DBSA/DVB composite as well as due to the good EMI shielding properties of VGCF-H itself. High value of EMI SE with 5wt% of VGCF with 50 wt% DVB composite can be assigned to the synergic effect of good dispersion of VGCF into the system and high electrical conductivity of the system. The main factors affecting EMI SE are thickness of sample, electrical conductivity and multi-

phases in the system. With more number of phases, including air voids, improved EMI SE has been reported. Therefore, the argument of synergic effect stands valid in this case. **Table 9.2** shows EMI-SE values of some the common materials from literature.

Table 9.2 EMI-SE values of some of the common materials.

Sample name	Thickness (mm)	EMI SE (dB)	Frequency (Hz)	Reference
Copper	3.1	100.6 ± 4.9	1-2 GHz	[92]
Nickel	3.1	85.8 ± 2.0	1-2 GHz	[92]
Pure epoxy	NA	0.3	NA	[93]
CF/epoxy (30%V_f)	2	29.4	12.4 GHz	[94]
VGCF DVB 50	3	55	18 GHz	Present work

From the **Table 9.2**, it can be seen the effectiveness of PANI-based composite for EMI applications. EMI-SE of pure epoxy has been reported very low of value 0.3 dB, due to its transparency. PANI-base matrix has shown far better EMI SE compared to pure epoxy. In this work, a thermoset composite has been reported with 51 dB of EMI shielding effectiveness in X-band, 1.97 S/cm of electrical conductivity and up to 1.71 of GPa flexural modulus.

Chapter 10 Conclusion

10.1 Summary

A highly conductive composite material with good mechanical properties is the need of the hour in present industrial and academic fields. Therefore, a thermoset conductive composite with high mechanical and electrical properties has been developed in this work and its application have been investigated especially its structural applications.

In Chapter 1, a brief introduction to the conductive polymers was presented and the importance of research in this filed was explained. Special attention was given to Polyaniline (PANI) because PANI has a special status among all the conducting polymers. PANI has been the center of research due to its ease in availability, ability to tune electrical conductivity and remarkable optical properties. Different dopants and matrices were discussed. It was established that, emeraldine base form of PANI can be rendered conductive by doping with a protonic acid. Reason to choose DBSA as dopant and DVB as matrix were explained by explaining their individual properties. Finally, it was confirmed that dodecylebenzenesulfonic acid (DBSA) will be used as a dopant for PANI due to its surfactant properties which improves the solubility of the PANI-DBSA complex in the matrix i.e. DVB.

In Chapter 2, different characterization techniques were presented in details. It was shown how prepared composite were characterized using various techniques like; Fourier transform infra-red spectroscopy (FTIR), ultra violet-visible-near infrared red spectroscopy (UV-vis-NIR), thermogravimetric analysis (TGA), thermal optical microscopy, electromagnetic interference (EMI) shielding measurements and four-probe electrical conductivity. The effect of dispersion on electrical and mechanical properties was also elaborated using scanning electron microscope (SEM) micrographs.

In Chapter 3, A detailed parametric study was presented to optimize the doping temperature and effective molar ratio between PANI and DBSA.

Chapter 4, mainly focused on the unique one-step synthesis process of PANI-DBSA/DVB composite. It was demonstrated in this work that doping of PANI and curing of DVB can took place at the same time. It was demonstrated that a PANI-DBSA/DVB composite has very high electrical and good mechanical properties after curing. However, due to the low liquid state duration (early start of curing at room temperature) of this matrix, a parametric study was done to optimize the present system.

In Chapter 5, Roll-milling process and control doping process of PANI were introduced for the mass production of this thermosetting conductive resin system. High electrical & mechanical properties with good liquid state duration were achieved.

To improve electrical conductivity and mechanical properties of the system, an additional conductive filler VGCF was also used in Chapter 6. With addition of additional conductive filler VGCF-H, higher electrical conductivity and better mechanical properties were achieved. The idea of using additional conductive fillers was derived by the hypothesis that PANI-DBSA agglomerates are the conductive islands in the insulating DVB matrix. Therefore, additional conductive fillers can be used as the conductive connecting bridge between those islands, simultaneously improving the mechanical properties. Different combinations of dopant ratios and conductive fillers were tried with the main PANI-DBSA/DVB matrix and their effect on composite properties were investigated.

In Chapter 7, dedoping phenomenon of this conductive composite system was explained using various techniques. Effect of curing temperature and curing time was explained.

Applications of this composite system were studied in Chapter 8. This conductive resin system was used to impregnate FRPs to prepare highly conductive FRPs. Carbon fiber reinforced composite prepared by using PANI-based thermosetting resin (CF/PANI) shown approximately 36 times higher electrical conductivity as compared to epoxy based CFRPs (CF/Epoxy) in the direction of thickness and approximately 6 times higher in the direction of fiber.

It is observed that high electric and dielectric properties contribute to the high EMI shielding efficiency. Therefore, this composite find its application in EMI shielding technology as well.

Chapter 9 was dedicated to the EMI SE properties of PANI-based composites. The composite with VGCF-H as additional conductive filler shown 73 dB shielding effectiveness at 13.2 GHz with the composition of 5 wt. % VGCF, 45 wt. % PANI-DBSA and 50 wt. % DVB in the composite. Electrical conductivity up to 1.97 S/cm with the addition of 5 wt. % VGCF-H and flexural modulus up to 1.71 GPa with 3 wt. % of VGCF-H were also achieved. These results confirmed that a polymer thermoset conductive composite with improved electrical, mechanical and very high EMI shielding effectiveness was successfully prepared.

10.2 Future prospective

These outstanding results make the PANI-DBSA/DVB composite a potential candidate for lightning strike protection (LSP), structural capacitor and EMI shielding material. This work gives a start towards unravelling the new horizon of applications of structural conductive composites. The capability of PANI-based CFRPs to supress thunder lightning strike damage is already in progress. We have obtained some very encouraging results using CF/PANI. However, due to the low mechanical properties of pure CF/PANI, we are looking into the hybrid composites having PANI-based and epoxy based CFRPs together to obtain the best optimum results. In aerospace industry, good EMI properties of PANI-DBSA/DVB composite can be utilized in aviation electronics. Five crashes of Blackhawk helicopters shortly after their introduction into service in the late 1980's were found to be due to electromagnetic interference from very strong radar and radio transmitters with the electronic flight control systems. Therefore, the EMI problem is really important to tackle in aviation industry. Metal based gasket are generally used to protect the sensitive electric circuitry of aircrafts from unwanted electromagnetic interference. But metals comes with weight, therefore PANI-based structural composite could provide solution to that problem. CF/PANI can also be used to prepare suitcases for EMI shielding protection for critical equipment in defence sector. Radar absorption would also be achievable with further improvement in this system and it would be of great importance in future military aircrafts.

Energy harvesting is one of the most researched field at present. Researchers are constantly looking for a material having high dielectric values and good ionic conductivity to prepare

good capacitors and batteries. We have found good dielectric properties of PANI-DBSA/DVB composite and also good ionic conductivity. Therefore, this material finds its potential applications in structural capacitor/batteries.

10.3 Future work and recommendations

In this thesis, a new PANI-based thermoset matrix with good electrical and mechanical properties was introduced. After optimization, longer liquid state of this matrix at room temperature was also obtained. However, this better stability came with the trade of relationship with other properties. Therefore, in future further work is recommended to obtain better liquid state duration without compromising with the properties. To achieve this goal, hybrid doping and hybrid curing profiles are recommended.

Mechanical properties of CF/PANI were also found to be lower compared to CF/epoxy. Effect of sizing on the interface properties between carbon fabric and matrix could be one of the reason. Therefore, a detail study is recommended to obtain the best mechanical properties of CF/PANI composite without losing its electrical conductivity properties.

In this work, DVB has been used as a matrix which show good compatibility with PANI-system. However, DVB found to have lower mechanical properties compared to commercially available epoxies. Therefore, it is highly recommended to search another alternative matrix with good compatibility with PANI-based system to compete in commercial market.

Electrical conductivity and mechanical properties are the function of PANI-DBSA content in the system. Therefore, it was important to know the effect of PANI-DBSA concentration on mechanical properties. For this purpose, Kerner-Nielsen model was used to predict the flexural modulus of the composite w.r.t. PANI-DBSA content in the composite. We assumed few constant as similar to of a carbon-black filled epoxy system i.e. K_E the Einstein coefficient and ϕ_m the maximum packing factor. We got very good agreement between theoretical and experimental values. However, K_E the Einstein coefficient and ϕ_m the maximum packing factor should be calculated specifically for the PANI-DBSA agglomerates and predict the composite mechanical properties again.

References

1.   Gibson, R. F. A review of recent research on mechanics of multifunctional composite materials and structures. *Compos. Struct.* **92,** 2793–2810 (2010).

2.   Hong, Y. K. *et al.* Method and apparatus to measure electromagnetic interference shielding efficiency and its shielding characteristics in broadband frequency ranges. *Rev. Sci. Instrum.* **74,** 1098–1102 (2003).

3.   Ghavamian, A., Maghami, M. R., Dehghan, S. & Gomes, C. Concerns of corrosive effects with respect to lightning protection systems. *Eng. Fail. Anal.* **57,** 434–443 (2015).

4.   Hussain, F. Review article: Polymer-matrix Nanocomposites, Processing, Manufacturing, and   Application: An Overview. *J. Compos. Mater.* **40,** 1511–1575 (2006).

5.   Long, Y., Chen, Z., Wang, N., Li, J. & Wan, M. Electronic transport in PANI-CSA/PANI-DBSA polyblends. *Phys. B Condens. Matter* **344,** 82–87 (2004).

6.   Li, J. Y., Huang, C. & Zhang, Q. Enhanced electromechanical properties in all-polymer percolative composites. *Appl. Phys. Lett.* **84,** 3124–3126 (2004).

7.   Deng, H. *et al.* Progress on the morphological control of conductive network in conductive polymer composites and the use as electroactive multifunctional materials. *Prog. Polym. Sci.* **39,** 627–655 (2014).

8.   Pud, A., Ogurtsov, N., Korzhenko, A. & Shapoval, G. Some aspects of preparation methods and properties of polyaniline blends and composites with organic polymers. *Prog. Polym. Sci.* **28,** 1701–1753 (2003).

9.   Shirakawa, H., Louis, E. J., MacDiarmid, A. G., Chiang, C. K. & Heeger, A. J. Synthesis of electrically conducting organic polymers: halogen derivatives of

polyacetylene, (CH). *J. Chem. Soc. Chem. Commun.* 578–580 (1977). doi:10.1039/C39770000578

10. Del Castillo-Castro, T., Castillo-Ortega, M. M. & Herrera-Franco, P. J. Electrical, mechanical and piezo-resistive behavior of a polyaniline/poly(n-butyl methacrylate) composite. *Compos. Part A Appl. Sci. Manuf.* **40,** 1573–1579 (2009).

11. Lee, J. & Kim, E. Effect of structural and morphological changes on the conductivity of stretched PANI-DBSA/HIPS film. *Bull. Korean Chem. Soc.* **32,** 2661–2665 (2011).

12. Afzal, A. B., Akhtar, M. J., Nadeem, M. & Hassan, M. M. Dielectric and impedance studies of DBSA doped polyaniline/PVC composites. *Curr. Appl. Phys.* **10,** 601–606 (2010).

13. Bhadra, S., Singha, N. K. & Khastgir, D. Dielectric properties and EMI shielding efficiency of polyaniline and ethylene 1-octene based semi-conducting composites. *Curr. Appl. Phys.* **9,** 396–403 (2009).

14. Moreira, V. X., Garcia, F. G. & Soares, B. G. Conductive epoxy/amine system containing polyaniline doped with dodecylbenzenesulfonic acid. *J. Appl. Polym. Sci.* **100,** 4059–4065 (2006).

15. Saravanan, S., Joseph Mathai, C., Anantharaman, M. R., Venkatachalam, S. & Prabhakaran, P. V. Investigations on the electrical and structural properties of polyaniline doped with camphor sulphonic acid. *J. Phys. Chem. Solids* **67,** 1496–1501 (2006).

16. Chiang, C. J. *et al.* In situ fabrication of conducting polymer composite film as a chemical resistive CO_2 gas sensor. *Microelectron. Eng.* **111,** 409–415 (2013).

17. Olayo, R., Encinas, J. C. & Rodri, D. E. Preparation and Characterization of Electroconductive Polypyrrole – Thermoplastic Composites. 1498–1506 (2001).

18. Ramamurthy, P. C., Harrell, W. R., Gregory, R. V., Sadanadan, B. & Rao, A. M. Mechanical and Electrical Properties of Solution-Processed Polyaniline/Multiwalled Carbon Nanotube Composite Films. *J. Electrochem. Soc.* **151,** G502 (2004).

19.   Jia, W. *et al.* Polyaniline-DBSA/organophilic clay nanocomposites: Synthesis and characterization. *Synth. Met.* **128,** 115–120 (2002).

20.   Acevedo, D. F., Salavagione, H. J., Miras, M. C. & Barbero, C. a. Synthesis, properties and aplications of functionalized polyanilines. *J. Braz. Chem. Soc.* **16,** 259–269 (2005).

21.   Ziadan, K. M. Conducting Polymers Application. *Intech* **Chapter 1,** 3–24 (2012).

22.   Street, J. L. B. and G. B. Polarons, Bipolarons and Solitons in Conducting polymers. *accounts Chem. Res.* **18,** 309–315 (1985).

23.   Saini, P. & Arora, M. Microwave Absorption and EMI Shielding Behavior of Nanocomposites Based on Intrinsically Conducting Polymers , Graphene and Carbon Nanotubes. *New Polym. Spec. Appl.* 71–112 (2012). doi:10.5772/48779

24.   Kumar, V., Yokozeki, T., Goto, T. & Takahashi, T. Mechanical and electrical properties of PANI-based conductive thermosetting composites. *J. Reinf. Plast. Compos.* (2015). doi:10.1177/0731684415588551

25.   Haba, Y., Segal, E., Narkis, M. & Siegmann, a. Polymerization of aniline in the presence of DBSA in an aqueous dispersion. *Synth. Met.* **106,** 59–66 (1999).

26.   Li, J., Tang, X., Li, H., Yan, Y. & Zhang, Q. Synthesis and thermoelectric properties of hydrochloric acid-doped polyaniline. *Synth. Met.* **160,** 1153–1158 (2010).

27.   Faez, R. Reactive doping of PAni-CSA and ITS use in conducting coatings. (2002). at <http://www.bv.fapesp.br/pt/auxilios/78962/reactive-doping-of-pani-csa-and-its-use-in-conducting-coatings/>

28.   Abed, M. Y., Youssif, M. A., Aziz, H. a. & Shenashen, M. a. Synthesis and enhancing electrical properties of PANI and PPA composites. *Egypt. J. Pet.* **23,** 271–277 (2014).

29.   Khalid, M. *et al.* Electrical Conductivity Studies of Polyaniline Nanotubes Doped with Different Sulfonic Acids. *Indian J. Mater. Sci.* **2013,** 1–7 (2013).

30.   Trznadel, M. & Rannou, P. Effect of solvent-dopant competition on the conductivity of

polyaniline films. *Synth. Met.* **101,** 842 (1999).

31.   Babazadeh, M. Aqueous dispersions of DBSA-doped polyaniline: One-pot preparation, characterization, and properties study. *J. Appl. Polym. Sci.* **113,** 3980–3984 (2009).

32.   Dombroske, A. E. M. & Cited, R. United States Patent [191 [45] Date of Patent : 291–304 (1994).

33.   Bouanga, C. V. *et al.* Study of dielectric relaxation phenomena and electrical properties of conductive polyaniline based composite films. *J. Non. Cryst. Solids* **356,** 611–615 (2010).

34.   Del Castillo-Castro, T. *et al.* Synthesis and characterization of composites of DBSA-doped polyaniline and polystyrene-based ionomers. *Compos. Part A Appl. Sci. Manuf.* **38,** 639–645 (2007).

35.   Lu, J., Moon, K. S., Kim, B. K. & Wong, C. P. High dielectric constant polyaniline/epoxy composites via in situ polymerization for embedded capacitor applications. *Polymer (Guildf).* **48,** 1510–1516 (2007).

36.   Krakovský, I., Varga, M., Gallego Ferrer, G., Sabater I Serra, R. & Salmerón-Sánchez, M. Structure and properties of epoxy/polyaniline nanocomposites. *J. Non. Cryst. Solids* **358,** 414–419 (2012).

37.   Diniz, F. B., De Andrade, G. F., Martins, C. R. & De Azevedo, W. M. A comparative study of epoxy and polyurethane based coatings containing polyaniline-DBSA pigments for corrosion protection on mild steel. *Prog. Org. Coatings* **76,** 912–916 (2013).

38.   Massoumi, B., Farjadbeh, F., Mohammadi, R. & Entezami, a. a. Synthesis of conductive adhesives based on epoxy resin/nanopolyaniline and chloroprene rubber/nanopolyaniline: Characterization of thermal, mechanical and electrical properties. *J. Compos. Mater.* (2012). doi:10.1177/0021998312446498

39.   Belaabed, B., Lamouri, S., Naar, N., Bourson, P. & Ould Saad Hamady, S.

Polyaniline-doped benzene sulfonic acid/epoxy resin composites: structural, morphological, thermal and dielectric behaviors. *Polym. J.* **42,** 546–554 (2010).

40. Jeon, B. H., Kim, S., Choi, M. H. & Chung, I. J. Synthesis and characterization of polyaniline-polycarbonate composites prepared by an emulsion polymerization. *Synth. Met.* **104,** 95–100 (1999).

41. Zilberman, M. *et al.* Conductive blends of thermally dodecylbenzene sulfonic acid-doped polyaniline with thermoplastic polymers. *J. Appl. Polym. Sci.* **66,** 243–253 (1997).

42. Xinli, Y. W. and. Preparation of polystyrene/polyaniline core/shell structured particles and their epoxy-based conductive composites. *Polym. Int.* **56,** 126–131 (2007).

43. Tsotra, P., Gatos, K. G., Gryshchuk, O. & Friedrich, K. Hardener type as critical parameter for the electrical properties of epoxy resin/polyaniline blends. *J. Mater. Sci.* **40,** 569–574 (2005).

44. George, B. & Mathew, B. Effect of the Degree of Dvb Crosslinking on the Metal Ion Specificity of Polyacrylamide-Supported Glycines. *J. Macromol. Sci. Part A* **38,** 429–449 (2001).

45. Gettinger, C. L., Heeger, a. J., Pine, D. J. & Cao, Y. Solution characterization of surfactant solubilized polyaniline. *Synthetic Metals* **74,** 81–88 (1995).

46. Ep, B., Cao, Y., Heeger, A. J. & Smith, P. Processible forms of electrically conductive polyaniline and conductive products formed therefrom. (2015).

47. Kumar, V., Yokozeki, T., Goto, T. & Takahashi, T. Synthesis and characterization of PANI-DBSA/DVB composite using roll-milled PANI-DBSA complex. *Polymer (Guildf).* **86,** 129–137 (2016).

48. Haba, Y., Segal, E., Narkis, M., Titelman, G. I. & Siegmann, a. Polyaniline – DBSArpolymer blends prepared via aqueous dispersions. 189–193 (2000).

49. Goto, T., Awano, H., Takahashi, T., Yonetake, K. & Sukumaran, S. K. Effect of

processing temperature on thermal doping of polyaniline without shear. *Polym. Adv. Technol.* **22,** 1286–1291 (2011).

50. Kilmartin, P. A. *et al.* Free radical scavenging and antioxidant properties of conducting polymers examined using EPR and NMR spectroscopies. *Synth. Met.* **153,** 153–156 (2005).

51. Gizdavic-Nikolaidis, M., Travas-Sejdic, J., Bowmaker, G. A., Cooney, R. P. & Kilmartin, P. A. Conducting polymers as free radical scavengers. *Synth. Met.* **140,** 225–232 (2004).

52. Faez, R. & De Paoli, M.-A. A conductive rubber based on EPDM and polyaniline. *Eur. Polym. J.* **37,** 1139–1143 (2001).

53. Malinauskas, a. Chemical deposition of conducting polymers. *Polymer (Guildf).* **42,** 3957–3972 (2001).

54. de Souza, F. G. & Soares, B. G. Methodology for determination of Pani.DBSA content in conductive blends by using UV-Vis spectrometry. *Polym. Test.* **25,** 512–517 (2006).

55. Xie, H. Q., Ma, Y. M. & Guo, J. S. Secondary doping phenomena of two conductive polyaniline composites. *Synth. Met.* **123,** 47–52 (2001).

56. Babu, V. J. Conducting Polyaniline-Electrical Charge Transportation. *Mater. Sci. Appl.* **04,** 1–10 (2013).

57. T. Taka, J. L. and K. L. CONDUCTIVITY AND STRUCTURE OF DBSA-PROTONATED POLYANILINE. *Solid State Commun.* **92,** 393–396 (1994).

58. Zheng, W. Y. *et al.* Self-Assembly of the Electroactive Complexes of Polyaniline and Surfactant. *Macromol. Chem. Phys.* **196,** 2443–2462 (1995).

59. Trchov??, M., ??ed??nkov??, I., Tobolkov??, E. & Stejskal, J. FTIR spectroscopic and conductivity study of the thermal degradation of polyaniline films. *Polym. Degrad. Stab.* **86,** 179–185 (2004).

60. Peikertová, P., Matějka, V., Kulhánková, L. & Neuwirthová, L. Thin Polyaniline

Films : Study of the Thermal Degradation. (2011).

61. Šeděnková, I., Trchová, M. & Stejskal, J. Thermal degradation of polyaniline films prepared in solutions of strong and weak acids and in water - FTIR and Raman spectroscopic studies. *Polym. Degrad. Stab.* **93,** 2147–2157 (2008).

62. Spitalsky, Z., Tasis, D., Papagelis, K. & Galiotis, C. Carbon nanotube-polymer composites: Chemistry, processing, mechanical and electrical properties. *Prog. Polym. Sci.* **35,** 357–401 (2010).

63. Jianming, J., Wei, P., Shenglin, Y. & Guang, L. Electrically conductive PANI-DBSA/Co-PAN composite fibers prepared by wet spinning. *Synth. Met.* **149,** 181–186 (2005).

64. Bilal, S., Gul, S., Ali, K. & Shah, A. U. H. A. Synthesis and characterization of completely soluble and highly thermally stable PANI-DBSA salts. *Synth. Met.* **162,** 2259–2266 (2012).

65. Yasser Zare, H. G. D. Analysis of Tensile Modulus of PP/Nanoclay/CaCO3 Ternary Nanocomposite Using Composite Theories. *J. Appl. Polym. Sci.* **123,** 2309–2319 (2012).

66. J. JANCAR, A. T. D. The mechanical properties of ternary composites of polypropylene with inorganic fillers and elastomer inclusions. *J. Mater. Sci. 29(1994)* **29,** 4651–4658 (1994).

67. Fu, S. Y., Feng, X. Q., Lauke, B. & Mai, Y. W. Effects of particle size, particle/matrix interface adhesion and particle loading on mechanical properties of particulate-polymer composites. *Compos. Part B Eng.* **39,** 933–961 (2008).

68. Chew, T., Daik, R. & Hamid, M. Thermal Conductivity and Specific Heat Capacity of Dodecylbenzenesulfonic Acid-Doped Polyaniline Particles—Water Based Nanofluid. *Polymers (Basel).* **7,** 1221–1231 (2015).

69. Ayad, M. & Zaghlol, S. Nanostructured crosslinked polyaniline with high surface area: Synthesis, characterization and adsorption for organic dye. *Chem. Eng. J.* **204-205,**

79–86 (2012).

70. Via, Michael D.King, J. A. *et al.* Tensile Modulus Modeling of Carbon Black/ Polycarbonate, Carbon Nanotube/Polycarbonate, and Exfoliated Graphite Nanoplatelet/Polycarbonate Composites. *J. Appl. Polym. Sci.* **124,** 2269–2277 (2013).

71. Daniel Loˊpez Gaxiola, Mary M. Jubinski, Jason M. Keith, Julia A. King, I. M. Effects of Carbon Fillers on Tensile and Flexural Properties in Polypropylene-Based Resins. *Polym. Polym. Compos.* **21,** 449–456 (2013).

72. Ravichandran, R., Sundarrajan, S., Venugopal, J. R., Mukherjee, S. & Ramakrishna, S. Applications of conducting polymers and their issues in biomedical engineering. *J. R. Soc. Interface* **7 Suppl 5,** S559–S579 (2010).

73. El-ghaffar, M. A. A., Shaffei, K. A. & Abdelwahab, N. Evaluation of Some Conducting Polymers as Novel Antioxidants for Rubber Vulcanizates. **2014,** (2014).

74. Han, Y. G., Kusunose, T. & Sekino, T. One-step reverse micelle polymerization of organic dispersible polyaniline nanoparticles. *Synth. Met.* **159,** 123–131 (2009).

75. MacDiarmid, A. G. & Epstein, A. J. The concept of secondary doping as applied to polyaniline. *Synth. Met.* **65,** 103–116 (1994).

76. Cheng, X. *et al.* Highly conductive graphene oxide/polyaniline hybrid polymer nanocomposites with simultaneously improved mechanical properties. *Compos. Part A Appl. Sci. Manuf.* **82,** 100–107 (2016).

77. Singh, B. P. *et al.* Effect of length of carbon nanotubes on electromagnetic interference shielding and mechanical properties of their reinforced epoxy composites. *J. Nanoparticle Res.* **16,** 1–11 (2014).

78. Tao, K. *et al.* Effects of carbon nanotube fillers on the curing processes of epoxy resin-based composites. *J. Appl. Polym. Sci.* **102,** 5248–5254 (2006).

79. Proke??, J. & Stejskal, J. Polyaniline prepared in the presence of various acids: 2. Thermal stability of conductivity. *Polym. Degrad. Stab.* **86,** 187–195 (2004).

80. Han, M. G., Cho, S. K., Oh, S. G. & Im, S. S. Preparation and characterization of polyaniline nanoparticles synthesized from DBSA micellar solution. *Synth. Met.* **126,** 53–60 (2002).

81. Roichman, Y., Titelman, G. ., Silverstein, M. ., Siegmann, a & Narkis, M. Polyaniline synthesis: influence of powder morphology on conductivity of solution cast blends with polystyrene. *Synth. Met.* **98,** 201–209 (1999).

82. Jia, W. *et al.* Electrically conductive composites based on epoxy resin with polyaniline-DBSA fillers. *Synth. Met.* **132,** 269–278 (2003).

83. Jia, W. *et al.* Electrically conductive composites based on epoxy resin with. **132,** 269–278 (2003).

84. Vavouliotis, A., Paipetis, A. & Kostopoulos, V. On the fatigue life prediction of CFRP laminates using the Electrical Resistance Change method. *Compos. Sci. Technol.* **71,** 630–642 (2011).

85. Song, D. Y., Takeda, N. & Kitano, A. Correlation between mechanical damage behavior and electrical resistance change in CFRP composites as a health monitoring sensor. *Mater. Sci. Eng. A* **456,** 286–291 (2007).

86. Yokozeki, T. *et al.* Development and characterization of CFRP using a polyaniline-based conductive thermoset matrix. *Compos. Sci. Technol.* **117,** 277–281 (2015).

87. Hirano, Y. *et al.* Lightning damage suppression in a carbon fiber-reinforced polymer with a polyaniline-based conductive thermoset matrix. *Compos. Sci. Technol.* **127,** 1–7 (2016).

88. Tsotra, P. & Friedrich, K. Short carbon fiber reinforced epoxy resin/polyaniline blends: their electrical and mechanical properties. *Compos. Sci. Technol.* **64,** 2385–2391 (2004).

89. Rea, S., Linton, D., Orr, E. & Mcconnell, J. Electromagnetic shielding properties of carbon fibre composites in avionic systems. *Microw. Rev.* **11,** 29–32 (2005).

90. Dřínovský, J. & Kejík, Z. Electromagnetic Shielding Efficiency Measurement of Composite Materials. *Meas. Sci. Rev.* **9,** 109–112 (2009).

91. Saini, P., Choudhary, V., Singh, B. P., Mathur, R. B. & Dhawan, S. K. Polyaniline-MWCNT nanocomposites for microwave absorption and EMI shielding. *Mater. Chem. Phys.* **113,** 919–926 (2009).

92. Hallett, M., Human, R. a T. & Physiology, C. Letters To the Editor Letters To the Editor. *Carbon N. Y.* **15,** 1106–1107 (1992).

93. Singh, B. P. *et al.* Enhanced microwave shielding and mechanical properties of high loading MWCNT-epoxy composites. *J. Nanoparticle Res.* **15,** 1–12 (2013).

94. Singh, B. P., Choudhary, V., Saini, P. & Mathur, R. B. Designing of epoxy composites reinforced with carbon nanotubes grown carbon fiber fabric for improved electromagnetic interference shielding. *AIP Adv.* **2,** 1–7 (2012).

Achievements

Journal papers

1. Vipin Kumar*, T. Yokozeki et al. "Characterization of Physical Properties and Morphology of PANI-Based Conductive Composites," *J. Reinf. Plast. Compos.* 34, (2015) 1298–1305.

2. X. Cheng, V. Kumar, T. Yokozeki et al. "Highly conductive Graphene Oxide/Polyaniline hybrid polymer nanocomposites with simultaneously improved mechanical properties," *Composites: Part A* 82 (2016) 100–107.

3. Vipin Kumar*, T. Yokozeki et al. "Synthesis and characterization of PANI-DBSA/DVB composite using roll-milled PANI-DBSA complex", *Polymer 86 (2016) 129-137.*

To be submitted journal papers

4. Vipin Kumar*, T. Yokozeki et al. "Improved electrical, mechanical and EMI shielding properties of PANI-VGCF-DBSA/DVB hybrid nanocomposite".

5. Vipin Kumar*, T. Yokozeki et al. "Effect of SWCNT on flexural properties of PANI-DBSA/DVB nanocomposite".

6. Vipin Kumar*, T. Yokozeki et al. "Hybrid doping system for improved properties of PANI-based composites".

Conference papers

1. Vipin Kumar*, T. Yokozeki. "Characterization of Physical Properties and Morphology of PANI-Based Conductive Composites," US-Japan Conference on Composite Materials, September 8-10, (2014) Price Centre, University of California San Diego, La Jolla, CA USA.

2. Vipin Kumar*, T. Yokozeki. "Characterization of Physical Properties and Morphology of PANI-Based Conductive Composites," CON-EX 2014, 59th FRP conference, Oct 2-3, (2014) Kyoto Institute of Technology. Kyoto, Japan.

3. Vipin Kumar*, T. Yokozeki. "Synthesis And Characterization Of Conductive CFRP & GFRP Using PANI-Based Electrically Conductive Thermoset Polymer Matrix," ICCM 20 conference, July 19-24, (2015), Copenhagen, Denmark.

4. Vipin Kumar*, T. Yokozeki. "Improved electrical, mechanical and EMI shielding properties of PANI-VGCF-DBSA/DVB hybrid nanocomposite," proceeding to ECCM 17 conference, June 26-30, 2016, Munich, Germany.

International workshops & symposiums

1. Vipin Kumar, T. Yokozeki*. "Mechanical and Electrical Properties of PANI-Based Conductive Thermosetting Composites," 1st Joint Turkey-Japan Workshop on Polymeric Composite Materials, Sabancı University, 12-13 May 2014, Istanbul, TURKEY.

2. Vipin Kumar*, T. Yokozeki. 2015. "Mechanical and Electrical Properties of Conductive Thermoset FRPs," 2nd TJC on Polymeric Composite Materials, 7-9 May 2015, Cesme/Izmir, Turkey.

3. Vipin Kumar*, T. Yokozeki. 2015. "Synthesis And Characterization Of Conductive CFRP & GFRP Using PANI-Based Electrically Conductive Thermoset Polymer Matrix," International Symposium on Nanoengineered Composites: Properties, modelling and applications, July 15-17, 2015, Roskilde, Denmark.

4. Vipin Kumar*, T. Yokozeki. 2015. "Conductive polymer composites," India-Japan workshop "Advanced Carbon Fiber Polymer Composites and its Applications", October28, 2015, NPL, New Delhi.